Technische Universität München

Wissenschaftszentrum Weihenstephan für Ernährung, Landnutzung und Umwelt,

Lehrstuhl für Biotechnologie der Nutztiere, Prof. Angelika Schnieke, Ph.D.

Porcine models of cardiovascular disease

Daniela Barbara Huber

Vollständiger Abdruck der von der Fakultät Wissenschaftszentrum Weihenstephan für Ernährung, Landnutzung und Umwelt der Technischen Universität München zur Erlangung des akademischen Grades eines

Doktors der Naturwissenschaften

genehmigten Dissertation.

Vorsitzender:

Prof. Dr. Siegfried Scherer

Prüfer der Dissertation:

1. Prof. Angelika Schnieke, Ph.D.
2. Prof. Dr.Wolfgang Wurst

Die Dissertation wurde am 20.03.2019 bei der Technischen Universität München eingereicht und durch die Fakultät Wissenschaftszentrum Weihenstephan für Ernährung, Landnutzung und Umwelt am 16.09.2019 angenommen.

Table of content

Table of content

Table of content

Abstract

Cardiovascular diseases - disorders affecting the heart and blood vessels - are still the leading cause of death globally. It is well known that the risk of developing such conditions is in part due to lifestyle factors, for example diet, physical inactivity, tobacco and alcohol use, but the most important determinants of cardiovascular health, age and genetic predisposition, are not so easily modified. It is important to understand the role of such factors in disease development.

In vivo models are very valuable for research, and modelling age-related cardiac changes in animals would be a powerful method to investigate cardiovascular biology. The subject of this thesis is the generation of two models of cardiovascular disease predisposition in pigs; one based on ageing and a second on a known genetic predisposition that affects younger people.

Ageing is a complex and multifarious condition and therefore difficult to represent in an animal model. It has however been shown that mice with mutations in the excision repair cross-complementation group 1 (*ERCC1)* gene, which plays a central role in DNA repair, show a phenotype that is similar to age-related pathologies. Thus, the idea was to introduce similar mutations in the porcine *ERCC1* locus and target expression of the mutant gene to the heart, and so generate a 'locally-aged' heart that is susceptible to age-related heart disease. In order to avoid a severe phenotype, double heterozygous pigs were to be developed. One allele of the *ERCC1* gene was designed to have a Δ7 mutation (deletion of the last seven amino acids). The second allele was designed to carry loxP sites flanking one or two exons (conditional knockout) to inactivate it in a tissue-, and time-specific manner by Cre recombinase. Primary somatic stem cells and gene targeting via homologous recombination (HR) was used to introduce the desired changes in the porcine *ERCC1* gene. Several different strategies were designed to generate gene targeted cells, e.g. promotor trap targeting vectors, CRISPR/Cas9-mediated (clustered regularly interspaced short palindromic repeats/CRISPR associated protein 9) gene targeting and double-cut vectors were used. Although first screenings of single cell clones showed targeting of the *ERCC1* locus, additional rearrangements occurred in all viable cell clones. As it was not possible to derive cell clones carrying correct loxP sequences or Δ7 mutations at the *ERCC1* locus, it was concluded that the function of this gene is required for cell survival and recombination and

therefore new strategies were developed. Adeno-associated viruses (AAVs) can be used to deliver the CRISPR/Cas9 system specifically into cardiac cells and generate a knockout of the *ERCC1* gene *in vivo*. Alternatively, by introducing a modified *ERCC1* minigene in the *ROSA26* locus, integration of the desired modifications is shifted to another locus while the endogenous *ERCC1* alleles remain functional. Using the CRISPR/Cas9 system the endogenous alleles can then be inactivated at any timepoint.

The second model was designed to mimic the genetic myocardial disease, hypertrophic cardiomyopathy (HCM), which in severe form can cause death in infancy. Hence, there is a strong interest to develop gene therapy strategies. To test their efficiency a translational animal model is required. Since the cardiac myosin-binding protein C *(MYBPC3)* gene is frequently mutated in HCM, it was decided to develop a porcine model carrying human founder *MYBPC3* mutations. Mutating the *MYBPC3* locus was successful and two different human mutations could be mimicked in porcine cells by the use of the CRISPR/Cas9 system. Cells have been used for SCNT (somatic cell nuclear transfer) and two pregnancies were established. One pregnancy resulted in a late abortion and one in the birth of a non-viable piglet. Analysis of the latter revealed signs of hypertrophy and mutations on both alleles. Since at this time only homozygous and compound heterozygous single cell clones were used for SCNT it was decided to use heterozygous single cell clones for further rounds of SCNT.

Zusammenfassung

Kardiovaskuläre Erkrankungen sind Erkrankungen des Herz-Kreislauf-Systems und stellen die häufigste Todesursache weltweit dar. Das Risiko daran zu erkranken wird durch gewisse Faktoren erhöht, wie zum Beispiel Ernährung, Mangel an Bewegung, Tabak- und Alkoholkonsum. Aber die wichtigsten Faktoren, die zugleich schwer zu beeinflussen sind, sind das Alter und genetische Veranlagung. Deswegen ist es wichtig zu verstehen, welche Rolle diese Faktoren bei der Entstehung der Krankheit haben.

In vivo Modelle sind sehr wertvoll für die Forschung und insbesondere solche, die altersbedingte Veränderungen des Herzens zeigen, wären äußerst hilfreich für die Erforschung von kardiovaskulären Mechanismen. Das Thema dieser Arbeit ist die Generierung zweier Schweinemodelle für kardiovaskuläre Erkrankungen; eine basiert auf dem Altern und eine zweite auf einer bekannten genetischen Prädisposition, die junge Menschen betrifft.

Altern ist ein komplexer und variabler Prozess, dementsprechend schwer ist es diesen in einem Tiermodell darzustellen. Es wurde jedoch gezeigt, dass Mäuse mit Mutationen in dem DNA-Reparaturgen *ERCC1* einen Phänotyp aufweisen, der ähnlich ist zu altersbedingten Pathologien. Deswegen wurde beschlossen, vergleichbare Mutationen in den porzinen *ERCC1*-Locus einzuführen und die Expression des mutanten Gens spezifisch im Herzen zu erreichen, damit ein „gealtertes“ und somit für altersbedingte Herzerkrankungen anfälliges Herz erzeugt wird. Um einen schweren Phänotypen zu vermeiden, wurde entschieden, einen doppelt heterozygoten Genotyp zu generieren. In ein Allel des *ERCC1*-Gens sollte eine Δ7-Mutation (Deletion der letzten sieben Aminosäuren) eingeführt werden. Das zweite Allel wurde mit loxP-Stellen, die ein oder zwei Exons flankieren (konditionaler Knockout), designed, damit das Gen mit Hilfe der Cre-Rekombinase gewebe- und zeitspezifisch inaktiviert werden kann. Die gewünschten Veränderungen sollten in primäre somatische Stammzellen mittels Gen-*Targeting* über Homologe Rekombination eingeführt werden. Verschiedene Strategien, wie zum Beispiel *Promotortrap*-*Targeting*-Vektoren, Gen-*Targeting* mittels CRISPR/Cas9 und *doublecut* Vektoren wurden verwendet.

Obwohl erste Analysen von Einzelzellklonen ein *targeting* des *ERCC1*-Locus zeigten, traten in allen überlebensfähigen Zellklonen zusätzlich unerwünschte Veränderungen auf. Da es nicht möglich war, Zellklone zu generieren, die korrekte loxP-Sequenzen oder Δ7-Mutationen am

ERCC1-Locus trugen, wird angenommen, dass die Funktion des Gens für das Überleben der Zellen benötigt wird und es wurden neue Strategien entwickelt, um das Gen zu mutieren.

Einerseits wurden AAVs designed, um das CRISPR/Cas9-System spezifisch in Herzzellen einzubringen und einen Knockout des *ERCC1*-Gens *in vivo* zu erzeugen. Andererseits sollte durch die Einführung eines modifizierten *ERCC1*-Minigens in den *ROSA26*-Locus die Einbringung der gewünschten Modifikationen zu einem anderen Locus verschoben werden und die endogenen *ERCC1*-Allele bleiben funktionell. Mit Hilfe des CRISPR/Cas9-Systems können die endogenen Allele zu jedem Zeitpunkt zerstört werden.

Das zweite Modell sollte die genetische myokardiale Krankheit „Hypertrophe Kardiomyopathie“ (HCM) nachahmen, welche in schwerer Form den Säuglingstod verursachen kann. Zur Behandlung der Krankheit werden entsprechende Gentherapien entwickelt. Um diese zu testen, ist ein translatorisches Tiermodell erforderlich. Da das Gen *MYBPC3* häufig in HCM mutiert ist, wurde beschlossen, ein Schweinemodell zu entwickeln, welches sogenannte Gründer-Mutationen des Menschen trägt. Die Einführung der Mutationen in den *MYBPC3*-Locus war erfolgreich und zwei verschiedene menschliche Mutationen konnten in Schweinezellen durch Verwendung des CRISPR/Cas9-Systems nachgeahmt werden. Die Einzelzellklone wurden für den Kerntransfer verwendet und es konnten zwei Trächtigkeiten etabliert werden. Eine Trächtigkeit führte zu einem späten Abgang und eine zur Geburt eines nicht lebensfähigen Ferkels. Die Analyse von letzterem zeigte Anzeichen von Hypertrophie und Mutationen auf beiden Allelen des *MYBPC3* Gens. Da zu dieser Zeit nur homozygote und gemischt heterozygote Einzelzellklone für den Kerntransfer verwendet wurden, wurde beschlossen, bei weiteren Kerntransfer-Runden nur heterozygote Einzelzellklone zu verwenden.

1 Introduction

1.1 Cardiovascular diseases

Cardiovascular diseases (CVDs) are a group of disorders affecting the heart and blood vessels and are still the leading cause of death globally, with around 15 million deaths per year causing immense health and economic problems worldwide (www.who.int/cardiovascular_diseases/publications/atlas_cvd/, accessed on 03 January 2018). In Germany, CVDs are the biggest killer (see Figure 1) with around 360 000 people dying in 2015 alone (www.destatis.de/DE/ZahlenFakten/GesellschaftStaat/Gesundheit/Todesursachen, accessed on 03 January 2018).

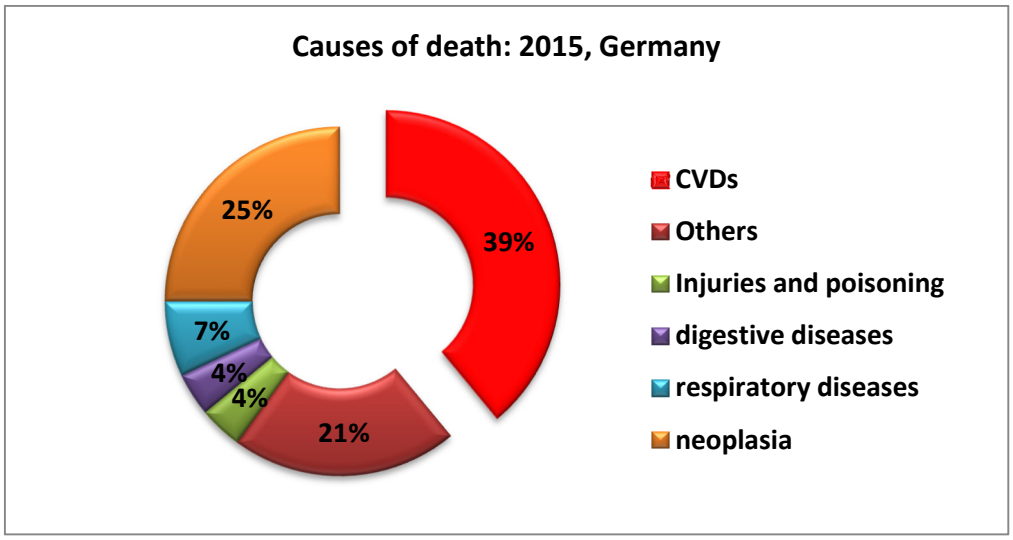

Figure 1: Causes of death in 2015.
Causes of death in 2015 in Germany. CVDs cause more than one third (39 %) of all deaths in Germany. (www.destatis.de/DE/ZahlenFakten/GesellschaftStaat/Gesundheit/Todesursachen, accessed on 03 January 2018)

CVDs include coronary artery disease, stroke, heart failure, cardiomyopathy, heart arrhythmia and many other disorders (http://www.who.int/cardiovascular_diseases/en/, accessed on 05 January 2018). It is well known that the risk of developing such conditions relates to lifestyle factors, for example diet, physical inactivity, tobacco and alcohol use. But the most important determinants of cardiovascular health, age and genetic predisposition, cannot easily be modified. It is thus important to understand the relationship of these factors with CVDs.

1.1.1 Ageing, the main risk factor for CVD

Increasing life expectancy and decreasing birth rates are leading to ageing societies worldwide (see Figure 2). This trend is likely to continue and a significant increase in people older than 64 is expected (http://ec.europa.eu/eurostat/statistics-explained/index.php/Population_structure_and_ageing, accessed on 03 January 2018).

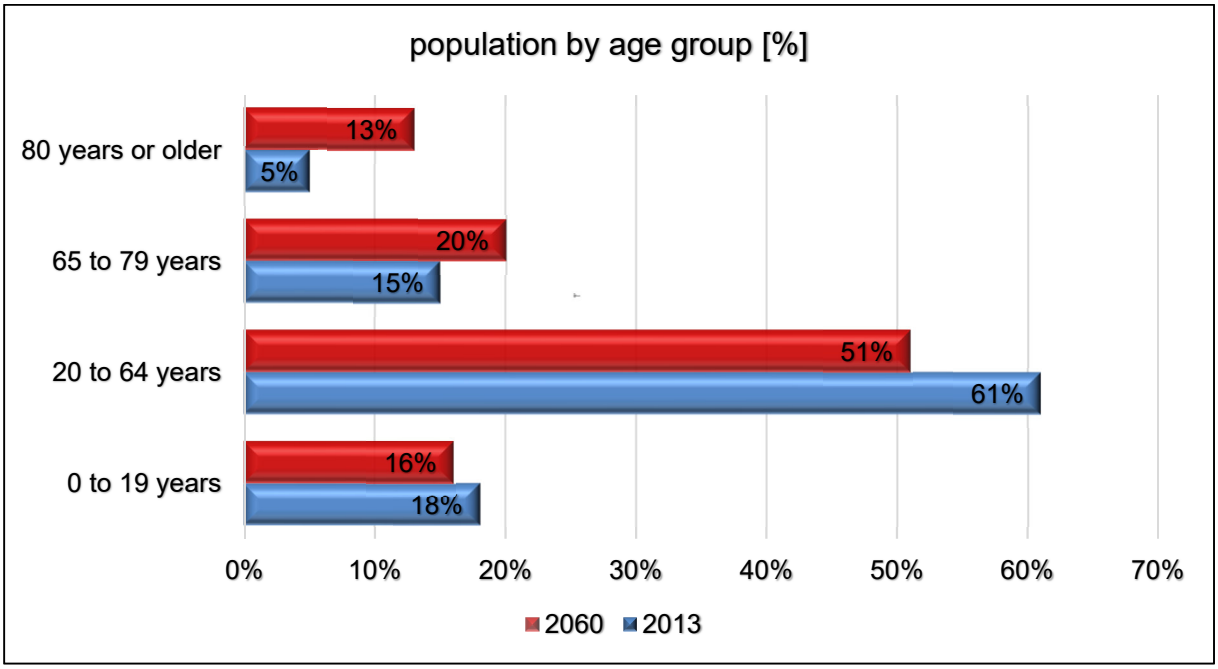

Figure 2: Estimated population by age group in 2060 compared to 2013 in Germany.
In 2013 about 20 % of the population was older than 64, whereas in 2060 the estimated percentage is increasing to one third. (www.destatis.de/EN/FactsFigures/SocietyState/Population/PopulationProjection/PopulationProjection.html, accessed on 03 January 2018)

These demographic changes can produce immense problems regarding health care systems and disease therapies. Age is a crucial risk factor for many human diseases, including the formation and progress of CVDs (Niccoli and Partridge 2012). Thus, it is important to understand the relationship between cardiac ageing and age-related heart diseases.

Ageing is a process in which physiological functions decrease and numerous molecular changes, such as altered gene expression and metabolite levels, somatic mutations, epimutations and accumulated molecular damage take place (Lee et al. 2017). The heart undergoes several structural changes, e.g. loss of a significant number of myocytes as a result of apoptotic and necrotic cell death (Pollack and Leeuwenburgh 2001). Several million myocytes of the ventricles get lost during the life span of humans beyond sexual maturity and the continuous loss leads to a decrease in cardiac mass (Olivetti et al. 1991). In rat models, myocyte cell death occurred as a function of age and affects several parts of the

heart, such as the left ventricle, the interventricular septum amd right ventricle free wall (Kajstura et al. 1996).

The size of the cardiomyocytes progressively increases and increased myocardial thickness can be observed. But the overall mass of the heart does not change in women and can even decrease in men, because the left ventricle shortens about 9 % in women and 11 % in men along its long axis, whereas the basal end-diastolic dimension remains unchanged. Due to such structural changes the overall shape of the heart alters from an elongated elliptical to a more spheroid shape (Olivetti et al. 1991, Hees et al. 2002). Additionally, an age-dependent increase in diastolic and systolic stiffness just as aortic stiffness has been shown and the latter is independent of mean blood pressure, or other risk factors and occurs in populations across many countries (Boss and Seegmiller 1981, Benetos et al. 2002). These changes have an important influence on cardiac wall stress, overall contractility and lead to a higher risk for cardiac disorders (Strait and Lakatta 2012).

Other deficits occurring in the process of ageing affect cardiac function, e.g. the diastolic filling rate progressively slows after the age of 20 years leading to an average reduction up to 50 % by 80 years old (Lakatta 2002). Maximal oxygen consumption declines, starting at age 20-30 and falling by approximately 10 % per decade (Strait and Lakatta 2012, Hawkins and Wiswell 2003). Although the cardiac system is capable of damage repair (Hees et al. 2002), regenerative capacity declines with age. Ageing is not itself the cause of heart failure, but age-related changes increase the probability of disease (Strait and Lakatta 2012). It is thus crucial to further investigate the connection between ageing and heart diseases and to improve preventive and therapeutic measures against these effects.

Since the heart functions within the context of whole body physiology, it is not possible to conduct full investigations *in vitro*. Therefore, it is currently necessary to generate animal models. For many reasons pigs are a suitable species with which to model heart diseases (for further details see 1.2.1).

1.1.1.1 models of ageing

Ageing is complex and heterogeneous and studying it can be challenging, especially if suitable *in vitro* and *in vivo* models are missing. Hence, even though human progeroid syndromes are relatively rare, they give valuable insights not only in the specific disease itself, but also into important mechanisms of ageing. Progeroid syndromes are a group of

genetic disorders characterised by shortened lifespan and premature and early appearance of clinical features that are normally associated with advanced age (Harkema et al. 2016). To examine the underlying mechanisms of ageing induced pluripotent stem cells (iPSCs) have been isolated from several progeroid syndromes and differentiated along multiple lineages (Carrero et al. 2016). Although, *in vitro* experiments can give some information about the process of ageing, *in vivo* studies are essential to understand the genetic pathways and the biological changes of the whole organism. Hence, model organisms, including *C. elegans* and mouse, have been established to elucidate underlying mechanisms of progeroid syndromes and age-related diseases. *C. elegans* represents a simple model organism that has given important insights into response mechanisms to age-related damages (Edifizi and Schumacher 2015). Nevertheless, mouse models are necessary to further understand the correlation between genomic maintenance and ageing. Findings showed that accumulation of DNA lesions during ageing is a major driver of ageing and age-related diseases. Defects in the nuclear envelope and DNA repair mechnaisms mainly cause progeroid syndromes (see Figure 3) (Carrero et al. 2016, Harkema et al. 2016).

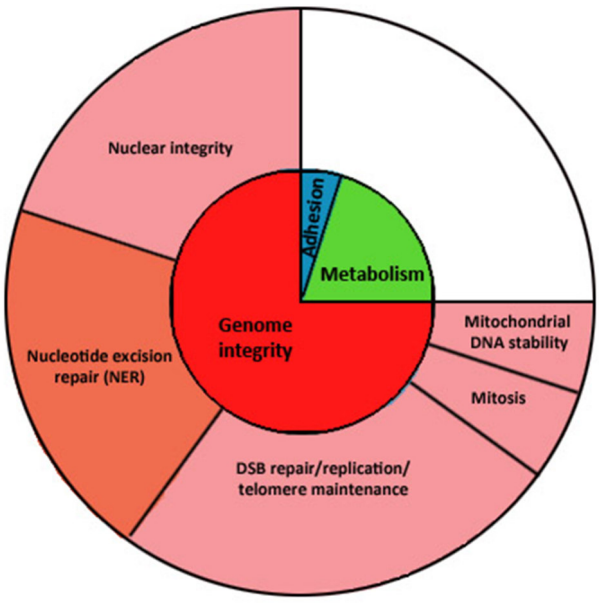

Figure 3: Main causes of progeroid syndromes.
20 human progeroid syndromes analysed and categorised by the primary effect of the genetic cause. Defects in the genome integrity are the major cause of progeroid syndromes (adapted from (Vermeij et al. 2016)).

As a result, several mouse models with mutations in genes important for DNA integrity have been generated. The following sections describe such mouse models. Additional model organisms mimicking ageing have been reviewed 2016 by Carrero and colleagues.

Mouse models of Hutchinson-Gilford progeria syndrome, e.g. *Zmpste24-null* (Zmpste24$^{-/-}$; zinc metallopeptidase STE24) mice, showed growth retardation, cardiomyopathy, muscular dystrophy, lipodystrophy, premature death and defects in DNA repair (Bergo et al. 2002, Pendas et al. 2002, Carrero et al. 2016). Whereas mice with mutations in the *Lmna* (lamin A) gene phenocopy the main clinical manifestations of the disease, such as shortened lifespan and bone and cardiovascular alterations (Osorio et al. 2011, Carrero et al. 2016).

Other mouse models have been generated for the Cockayne syndrome (Cs). This progeroid syndrome is associated with mutations in the *CSA* (Cockayne syndrome A ortholog or *ERCC8*) or *CSB* (Cockayne syndrome B ortholog or *ERCC6*) gene. Mutations in the *ERCC3*, *ERCC2* and *XPG* (Xeroderma pigmentosum, complementation group G or *ERCC5*) genes occur in patients that have symptoms of Cs but also show symptoms of xeroderma pigmentosum (xp), such as a severe photosensitivity and increased skin cancer risk (Karikkineth et al. 2017). All these genes encode proteins involved in DNA repair, more precisely in the nucleotide excision repair pathway (NER). Mouse models with mutations in the murine *Csb* (*Csb*$^{m/m}$) or *Csa* (*Csa*$^{-/-}$) gene represent mild cases of Cs, since they show symptoms such as motor dysfunction, cachectic dwarfism, loss of cells in the retina and sensorineural hearing loss, but no additional major neurodegenerative deficits (van der Horst et al. 1997, van der Horst et al. 2002, Karikkineth et al. 2017). Severe symptoms, such as profound neurodegeneration and early death could be observed in offspring of *Csb*$^{m/m}$ or *Csa*$^{-/-}$ mice that have been crossed with mice deficient in other NER-related genes, such as *Xpc* (Xeroderma pigmentosum, complementation group C) or *Xpa* (Xeroderma pigmentosum, complementation group A) (Laposa et al. 2007, Brace et al. 2013, van der Pluijm et al. 2007, Jaarsma et al. 2011).

Xeroderma pigmentosum is another example of a progeroid syndrome caused by mutations in NER genes. Mutations frequently occurring in xp patients have been generated in mouse models. The *Xpa*$^{-/-}$ and *Xpc*$^{-/-}$ mice show features of the disease, such as reduced lifespan and increased incidence of cancer (Melis et al. 2008). Other mice with a conditional knockout (KO) of the *Xpg* gene (*Xpg*$^{-/-}$) suffer from osteoporosis, retinal photoreceptor loss, liver ageing, extensive neurodegeneration and a short lifespan of 4-5 months (Barnhoorn et al. 2014). Patients with mutations in the *XPD* (Xeroderma pigmentosum, complementation group D) gene can either develop xp or trichothiodystrophy (TTD), depending on the site of

mutation (Taylor et al. 1997). A mouse model with mutations in the *Xpd* gene has been generated to mimick TTD. These mice show a remarkable extent of symptoms of the human disorder, such as brittle hair, developmental abnormalities, reduced lifespan, UV-sensitivity and skin abnormalities (de Boer et al. 1998). Other mouse models have mutations in the *Ercc1* (Excision repair cross-complementation group 1) gene (e.g. *Ercc1*$^{\Delta/-}$), which plays an important role in the NER pathway. These mice have the broadest spectrum of age-related pathologies recorded, including progressive frailty, a feature frequently observed in natural human ageing and their phenotype is most similar to age-related pathologies in human patients (Weeda et al. 1997, Vermeij et al. 2016). For further information see 1.1.1.2.3.

1.1.1.2 Excision repair cross-complementation group 1 (ERCC1)

1.1.1.2.1 Structure and Function

In 1983, the *ERCC1* gene was identified and the genomic DNA for *ERCC1* was the first human DNA repair gene cloned (Rubin et al. 1983, Westerveld et al. 1984a). The human *ERCC1* gene is located on chromosome 19, consists of ten exons, of which nine code for protein, and spans 15 kb. At least four different transcript variants are annotated, but there is only one transcript (www.ncbi.nlm.nih.gov/gene/2067; transcript variant 2 encoding isoform 2, accessed on 30 March 2018) encoding functional ERCC1 protein. The significance of the other transcripts is unknown (van Duin et al. 1986, van Duin et al. 1987).

The *ERCC1* gene encodes a protein that is involved in the NER pathway and recombinational processes and forms a heterodimer with the XPF (excision repair cross-complementation group 4) protein. It consists of 297 amino acids and has a calculated molecular weight of 32.56 kDa (van Duin et al. 1986, Sijbers et al. 1996). N-terminal deletion of the first 91 amino acids of *ERCC1* comprising almost one third of the protein has no effect on the correcting ability of the protein indicating that this region is not essential for NER or cross-link repair function. However, findings show that substitution of a single amino acid (C_{76} → W) within this region leads to a non-functional protein suggesting a role in protein folding (Sijbers et al. 1996). Residues 93-120 are required for the interaction with XPA protein, whereas the C-terminal end of the protein contains a helix-turn-helix structure and residues 224-292 are responsible for initial and stable binding to XPF (Li et al. 1994, de Laat et al. 1998). Intriguingly, loss of only the last five to seven amino acids of the C-terminal end already affects ERCC1 repair function indicating that these residues are important for XPF binding.

However, dramatically destabilisation of the protein does not occur in these cases (de Laat et al. 1998, Weeda et al. 1997).

The ERCC1 and XPF proteins have to form a stable heterodimer complex to function as an endonuclease. Analysis of the structure of the complex revealed that only XPF contains the nuclease domain, but it needs ERCC1 for nuclease activity (Tripsianes et al. 2005). Due to this function, the ERCC1-XPF complex is involved in several pathways, including interstrand crosslink repair, double-strand break (DSB) repair, telomere maintenance, homologous recombination and NER (Ahmad et al. 2008, Munoz et al. 2005, Al-Minawi et al. 2009, van Duin et al. 1986, Manandhar et al. 2015, Wood 2010).

Since DNA damage occurs constantly DNA repair mechanisms, such as the NER pathway, are crucial for the genome integrity. If helix disrupting DNA alterations appear, mostly induced by ultraviolet radiation or some mutagens, the NER pathway gets activated. In case of the global genomic NER pathway XPC-RAD23B (Xeroderma pigmentosum, complementation group C-RAD 23 homolog B) recognises the damage, binds to the DNA and TFIIH (transcription factor II Human, containing Xeroderma pigmentosum, complementation group B (XPB) and XPD), XPA and RPA (replication protein A) are recruited and DNA gets unwound (see Figure 4). The ERCC1-XPF complex binds and creates a 5` incision where the DNA strand departs 5` to 3` from the junction, whereas XPG generates a 3` incision. A 27-30 oligonucleotide is cut out and the gap is restored by repair synthesis factors (Evans et al. 1997, Volker et al. 2001, O'Donovan et al. 1994, Friedberg 2001). Transcription coupled NER takes place only at transcriptionally active genes and is initiated by the stalling of RNA polymerase II at a lesion (Hanawalt 2002). In both NER subpathways ERCC1-XPF and XPG generate incisions on the damaged DNA strand (Liu et al. 2010).

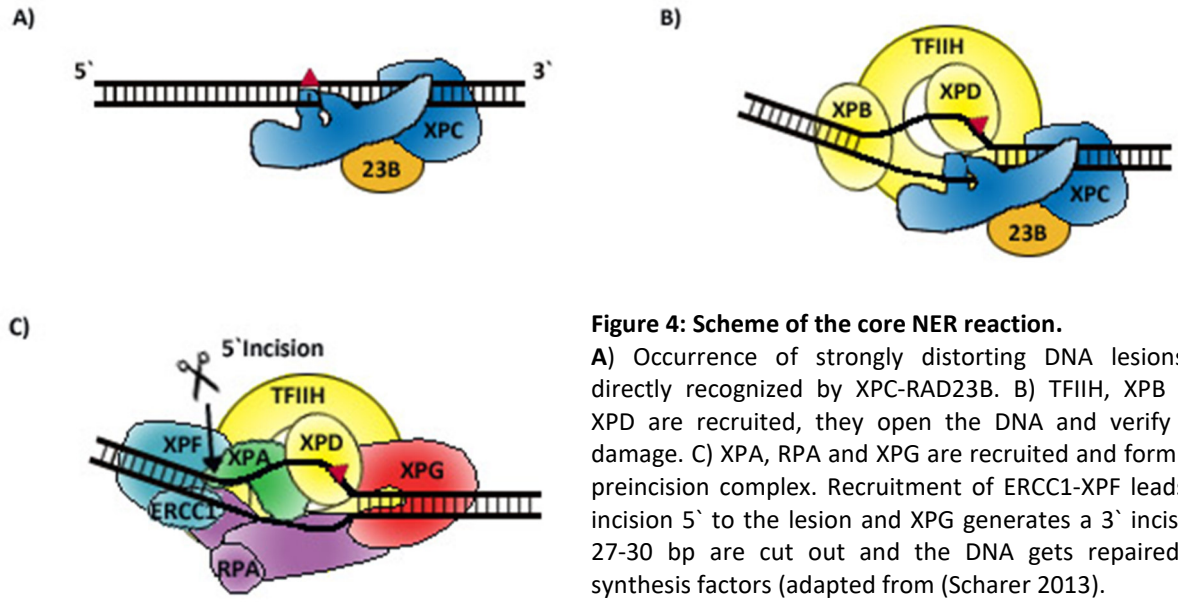

Figure 4: Scheme of the core NER reaction.
A) Occurrence of strongly distorting DNA lesions is directly recognized by XPC-RAD23B. B) TFIIH, XPB and XPD are recruited, they open the DNA and verify the damage. C) XPA, RPA and XPG are recruited and form the preincision complex. Recruitment of ERCC1-XPF leads to incision 5` to the lesion and XPG generates a 3` incision. 27-30 bp are cut out and the DNA gets repaired by synthesis factors (adapted from (Scharer 2013).

1.1.1.2.2 ERCC1 defects in human

Although the *ERCC1* gene was the first mammalian repair gene to be cloned (Westerveld et al. 1984b) and many photosensitive patients have been screened over decades the first patients with *ERCC1* mutations have only been identified in 2007. Hence the gene has a different nomenclature than the standard XP nomenclature (XP-x) (Gregg et al. 2011). Only three patients with defects in the *ERCC1* gene have been reported. In 2007 the first patient was discovered with compound heterozygous mutations in the *ERCC1* gene suffering from cerebro-oculofacio-skeletal syndrome, a rare disorder in which patients undergo rapid neurologic decline. The patient had severe pre- and postnatal developmental failures, including microcephaly and neurological alterations (Jaspers et al. 2007). The second patient with different compound heterozygous mutations developed neurological symptoms beginning at the age of 15 and he died by the age of 37 due to severe neurodegeneration resulting in dementia and cortical atrophy (Gregg et al. 2011). The third and last patient was homozygous for the mutation, which also occured on one allele of the first patient, showed neurological and skeletal abnormalities and died at the age of 2.5 years (Kashiyama et al. 2013).

The fact that there are only three known individuals having mutations in the *ERCC1* gene, the severe phenotype of these patients, and findings in mouse models all indicate that the gene is a crucial and rate-limiting factor in the NER pathway (Weeda et al. 1997).

Platinum based chemotherapeutics, such as cisplatin, are extensively used to treat several cancer types, e.g. breast, prostate, ovarian and others. The application of platinum compounds results in several forms of DNA damage, such as bulky lesions and intrastrand crosslinks, which are removed by the NER pathway (McNeil et al. 2015). Hence, the ERCC1-XPF complex interferes with the chemotherapeutics and its inhibition together with chemotherapeutics can increase the efficiency of the treatment of some cancers (Arora et al. 2010).

1.1.1.2.3 Mouse models

Different mouse models have been generated and provided important insights into the function and role of the *ERCC1* gene. The first *ERCC1*-deficient mouse model has been produced by disrupting exon five. This mutation leads to a truncated transcript version lacking the last four exons where the XPF interaction domain is located (McWhir et al. 1993). Homozygous mice (*Ercc1*$^{-/-}$) have been runted at birth and showed progressive damage in the liver from polyploidy, progressing to aneuploidy and died before weaning with liver failure (McWhir et al. 1993).

Another group has generated two types of mouse strains. One knockout strain (*Ercc1*$^{-/-}$) lacked exon seven leading to an abortion of the helix-hairpin-helix motif necessary for binding of XPF. The other strain had a truncated *Ercc1* allele (*Ercc1*^{*292} or *Ercc1*$^{\Delta 7}$) at the C-terminus leading to a protein lacking the last seven amino acids (Weeda et al. 1997). No *Ercc1* mRNA was detected in knockout strains, whereas *Ercc1*^{*292} mice showed normal levels of mRNA. This indicates that the knockout allele is transcriptionally inactivated, whereas the *Ercc1*^{*292} allele is still transcribed. Nevertheless, each mutation has a dramatic effect on NER indicating that Ercc1 function is dependent on dimerisation. Both strains showed the same liver abnormalities and severe runting, as reported previously (McWhir et al. 1993, Weeda et al. 1997). But the main phenotypic difference was the lifespan of the two strains. *Ercc1* knockout mice all died before day 38, whereas *Ercc1*^{*292} mice lived up to six months (Weeda et al. 1997).

Mice with a combination of the mutant alleles (*Ercc1*$^{-/\Delta 7}$) have been compared with their wt siblings, to investigate age-related symptoms. The *Ercc1*$^{-/\Delta 7}$ strain showed a much smaller body size, the median life span was markedly reduced compared to wildtype siblings (20 and 118 weeks) and multiple signs of ageing, such as a decline in whole body and organ weight,

numerous histopathological lesions, e.g. abnormal nuclear morphology and intranuclear cytoplasmic inclusions of liver cells and changes in immune parameters were observed. Studies of their complete life span revealed that nearly all age-related changes occurred to some extent in DNA repair proficient wt mice, but in *Ercc1*$^{-/\Delta 7}$ mice age-related changes occur much faster confirming the use of these mice for studies of ageing (Dolle et al. 2011).

Since these mouse models are very short lived they lack symptoms of xp, for instance the increased incidence of skin cancer. To overcome this problem, the liver phenotype was corrected using a transgene that was under the control of a liver-specific gene promotor. Nevertheless, these mice died after eight to twelve weeks with kidney and additional abnormalities (Selfridge et al. 2001).

Another approach was the skin-specific knockout of the *Ercc1* gene using the Cre-lox system to generate a model of UV-induced skin cancer. After crossing of *Ercc1*$^{flox/-}$ mice with transgenic mice expressing Cre recombinase under the control of the bovine keratin five promotor 100 % knockout of the *Ercc1* gene was achieved in the epidermis. Mice with *Ercc1* deficiency in the skin had normal viability, have been hypersensitive to short-term effects of UV irradiation and UV irradiation-induced skin cancer and developed actinic keratosis and squamous cell carcinomas (Doig et al. 2006).

All these mouse models showed that mutations in the *Ercc1* gene lead to severe phenotypes indicating the importance of the gene not only in the NER pathway. Nevertheless, mouse models have limitations, e.g. due to their short lifespan they are less suitable for longitudinal studies, which are crucial for studies of ageing.

1.1.2 Hypertrophic cardiomyopathy (HCM)

Besides molecular ageing natural mutations can result in a predisposition to cardiac failure. One of these is HCM, a myocardial disease in which a part of the heart muscle (myocardium) is enlarged (hypertrophic) causing functional impairment, such as diastolic dysfunction. In this disorder abnormal, increased size of myocytes leads to left ventricular thickening, the muscle cell arrangement is disorganised as opposed to a normal parallel myocyte pattern (myocardial disarray) and increased interstitial fibrosis can occur (Putinski et al. 2013, Sabater-Molina et al. 2018)

The disease develops without an obvious, identifiable cause and is relatively common, estimated as 1:500 in the general population (Hensley et al. 2015). Although HCM is frequently asymptomatic some patients develop severe systolic dysfunction, heart failure and it is the leading cause of sudden cardiac death in young adults (Maron and Maron 2013). HCM is a genetic disorder being transmitted in an autosomal dominant manner with variable expression and is caused by heterozygous mutations in one of several genes encoding components of the cardiac sarcomere. More than 1440 mutations in at least 11 genes have been found to cause HCM, with mutations in the *MYH7* (myosin heavy chain) and *MYBPC3* (cardiac myosin-binding protein C) genes responsible for 75- 80 % of cases (Hensley et al. 2015).

The loci heterogeneity influences the severity of HCM leading to a wide range of clinical outcomes from asymptomatic, mildly symptomatic to sudden cardiac death. This makes diagnosis difficult and HCM is usually detected incidentally or after diagnosis of a family member with sudden cardiac death. Identification of the disorder relies on physical examination, two-dimensional echocardiography, electrocardiography (ECG), family history and analysis of specific mutations. For example, mutant forms of *MYBPC3* can be identified by genetic testing (Carrier et al. 2010).

Current therapies to treat HCM use pharmacological agents or surgical interventions. Nevertheless, the treatments can only relief the symptoms, but fail to address and correct the cause of the disease (Mohamed et al. 2017). In the absence of alternative treatments other than heart transplant, gene therapy is a realistic option to treat HCM.

Since *MYBPC3* is frequently mutated in HCM several gene therapies concentrate on this gene. One group showed the possibility to correct *MYBPC3* mutations in human preimplantation embryos by gene editing using the CRISPR/Cas9 system (clustered regularly interspaced short palindromic repeat/CRISPR-associated protein 9) (see section 1.2.2.2). Precise DSBs have been introduced at the mutant paternal allele inducing an endogenous homology-directed repair (HDR) mechanism, exclusively directed by the maternal wt allele as a repair template. Although targeting efficiency was high, drawbacks, such as indels resulting from non-homologous end joining (NHEJ) and mosaicism display serious safety issues, which must be overcome before clinical application can be considered (Ma et al. 2017).

Other approaches use mRNA-based therapies for the treatment of HCM. It was shown that antisense oligoribonucleotides could induce exon skipping in *Mybpc3* mutated mice leading to modified in-frame mRNA and protein (Gedicke-Hornung et al. 2013). Furthermore, the cardiac isoform of the myosin-binding protein C (cMyBP-C) of *Mybpc3* mutated mice could be repaired by inducing 5`-*trans*-splicing between the mutant endogenous *Mybpc3* pre-mRNA and an engineered pre-*trans*-splicing molecule carrying wt *Mybpc3* complementary DNA (cDNA) (Mearini et al. 2013). Additionally, a single dose administration of adeno-associated virus (AAV) with full-length *Mybpc3* was sufficient to prevent the disease phenotype in *Mybpc3* mutated mice and to suppress production of mutant mRNA species (Mearini et al. 2014).

These RNA-based therapies are promising, but mice have many physiological differences to humans and it is possible that rodents respond differently to these therapies than humans. For this reason, further analysis of positive and negative effects is necessary in species that are more similar to humans. Pigs are currently the best option to model heart diseases, because they resemble humans in body size and the anatomy and physiology of many organs, including the heart. Pigs are thus better suited to establish clinical procedures and therapies designed for humans, than mice whose hearts are far smaller (Flisikowska et al. 2013). A porcine model with a truncating mutation in the *MYBPC3* gene would thus be useful.

1.1.2.1 MYBPC3

1.1.2.1.1 Structure and Function

The human *MYBPC3* gene is located on chromosome 11p11.2 and encodes the cMyBP-C, which is expressed exclusively in the heart muscle. Two other myosin-binding protein C isoforms are expressed in skeletal muscle and encoded by *MYBPC1* and *MYBPC2* (Fougerousse et al. 1998). The genomic sequence is more than 21 kb in size, contains 35 exons, 34 of which are coding and two exons are unusually small, three nucleotides each (Carrier et al. 1997). Three different transcript variants are known, but all encode the same 140.78 kDa protein comprising 1274 amino acids (www.ensembl.org/index.html, accessed on 22 August 2018).

The cardiac myosin-binding protein C is a component of the sarcomere (see Figure 5 A) and plays an important role in maintaining cardiac muscle structure. The protein is a member of

the intracellular immunoglobulin superfamily and consists of eight immunoglobulin-like and three fibronectin-like domains. The cardiac isoform has a unique myosin-binding motif (m-domain) with multiple phosphorylation sites. This motif is believed to alter actomyosin interactions in the heart through interactions with actin (Carrier et al. 1997, Carrier et al. 2015, Howarth et al. 2012).

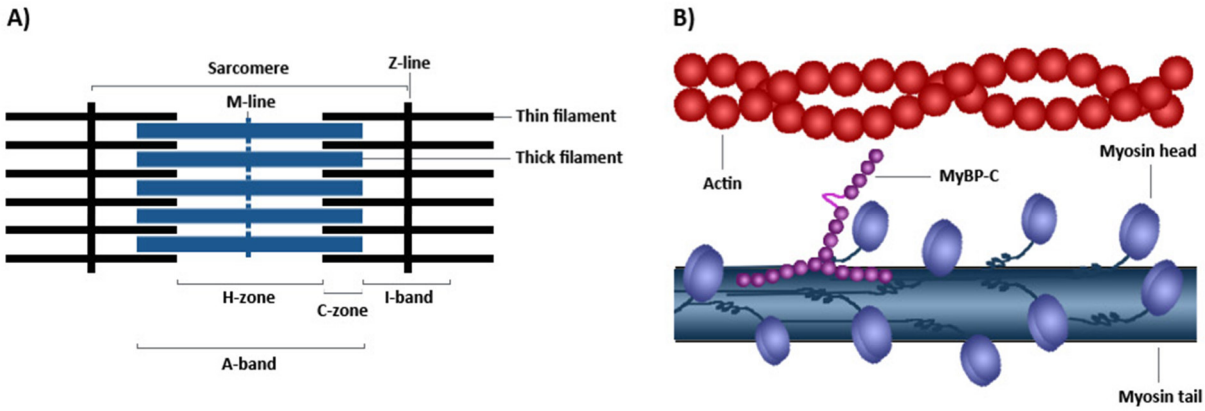

Figure 5: Localisation of the cardiac MyBP-C protein in the sarcomere of the heart muscle.
A) Schematic organisation of sarcomeres. Actin-containing thin filaments are anchored at Z-lines and myosin-containing filaments are anchored at the M-line (adapted from (Carrier et al. 2015). B) Schematic structure of the C-zone of sarcomeric A-bands. Cardiac MyBP-C protein is located in this region and interacts with both, myosin (thick) and actin filaments (adapted from (Tajsharghi 2008)).

Although sarcomere formation during embryogenesis is not dependent on cMyBP-C its absence is sufficient to trigger profound cardiac hypertrophy and impaired systolic and diastolic function (Harris et al. 2002). Since it interacts with both the thick and thin filament (see Figure 5 B) it is likely that cMyBP-C regulates and coordinates the positioning of myosin and actin. In this way, it seems to constrain actin-myosin interaction and as a consequence ultimately power output is limited. cMyBP-C contributes to the regulation of cardiac contraction at short sarcomere length and it is required for complete relaxation in diastole (Carrier et al. 2015).

The interactions of cMyBP-C with its binding partners depend on post-translational modifications. At least three phosphorylation sites (Ser273, 282 and 302 in the mouse sequence) are positioned in the MyBP-C motif (M motif). Phosphorylation takes place in a hierarchical order, starting with Ser282, triggering a change of confirmation to make Ser273 and Ser302 more accessible (Sadayappan et al. 2011). Another phosphorylation site at Ser133 in human cMyBP-C (mouse Ser131) has been found outside the M motif (Kuster et al. 2013). The phosphorylation status of cMyBP-C influences its binding characteristics and is

crucial for myofilament binding, sarcomere morphology and myocyte alignment. Interestingly, overall phosphorylation levels are markedly reduced in human and experimental heart failure (El-Armouche et al. 2007).

These findings give an idea of the function and role of the cMyBP-C, but the precise role of the protein and the underlying mechanisms leading to HCM remain to be elucidated.

1.1.2.1.2 MYBPC3 Mutations leading to HCM

More than 350 individual *MYBPC3* mutations have been found to cause HCM, many of which (>60 %) are insertions, deletions or nonsense mutations, resulting in a frameshift and/or premature termination codon and splicing or branchpoint mutations. All these mutations are expected to produce C-terminal truncated cMyBP-C missing binding sites for myosin and/or titin (Carrier et al. 2015). Among these, founder mutations of *MYBPC3* were observed. These are specific mutations that represent a large percentage of HCM cases and occur in some populations from different countries (Carrier et al. 2015). Examples of founder mutations can be found in Table 1.

Table 1: Founder mutations of *MYBPC3* gene causing HCM, identified in some countries and populations.

Country	F[1]	Mutation[2]	Location	Consequence
Iceland	58 %	c.927-2A>G	Intron 11	PTC in exon 13
Italy, Veneto	19.5 %	c.912-913delTT	Exon 11	PTC in exon 12
The Netherlands	17 %	c.2373-2374insG	Exon 24	PTC in exon 25
Finland	17 %	c.3183C>T	Exon 29	PTC in exon 29
Japan	16 %	c.1775delT	Exon 18	PTC in exon 19
Italy, Tuscany	14 %	c.772G>A	Exon 6	PTC in exon 9
France	8.4 %	c.1928-2A>G	Intron 20	PTC in exon 22
The Netherlands	2.6 %	c.2827C>T	Exon 27	PTC in exon 27
The Netherlands	1.6 %	c.2864-2865delCT	Exon 27	PTC in exon 29

PTC: premature termination codon
[1] frequency of the mutation, expressed as total number of cases with HCM
[2] cDNA nomenclature, considering the A of ATG codon as 1
(adapted from (Carrier et al. 2015))

Although all of these mutations are truncating several studies showed that no truncated protein is detectable. Furthermore, full-length protein expression level was 20-30 % lower than in healthy individuals or HCM patients with mutations in other genes. These findings

indicate that haploinsufficiency is the main pathogenic mechanism for *MYBPC3* truncating mutations (Marston et al. 2012).

Since detection of truncated protein was not possible and expression of full length protein is reduced it is likely that either the mutant mRNA or the protein is unstable and one *MYBPC3* allele cannot compensate the loss. The ubiquitin-proteasome system and the autophagy-lysosome pathway are presumed to regulate degradation of mutant cMyBP-C and nonsense-mediated mRNA decay (NMD) for elimination of aberrant mRNA. The detailed process in which *MYBPC3* haploinsufficiency leads to the disease phenotype has not been fully elucidated (Vignier et al. 2009, Carrier et al. 2010, Carrier et al. 2015).

1.1.2.1.3 Mouse models for HCM

Several mouse models have been generated and provided important insights into the role of *MYBPC3* and the progress of HCM. Different homozygous (*Mybpc3*$^{-/-}$) and heterozygous (*Mybpc3*$^{-/+}$) knockout strains have been viable, fertile, lived for more than one year, showed normal offspring numbers and inheritance of the mutant allel was consistent with Mendelian ratios (Carrier et al. 2004, Harris et al. 2002, Chen et al. 2012). *Mybpc3*$^{-/-}$ mice and mice that express a truncated protein lacking titin and myosin binding site developed significant cardiac hypertrophy, showed elevated left ventricle-to-body weight, myocyte disarray and interstitial fibrosis (McConnell et al. 1999, Harris et al. 2002, Carrier et al. 2004). *Mybpc3*$^{-/+}$ KO mice have either not been distinguishable from wild-type littermates (Harris et al. 2002) or developed significant asymmetric septal hypertrophy at 10-11 months of age without impairment of left ventricle function (Carrier et al. 2004). Different mouse models carrying a *Mybcp3* transgene lacking a myosin binding site (Yang et al. 1999) or lacking both the titin and myosin binding sites (Yang et al. 1998) resembled the relatively benign clinical condition of patients with similar mutations. They exhibited a mild phenotype with no apparent heart enlargement and myocardium wall thickening, but subtle alterations in force production have been observed. Mice with a *Mybcp3* N-terminal deletion showed no evidence of HCM, but it is believed that N-terminal domains are important to effectively regulate cardiac-muscle contraction at the cross-bridge level (Witt et al. 2001). Another strain mimics a mutation very common in Italy (see Table 1) having a G>A transition on the last nucleotide of exon 6. Homozygous mice suffered from myocyte and left ventricle hypertrophy, whereas heterozygotes had no major phenotype (Vignier et al. 2009).

All these mouse models showed many similarities with human HCM patients and have provided important information about the *MYBPC3* gene and HCM. For example, they demonstrated that cMyBP-C is not essential for sarcomere formation during embryogenesis, but is important for sarcomere organisation and regulating systolic and diastolic function (Carrier et al. 2004, Harris et al. 2002, Chen et al. 2012). Nevertheless, developing therapies, testing of novel drugs and surgical methods is difficult in such small animals. Therefore, a large animal model would be a useful resource to investigate novel treatment options.

1.2 Large animal models

1.2.1 The need for large animal CVD models

The cardiovascular system is complex and difficult to investigate outside the context of the whole body. Hence, animal models are a valuable tool for the research of heart diseases. A suitable model system should represent the biology of human diseases, should be easy to manipulate, generated with low costs, possible to reproduce and ethically accepted. Mice are the most common animal species used to develop models of human disease. However, their small size, short lifespan and anatomical differences to humans are often disadvantages and this applies to heart surgery and therapy for age-related diseases. E.g. the major difference in heart size between mice and humans make experimental infarct models unreliable (Camacho et al. 2016). Although, manipulation of large animal models, such as pigs and non-human primates, often is more difficult and expensive, they offer certain advantages, because of their similarities in genetic, structure, function and diseases compared to humans (Camacho et al. 2016). Furthermore, regulatory authorities are now requiring data from species other than rodents before approving new drugs and therapies (e.g. the US Food and Drug Administration FDA, www.fda.gov/AboutFDA/Transparency/Basics/ucm194932.htm, accessed on 20 January 2018).

Several large animals, such as dog, sheep, pig, non-human primates, cattle and horses have been used to mimic certain types of heart diseases and to develop methods for myocardial regeneration, such as the use of a biologically derived extracellular matrix to regenerate the myocardium (Cui et al. 2005, Camacho et al. 2016). While non-human primates show the greatest similarities with humans, they are difficult and expensive to maintain and raise serious ethical issues. As mentioned previously, pigs are currently the best option to model

heart diseases, because of the high degree of similarity with human myocardium (Flisikowska et al. 2013). Porcine hearts have slightly faster *in vivo* contractile and relaxation kinetics compared to humans. Pigs can increase their heart rates from approximately 89-117 bmp at rest to 259-306 bpm during exercise. This increased heart rate of 128-219 % is very similar to the 140-170 % in humans. In comparison rodents have adapted to function at very high basic heart rate and the increase is only 40-50 % for rats and 20-40 % for mice (Milani-Nejad and Janssen 2014). Furthermore, the high heart/body weight ratio of pigs is similar to humans (Lelovas et al. 2014). As a consequence, pigs have long been used for experimental heart surgery, xenotransplantation and to model heart diseases (Reemtsma 1995, Manji et al. 2015, Flisikowska et al. 2013).

Different techniques regarding heart surgery have been evaluated and optimised in wt pigs. Among others, are examples of aortic stent grafts or cardiac plugs, which where applied and tested in porcine models (Johannes et al. 2012, Igor Rafael et al. 2011, Ferrari et al. 2015, Ferrari et al. 2017, de Beaufort et al. 2017). Another application of large animals in heart surgery is the use of porcine tissues for xenotransplantation, e.g. human valves of patients can be replaced by porcine valves (Manji et al. 2015, Myken and Bech-Hansen 2009). Genetically modified pigs that lack expression of the low density lipoprotein receptor can be used to investigate mechanisms and therapies of coronary atherosclerosis (Huang et al. 2017, Ogita et al. 2016).

Furthermore, pigs are used to induce myocardial infarction or ischemia by different surgery methods. These models contribute to the understanding of the pathophysiological mechanisms underlying these disorders and can be used to optimise treatment and surgery (Klocke et al. 2007, Keeran et al. 2017). Nevertheless, young patients respond differently to surgery and therapy than older individuals (Wang et al. 2014). Thus, a porcine model of an old heart would be a valuable tool to develop new therapies for age-related heart diseases.

Although HCM is a common disease in domestic cats (Freeman et al. 2017) and these cats could be used as a large animal model, pigs are preferable models. Feline models of HCM are not only limited due to the fact that in the majority of cats with HCM no genetic etiology has been identified, but also because of the reasons mentioned above, such as differences in physiology.

1.2.2 Generation of genetically modified animals

1.2.2.1 Reproductive technologies

In 1980 transgenic mice carrying foreign DNA sequences have been generated by microinjection of DNA into pronuclei of fertilised mouse oocytes (Gordon et al. 1980). Subsequently, first transgenic pigs, sheep and rabbits have been generated using the same procedure (Hammer et al. 1985). But high lipid levels in the cytoplasm of porcine eggs lead to high opacity and identification of nuclei is very difficult (Hammer et al. 1985). Additionally, the basic method only allows random transgene integrations, which is less precise compared to more recent methods such as gene targeting (see below) (Bouabe and Okkenhaug 2013). Most importantly, the procedure is inefficient regarding the proportion of transgenic animals produced (Pursel et al. 1989).

Genetic modification of mice radically changed and got easier by the development of gene targeting via homologous recombination (HR) in mouse embryonic stem (ES) cells (Thomas and Capecchi 1987). However, fully functional embryonic stem cells capable of contributing to the germline of any livestock species have not been generated (Nowak-Imialek and Niemann 2012). To solve this problem alternatives to ES cells had been searched for and nuclear transfer from primary somatic cells, transfected and analysed *in vitro*, had been developed and used (Schnieke et al. 1997, McCreath et al. 2000). The method was first established in sheep but soon it was applied to pigs and became the standard technique to generate genetically modified pigs (Lai et al. 2002).

Gene targeting via HR allows the introduction of exogenous DNA in a site-specific manner. HR takes places in all forms of life and is a DNA repair and recombination mechanism, where two similar or identical nucleotide sequences are exchanged between DNA molecules. Not only DNA double-stranded breaks, DNA gaps and DNA interstrand crosslinks can be repaired this way (Li and Heyer 2008), but it also enables genetic variation during meiosis (Grelon 2016). Transgenes or distinct mutations can be introduced via HR using a targeting vector that includes homologous regions flanking the region to be exchanged. Other elements, which are described in the next paragraph, can be added to a targeting vector to enrich positive targeted cells or avoid negative effects of vector elements.

Adding resistance genes, such as the neomycin resistance gene (neo) or puromycin (puro), enables selection of cells for a specific event. One possibility is to add a resistance gene with

all necessary elements for gene expression to a vector and select cells positive for transfection of the specific vector. Another possibility is to use a promotor trap targeting vector. The targeting vector carries a drug resistance gene lacking a promotor, therefore expression of the selection factor is dependent on correct site-specific targeting (Bouabe and Okkenhaug 2013, Gossler et al. 1989).

Some elements of a targeting vector, e.g. the resistance gene, can affect expression of neighbouring genes (Meier et al. 2010). In these cases, such elements can be removed by the use of recombinases, e.g. Cre or Dre, which cut out regions flanked by their specific recognition sites (loxP, rox) (Sauer and Henderson 1988, Sauer and McDermott 2004).

This system is not only helpful for removing disturbing elements, but site-specific recombination allows many forms of structural alterations. By flanking any DNA sequence of interest, it is possible to delete the specific part. If the recombinase is expressed under control of a cell type-, or tissue-specific promotor deletion can be controlled spatially. The expression of a site-specific recombinase can be restricted and controlled for example by using either an inducible promotor or a promotor that is active at a particular developmental stage of tissues or cells (Bouabe and Okkenhaug 2013).

Another way to transiently express the recombinase is to deliver it using tissue-specific AAVs. With this method possible adverse effects from stable recombinase expression can be avoided and deletion can be controlled timely or spatially (Kaspar et al. 2002, Werfel et al. 2014).

However, HR of a targeting vector into a genomic locus occurs at a much lower frequency than random integration and it is much less efficient in primary somatic cells than in mouse ES cells (Porteus 2007). This is where genome editing enabled new ways of gene manipulation and helped to simplify genetic manipulations.

1.2.2.2 Genome editing

Genome editing is the controlled manipulation and targeting of a genome by the use of tailor made endonucleases, with which specific changes, mostly insertions, deletions or replacement of DNA, are introduced in the genome of a cell or organism (Lee et al. 2016). Synthetic and highly specific endonucleases introduce a single-, or double-strand break at the site of interest. DNA repair mechanisms get activated and the DSBs can be repaired by

HDR or NHEJ. In the case of HDR a homologous template is used to precisely repair the broken region. The error prone mechanism of NHEJ indeed, religates the DSB and insertions or deletions (indels) are possible (Kramer et al. 1994, Moore and Haber 1996). NHEJ enables gene inactivation by indels resulting in a frameshift and premature stop codon. HDR on the other hand makes it possible to insert any exogenous DNA of interest by flanking it with homolougous regions (see Figure 6).

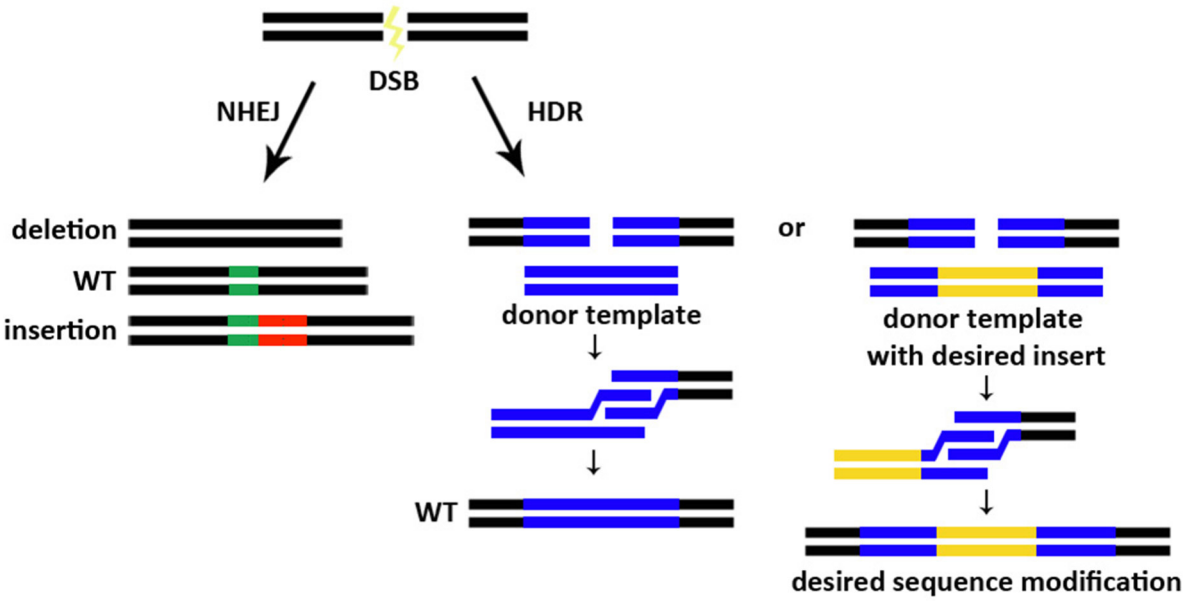

Figure 6: Repair mechanisms of DNA double-strand breaks.
By using the HDR mechanism it is possible to insert any desired sequence in a specific locus. (Adapted from (Sander and Joung 2014)).

Among others zinc finger nucleases (ZFN) (Bibikova et al. 2001) and transcription activator-like effector nucleases (TALENS) have been established, improved and used to manipulate mammalian genes (Miller et al. 2011, Carlson et al. 2012). The newest and most popular tool for genome editing is the CRISPR/Cas9 system. Several advantages such as less off-target effects, simple and cheap production and high efficiency ensured that CRISPR/Cas9 within a few years became the standard technique of genome editing (Mali et al. 2013, Zhou et al. 2015).

CRISPR and associated Cas genes have been found in procaryotes and represent a RNA-based adaptive immune system to target and destroy viruses (Barrangou et al. 2007). By adapting the system, genome editing in mammals became possible. To introduce DSBs two components have to be expressed a guide RNA (gRNA) consisting of CRISPR RNA (crRNA) fused with trans-activating crRNA (tracrRNA) and a Cas9 protein containing a nuclear

localisation signal (see Figure 7). The crRNA consists of 20 nucleotides, is designed to be complementary to a distinct genomic region and a protospacer adjacent motif (PAM), a three bp sequence specific for the Cas9 protein, which has to directly follow the DNA sequence targeted by Cas9. Whereas the crRNA determines the specifity of the gRNA the tracrRNA forms a scaffold that is necessary for the Cas9 protein to bind and cleave the target DNA (Mali et al. 2013, Garside and MacMillan 2014, Sander and Joung 2014).

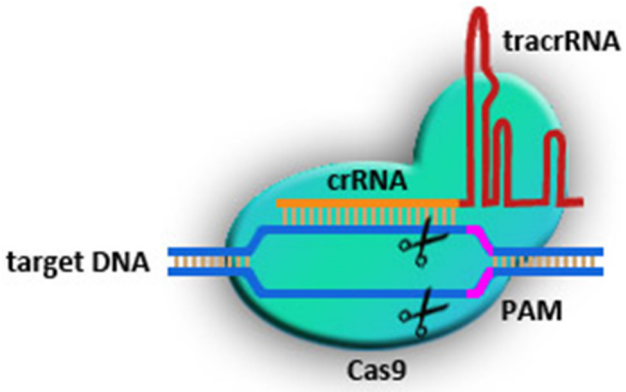

Figure 7: Schematic overview of genome editing by CRISPR/Cas9 system.
The gRNA consisting of crRNA and tracrRNA binds to DNA sequence and Cas9 is directed to the target site. The PAM motiv downstream of the gRNA binding region is crucial for binding and cleavage of Cas9 (adapted from (Ding et al. 2016)).

1.3 Goal

The aim of the PhD project was to generate genetically modified pigs which model two major risk factors for heart disease, ageing and genetic predisposition.

Most therapeutic interventions including heart surgery are being carried out in older patients where age related changes have occurred. To mimic this in a physiologically relevant animal model pigs were to be generated with a locally aged organ, the heart, by reducing its capacity for DNA repair. *ERCC1* is an essential component of the DNA repair machinery in eukaryotic cells. Modulating its activity in mice results in animals with early onset of age-related changes and a reduced lifespan. To avoid such a severe phenotype in pigs either a conditional *ERCC1* knockout where to be introduced into the porcine genome or a truncation of the last 7 amino acids of the *ERCC1* gene. Based on its function in double-strand break DNA repair and homologous recombination it was assumed that targeting the *ERCC1* gene might be challenging, but it had been successful in mice albeit with very low efficiency and by aiming to only mutate one allele ERCC1 function should not be abolished.

The second model aims at mimicking the genetic myocardial disease, hypertrophic cardiomyopathy (HCM), which in severe form can cause death in infancy. *MYBPC3* is frequently mutated in HCM and several gene therapies concentrate on this gene. It was therefore decided to introduce two common human mutations (Italian and Dutch mutation) into the porcine genome.

For both models the genetic modifications were to be introduced into the endogenous gene loci of porcine primary cells. Cell clones could then be used to generate piglets by somatic cell nuclear transfer.

2 Material and Methods

2.1 Material

2.1.1 Chemicals

Acetic acid	AppliChem, Darmstadt, GER
Advanced Protein Assay Reagent	Cytoskeleton, Denver, USA
Agarose	Sigma-Aldrich, Steinheim, GER
Ammonium persulfate (APS)	Carl Roth, Karlsuhe, GER
Boric acid	AppliChem, Darmstadt, GER
Bromphenol blue	Sigma-Aldrich, Steinheim, GER
Chloroform (99,8 %)	Sigma-Aldrich, Steinheim, GER
Clarity™ Western ECL Substrate	Biorad Laboratories, Munich, GER
Deoxynucleotide (dNTP) solution mix	New England Biolabs, Frankfurt, GER
DEPC-treated water	Thermo Fisher Scientific, Waltham, USA
Dithiothreitol (DTT)	Omnilab-Laborzentrum, Bremen, GER
Ethylenediaminetetraacetic acid (EDTA)	AppliChem, Darmstadt, GER
Ethanol (EtOH) absolute	Fisher Scientific, Loughborough, UK
Ethidium bromide	Sigma-Aldrich, Steinheim, GER
Formaldehyde solution 37 %	AppliChem, Darmstadt, GER
Glycerol anhydrous	AppliChem, Darmstadt, GER
Glycine	Carl Roth, Karlsruhe, GER
Hydrogen chloride 37 % (HCl)	Sigma-Aldrich, Steinheim, GER
Isopropyl β-D-1-thiogalactopyranoside (IPTG)	Bioline, Luckenwalde, GER
Magnesium chloride hexahydrate	Carl Roth, Karlsruhe, GER
Methanol (MeOH)	Sigma-Aldrich, Steinheim, GER
Milk powder	Carl Roth, Karlsruhe, GER
Nicotinamide adenine dinucleotide hydrate (NAD)	Sigma-Aldrich, Steinheim, GER
PEG-8000	Sigma-Aldrich, Steinheim, GER
Phenol:Chloroform:Isoamylalcohol (25:24:1)	AppliChem, Darmstadt, GER
PhosSTOP™	Roche, Mannheim, GER

Ponceau S	Sigma-Aldrich, Steinheim, GER
Propan-2-ol (isopropanol)	Fisher Scientific, Loughborough, UK
Rotiphorese® Gel 30 (37,5:1)	Carl Roth, Karlsuhe, GER
SCR7 ($C_{18}H_{14}N_4OS$)	Sigma-Aldrich, Steinheim, GER
Silicon fat	Obermeier, Bad Berleburg, GER
Sodium acetate	AppliChem, Darmstadt, GER
Sodium chloride (NaCl)	AppliChem, Darmstadt, GER
Sodium dodecyl sulfate (SDS)	Omnilab-Laborzentrum, Bremen, GER
Sodium fluoride	
Sodium hydroxide (NaOH)	Sigma-Aldrich, Steinheim, GER
Sucrose	Carl Roth, Karlsruhe, GER
TEMED	Carl Roth, Karlsruhe, GER
Tris, ultrapure	AppliChem, Darmstadt, GER
Tris-HCl	Sigma-Aldrich, Steinheim, GER
Tween 20	Sigma, Steinheim, GER
X-Gal	Bioline, Luckenwalde, GER

2.1.2 Consumables

Cloning rings	Brand, Wertheim, GER
Countess™ chamber slides	Invitrogen, Karlsruhe, GER
Cryo Vials	Corning Incorporated, Corning, USA
Electroporation Cuvettes (4 mm)	Biorad, Hercules, USA
Electroporation Cuvettes (2 mm)	Eppendorf, Hamburg, GER
Filter paper (extra thick blot paper)	Biorad Laboratories, Munich, GER
Filter pipette tips	Thermo Fisher Scientific, Waltham, USA
Glass pasteur pipettes	Brand, Wertheim, GER
MicroAmp™ Fast Optical 96-Well Reaction Plate Life Technologies	Life Technologies, Carlsbad, USA
MicroAmp™ Optical Adhesive Film	Life Technologies, Carlsbad, USA
Tubes (15 mL, 50 mL)	Greiner Bio-One, Frickenhausen, GER
Tubes (14 ml)	Corning Incorporated, Corning, USA
Reaction tubes (1.5 mL, 2 mL)	Zefa Laborservice, Harthausen, GER

Reaction tubes (0,5 mL)	Brand, Wertheim, GER
Reaction tubes (5 mL)	Starlab, Hamburg, GER
0.2 mL 8-Strip PCR Tubes	Starlab, Hamburg, GER
Petri dishes	Greiner Bio-One, Frickenhausen, GER
Plastic pipettes (sterile, 1-50 mL)	Corning Incorporated, Corning, USA
Scalpel	Braun, Melsungen, GER
Sterile filter 0.22 µm	Berrytec, Grünwald, GER
Syringes	BD Biosciences, Le Pont De Claix, FRA
Tissue culture flasks (T25, T75, T150)	Corning Incorporated, Corning, USA
Tissue culture plates (10 cm, 15 cm, 6-, 12-, 24-, 98-well)	Corning Incorporated, Corning, USA
Western blotting membranes, Nitrocellulose ("Amersham™ Protran®")	Sigma-Aldrich, Steinheim, GER

2.1.3 Equipment

7500 FastReal-Time PCR Cycler	Life Technologies, Carlsbad, USA
AxioCam	Carl Zeiss, Jena, GER
Bio Imaging System Gene Genius	Syngene, Cambridge, UK
Blue light table	Serva, Heidelberg, GER
Centrifuges "Sigma 3-16", "Sigma 1-15", "Sigma 1-15K", "Sigma 4K15"	Sigma, Osterode, GER
ChemiDoc™ Touch Imaging System	Biorad Laboratories, Munich, GER
CO_2 incubator "Forma Steri-Cycle 371"	Thermo Fisher Scientific, Waltham, USA
Countess™ automated cell counter	Invitrogen, Karlsruhe, GER
Digital Graphic Printer UP- D895MD	Syngene, Cambridge, UK
Dry block heater/cooler "PCH-2"	Grant instruments, Royston, UK
Electrophoresis system (buffer chamber, gel trays, combs)	Peqlab Biotechnologie, Erlangen, GER
Freezer -20°C "GS 2481"	Liebherr, Bulle, SUI
Freezer -80°C "Forma 900 Series"	Thermo Fisher Scientific, Waltham, USA
Fridge "TSE1283"	Beko, Neu-Isenburg, GER
Gel documentation imaging system "Quantum ST5"	Vilber Lourmat, Eberhardzell, GER

Glassware	Marienfeld GmbH, Landa, GER
Ice maker	Manitowoc Ice, Manitowoc, USA
Incubator “BD115”	Binder, Tuttlingen, GER
Magnetic stirrer “AREC_X”, “AGE”	VELP Scientific, Usmate, IT
Microscope “Axiovert 40CLF”, “Axiovert 200 M”	Carl Zeiss, Jena, GER
Microwave “MW17M70G-AU”	MDA Haushaltswaren, Barsbüttel, GER
Mini centrifuge “perfect spin mini”	Peqlab Biotechnologie, Erlangen, GER
Mini Trans-Blot® Cell	Biorad Laboratories, Munich, GER
Mr. Frosty^{R} freezing container	Thermo Fisher Scientific, Waltham, USA
Multiporator (Electroporator)	Eppendorf, Hamburg, GER
NanoDrop® Lite	Peqlab, Erlangen, GER
Nucleofector™	Lonza, Basel, SUI
Orbital shaker	Thermo Fisher Scientific, Waltham, USA
PCR Cycler “peqStar 2x”	Peqlab Biotechnologie, Erlangen, GER
Pipet-Lite RAININ (2 µl; 20 µl; 200 µl; 1000 µl)	Mettler Toledo, Gießen, GER
Pipetus “accu jet pro”	Brand, Wertheim, GER
Power supply “EPS 301”	Amersham Bioscience, Little Chalfont, UK
Qubit 4 Fluorometer	Thermo Fisher Scientific, Waltham, USA
Rocker shaker “Unitwist 3-D”	Uniequip, Munich, GER
Safety cabinet “HERAsafe HS 12”	Kendro Laboratory Products, Hanau, GER
Shake `n` stack hybridisation oven	Thermo Fisher Scientific, Waltham, USA
SpeedMill Plus	Analytik Jena, Jena, GER
Vortex mixer “Vortex Genie 2”	VELP Scientific, Usmate, IT
Water bath “WNB22”	Memmert, Schwabach, GER
Western Blot “Mini PROTEAN Tetra Handcast System”	Biorad Laboratories, Munich, GER

2.1.4 Prokaryotic cells

Table 2: Prokaryotic cells

name	genotype	source
E. coli ElectroMAX DH10B	F^{-}*mcr*A Δ(*mrr-hsd*RMS-*mcr*BC) Φ80*lac*ZΔM15 Δ*lac*X74 *rec*A1 *end*A1 *ara*D139Δ(*ara*, *leu*)7697 *gal*U *gal*K λ^{-}*rps*L *nup*G	Thermo Fisher Scientific, Waltham, USA

dam$^-$/*dcm*$^-$ competent *E. coli* (K12 Strain)	*ara-14 leuB6 fhuA31 lacY1 tsx78 glnV44 galK2 galT22 mcrA dcm-6 hisG4 rfbD1 R(zgb210::Tn10)* Tet^S *endA1 rspL136* (Str^R) *dam13::Tn9* (Cam^R) *xylA-5 mtl-1 thi-1 mcrB1 hsdR2*	New England Biolabs, Frankfurt, GER

2.1.5 Eukaryotic cells

Table 3: Eukaryotic cells

name	Isolation No.	genotype	sex	source
Porcine kidney fibroblasts (KDF)	250614 230715 280515	wt, bmp	m	Isolated during this work
Adipose-tissue derived porcine mesenchymal stem cells (MSC)	250614	wt, bmp	m	Isolated during this work
Adipose-tissue derived porcine mesenchymal stem cells (MSC)	110111	wt, LR	m	Chair of Livestock Biotechnology, Prof. A Schnieke, Freising, GER
Porcine kidney fibroblasts (KDF) R26 Fetus4	-	mTomato, mEGFP, LR	m	Chair of Livestock Biotechnology, Prof. A Schnieke, Freising, GER
Porcine kidney fibroblasts (KDF)	200416 130617	wt, LRxbmp	f	Isolated during this work
Porcine kidney fibroblasts (KDF) #912, #928	040717	wt, LRxbmp	m	Isolated during this work
Porcine earclip fibroblast (KDF) #266	-	CD46, CD55, CD59, HO1, A20, LR	m	Chair of Livestock Biotechnology, Prof. A Schnieke, Freising, GER

2.1.6 Enzymes and buffers

Table 4: Enzymes and buffers

enzyme	company
Antarctic Phosphatase	New England Biolabs, Frankfurt, GER
Calf Intestine Phosphatase (CIP)	New England Biolabs, Frankfurt, GER
Cre protein	Chair of Livestock Biotechnology, Prof. A Schnieke, Freising, GER
DNA polymerase I, Large (Klenow) Fragment	New England Biolabs, Frankfurt, GER
Exonuclease I	New England Biolabs, Frankfurt, GER
Fast SYBR® Green PCR Master Mix	Thermo Fisher Scientific, Waltham, USA
GoTaq® G2 DNA Polymerase, 5x Green GoTaq® Reaction Buffer	Promega, Mannheim, GER
PCR Extender Polymerase Mix, 10x Tuning Buffer, 10x HighFidelity Buffer	5 Prime, Hamburg, GER
Phusion DNA Polymerase	New England Biolabs, Frankfurt, GER
Proteinase K	Sigma, Steinheim, GER

Q5® High-Fidelity DNA Polymerase, 5x Q5 Reaction Buffer, 5X Q5 High GC Enhancer	New England Biolabs, Frankfurt, GER
restriction enzymes, NEBuffer™ 1.1, 2.1, 3.1, CutSmart® Buffer	New England Biolabs, Frankfurt, GER
RNase A (20 mg/mL)	Sigma, Steinheim, GER
SuperScript™ III Reverse Transcriptase, 5x First-Strand Buffer	Invitrogen, Karlsruhe, GER
T4 DNA Ligase, T4 DNA Ligase Buffer (10x)	New England Biolabs, Frankfurt, GER
T5 Exonuclease	New England Biolabs, Frankfurt, GER
Taq DNA ligase	New England Biolabs, Frankfurt, GER

2.1.7 Oligonucleotides

Table 5: Oligonucleotides
All Oligonucleotides were purchased from MWG Eurofins, Ebersberg, GER.

oligonucleotide	sequence (5`→ 3`)	No.
ERCC1_Ex0-5F	TGTCCAGGCAGAAGAAGTGT	4
ERCC1_In1F3	CCTGTGTCCTCATGAATGCG	7
ERCC1_Ex0-1F4	GCCCAGATGTCCTTTCCTCT	8
ERCC1_Ex0-1F	CTAGCACTGCCTCACACATG	10
ERCC1_Ex0-2F	CGATCTCCCTCCGTCTTC	12
ERCC1_In1F_Sq	AGGACTGGGGCTAGAGGTG	13
ERCC1_Ex0-9F	CGAGGCAAACGGAAAGAGAG	14
ERCC1_Ex1/2_F	GGAGGTGGTGGGTGGATC	15
ERCC1_Ex2F	CGAAGAGGGAGGCCAGAAG	17
ERCC1_In2F_Sq	GTTAAGAACAGGACGGCAGC	18
ERCC1_In2F_Sq3	GCAGAGGAGGGACGTGATAT	20
ERCC1_In3F_Sq	TCTTAACCCGCTGAACCACA	21
ERCC1_In4F	CTCTGGCTCCACTTTGAAGC	22
ERCC1_5F	CTGAATTGGAGCCGGGAGT	24
ERCC1_Ex4F_Sq	AACCCCGTGCTGAGGTTT	25
ERCC1_Ex5F	CTCCGCTACCACAACCTCC	27
ERCC1_Sq37_197_F	CGTTGTGGCTCAGAGGTAGT	28
ERCC1_In5F	GCCCTCTGCCTCCTAAATAGT	29
ERCC1_In5F_Bac	TGGGACCTTACTGTTGATCCA	30
ERCC1_In5F_Eco	TCTCTGTGTCTGTGAGGCTG	31
ERCC1_Bac_F	GGTTAGACGTCCCACCTGG	32
ERCC1_In6F	CCCTCATCTCTGCGCTTCTA	33
ERCC1_In5F_Sq	CTGTCGCTGTCACCGCTG	35
ERCC1_1F	CGAGCCTCCTACAGTTCGAC	36
ERCC1_In6F_Sq	AGGGGTTATAAGGCTCCAGG	37

ERCC1_In6F_Sq3	GGCTCAGCGGGTTAAGAATC	38
ERCC1_2F	TCTTGGCAGTTCATTTGCTG	40
ERCC1_In6F_Sq4	CAGTAAACTTGGGCGCCTTT	41
ERCC1_Ex6F	ACATACAAGGCCTATGAGCAGA	42
ERCC1_Ex7F_2	CAGAAGCCAGCAGATCTCCT	43
ERCC1_In7F_Sq	AGCAGCACTGAGTACCCA	45
ERCC1_In7F_Sq2	ACCTGTACTTTCTGAACCCCA	46
ERCC1_Ex8F	TGAATGTCTGACCACCGTGA	48
ERCC1_Ex0-2R	GAGGGAGATCGAGGCGTC	50
ERCC1_Ex2R	GGGGTCTGAAAATGAAGGCG	51
ERCC1_Ex2R2	CTTCTGGCCTCCCTCTTCG	52
ERCC1_In2R_Sq	AGCCAGTACTTAGCTGTGGG	57
ERCC1_Ex3R2	CTGGTTTGGGAGCCTGGTT	59
ERCC1_In3R_Sq2	ATTGAACCCGCAACCTCATG	60
ERCC1_In3R_Sq	CAGGTGGGACGTCTAACTTCT	61
ERCC1_Ex4R	CACATCGCCAAACTGCCAG	62
ERCC1_In4R_Sq	GGAGGCTCAGAGGGGTTAAG	63
ERCC1_Sq49_496R	CTGGGACTTGTTCGAGGGAA	64
ERCC1_Bac_R4	CAGCTCTGAATGGACCCCT	65
ERCC1_Bac_R2	TGGATCAACAGTAAGGTCCCA	66
ERCC1_In5R_Eco	GCCATCTTCAGCAACATGGA	68
ERCC1_In5R_Bac	GTGTGCTACAAGACCCCTCT	69
ERCC1_Ex6R	GAGGATCAGGGTGCAGTCG	71
ERCC1_6R	TGAAGAGAGCCTGACCTGAG	72
ERCC1_3R	CTGGAGAAGGAAGCATCAGG	75
ERCC1_Ex7R	ACTTCACGGTGGTCAGACAT	77
ERCC1_Ex10_R	CCCTCCCTCTTTCTCCCTTC	80
ERCC1_In3_R	ATCCCATGGCCCAGAACAC	81
ERCC1_Ex10_R2	CCCAGAAATGGATGTGGGGA	89
ERCC1_Ex10_R5	CAGGGCAGCCTAAGGATCTT	92
ERCC1_In6_R	GGAACTCCCTTGCTTCTGAT	95
ERCC1_In6_R 96	TTTGTTTCTGCTGAGCCACG	96
pSL_Ex2_F	GTACTTCTCGAGCTCTCGAAGAGGGAGGCCAGAAGC	97
Ex3_loxP_R	CGAAGTTATCCCCCTCCTCACCTGCCG	98
Ex3_loxP_Ex4_F	GGAGGGGGATAACTTCGTATAGCATACATTATACGAAGTTATAT GGAGAAGTGGGGCTTTG	99
Ex4_pSL_R	CGCGATCGATATCAGCCACATCGCCAAACTGCCA	100
ERCC1_In3F_2	GCTGTGGTAGTGGAGGGG	103
ERCC1_Ex10_F	TCTTTTCTCTCCCCTCCCCT	106
ERCC1_In9_F	TGTGACTGCTTCTCTCCTGG	107

ERCC1_OE_E10_F	AGCTTAGCTGCCCCCAACGACACAAGTAAGCATTTTCCTGGTCCAGG	114
ERCC1_OE_E10_R	CAGCTAAGCTCATCGGGAGTCGACCTATTATCACTCATGTAAGACGTCAA	115
ERCC1_Ex9F	CGGGAAGATCTGGCCTTGT	117
ERCC1_D7_STOP_F	TGAGTGATAATAGGTCGACTCCC	118
ERCC1_In5_F2	ATCACTGTCTGGGCACTCTC	122
ERCC1_In5_F3	GCCAGAGGTTAGGGAGTGTC	123
loxp-ERCC1-F	ATACGAAGTTATCCTTGTTTCTCCC	124
ERCC1_Ex6_F 125	ATCCTGGCCGATTGTACACT	125
ERCC1_Ex6_F2 126	TCTCTACCCAGAAAGATCCGC	126
ERCC1_Ex6_F3 127	CAACAAGCACTCAGGGACCT	127
ERCC1_loxP_F2	GCATACATTATACGAAGTTATCCTTGTTTCT	128
ERCC1_loxPF3 129	CTCTTATTTATAACTTCGTATAGCATACATTATACG	129
loxP_F1 130	ATAACTTCGTATAGCATACATTATACG	130
ERCC1_Ex10F 131	CTTCTTGAAAGCGTCCCGAT	131
ERCC1_In4F 133	CTGCTTCCTGAGACCTGCT	133
ERCC1_In4F 135	AAGGGGTCTGGGGATGAC	135
ERCC1_In4F3 136	GTCCTCCTGAGCTCGCCA	136
ERCC1_loxP5F 137	GGGGTCTGGGGATGATAACT	137
ERCC1_In4F_loxP	CCTAGGGATAACTTCGTATAGCAT	139
ERCC1_LoxPIn3F2	GGACCCTTTAATAACTTCGTATAGCATAC	149
ERCC1_Ex6_R2 150	TCTCCGGCTCACCTCCAG	150
ERCC1_Ex6_R3 151	GGATCAGTGTACAATCGGCC	151
ERCC1_In6_R2 152	TAGAATTCCCTCTCCAGCGG	152
ERCC1_In6_R3 153	CCTGGAGCCTTATAACCCCT	153
ERCC1_Ex6R4 154	CACATCTTAGCCAGGTCCCT	154
ERCC1_In5R5 155	CCAAGCTGTGTCTGTGACCT	155
ERCC1_Ex10R8 156	GGGAGATGATGGAGCCTGAG	156
ERCC1_In4R2 160	CTGCTCAGTGGAATGCAGAG	160
Oligo In4 R	CCAAGACCTCTGCCTCCTAC	167
ERCC1_In3_F3	GGATCCCGCACTCCCTTG	202
ERCC1_In3_F6	GAGGAGATGTCAGGCTGTCG	205
pbs-U6_F	CTCTTCGCTATTACGCCAGC	2g
pbs-U6_R	TCACTCATTAGGCACCCCAG	3g
T7_F2	TTGTAAAACGACGGCCAGTG	4g
T7_F	TAATACGACTCACTATAGG	5g
U6_F_Sq	TTCACCGAGGGCCTATTTCCCATG	8g
pbs-U6-T7_F	GTACAAAATACGTGACGTAGAAAG	9g
pbs-U6-trac_R	AAAAAAAGCACCGACTCGGTG	10g

ERCC1-del7_F	GACGTCTTACATGAGTAGTGAGCCCCTCTCCCTCCCC	13g
ERCC1_del7_R	GCTTAGCCTTCCGGCTCGTATGTTGTG	14g
CMV_pA_ROX_F	TGGGAAGACAATAGCAGGCA	23g
ERCC1_SA_R	GAAAGACCGCGAAGAGTTTG	28g
ERCC1_BS_R	CGGCTGTCCATCACTGTCCT	29g
NEO_R	TGTGACTGCTTCTCTCCTGG	30g
IRES_R	GCCCTCACATTGCCAAAAGA	31g
pX330-MCS_R	ACCAAGCTTACGTCGACTGT	35g
pJet_R3	TCGATTTTCCATGGCAGCTG	41g
pJet_F2	ACCATATCCATCCGGCGTAA	42g
MYBPC3_Ex6F	CCTGTTTGAGCTGCACATCA	1M
MYBPC3_In5_F	GCCCCAAGTCTCCTCTAACA	2M
MYBPC3_In5_F2 3M	CTGCTCCTTCCACTCTTCCA	3M
MYBPC3_Ex21F 4M	GACGAGTGGGTGTTTGACAG	4M
MYBPC3_Ex22F 5M	GCAGAGTCCGAGTAGAGACC	5M
MYBPC3_Ex7R	GATCGAAGGTCCAGGTCTCC	50M
MYBPC3_In6_R2	GGACAGGACCCTTGCAGAG	52M
MYBPC3_In6_R3 53M	TCACCTATTCACCTGTGCCC	53M
MYBPC3_Ex12R 54M	TAAGCCACTTGACCTCTGCG	54M
MYBPC3_Ex26R 55M	TTTACCAGCATTGTCGTCCG	55M
MYBPC3_Ex24R 56M	CAATGGGCATGAAGGGCTG	56M
ROX1_F	CTAGTAACTTTAAATAATGCCAATTATTTAAAGTTA	6b
ROX1_R	GATCTAACTTTAAATAATTGGCATTATTTAAAGTTA	7b
roxloxP_F	TCGATAACTTTAAATAATGCCAATTATTTAAAGTTAATAACTTCG TATAGCATACATTATACGAAGTTAT	8b
roxloxP_R	GGCCATAACTTCGTATAATGTATGCTATACGAAGTTATTAACTTT AAATAATTGGCATTATTTAAAGTTA	10b
TVlox5-CRI_In5 F	GTAAGCAGGGGTCACTCCCC TGG CTGAATTGGAGCCGGGAGT	82b
TVlox5-CRI_In5 R	GTAAGCAGGGGTCACTCCCC TGG CCAAGCTGTGTCTGTGACCT	83b
TVlox5-CRI_In4 F	GGTGTGACCCTAGGGCGT AGG TCTTAACCCGCTGAACCACA	84b
TVlox5-CRI_In4 R	GGTGTGACCCTAGGGCGT AGG CCAAGCTGTGTCTGTGACCT	85b
ERCC1_Ex5_C_F2	CGC CCC AGACTACATCCACCAGCGGC CTGAATTGGAGCCGGGAGT	88b
ERCC1_Ex5_C_R2	CGC CCC AGACTACATCCACCAGCGGC CCAAGCTGTGTCTGTGACCT	89b
BS R	GGCAGCAATTCACGAATC	-
hMYH7 ex.3 R	GCTCCTTCTCTGACTTGCGCAGG	1106
M13_rev	CAGGAAACAGCTATGACC	
pACTA1 F	GTGCTGTCCCTCTACGCCTC	-
pACTA1 R	GGTAGTCGGTGAGATCGCGG	-
pGAPDH F1	TGGTCACCAGGGCTGCTTTT	-

pGAPDH R1	GTTCTCCGCCTTGACTGTGC	-
pMYH7 F	CTCCGTCTTCTTTCCTTGCTGCTC	-
pNPPA F2	GGTGTTTCAGTTCCCAGGGC	-
pNPPA R2	TGCTCGCTTAGTACTTGTGGGG	-
pNPPB F2	CTCCGGGGAATACGCAGCC	-
pNPPB R	CGTTGGAGAAGCGGACACAGAG	-
pX330 seq F1	GGGAGAAAGGCGGACAGGTA	-
Random hexamers	NNNNNN	-
gRNA target site oligonucleotides		
CRISP18-MYBPC3_F (Ex6-1)	CACC TAATAATACGACTCACTATAG GCTGTGAGGTATCCACCA	15b
CRISP18-MYBPC3_R (Ex6-1)	AAAC TGGTGGATACCTCACAGCC TATAGTGAGTCGTATTATTA	16b
CRISP20-MYBPC3_F (Ex6-2)	CACC TAATAATACGACTCACTATAGGCAGCTGTCAAATTTGTCCT	17b
CRISP20-MYBPC3_R (Ex6-2)	AAAC AGGACAAATTTGACAGCTGCC TATAGTGAGTCGTATTATTA	18b
CRISP18-MYBPC3_F (Ex6-1)	CACC GCTGTGAGGTATCCACCA	62b
CRISP18-MYBPC3_R (Ex6-1)	AAAC TGGTGGATACCTCACAGC	63b
CRISP-MY_ex23_F1	CACC GCTGCCCGCCATCGTAGGC	64b
CRISP-MY_ex23_R1	AAAC GCCTACGATGGCGGGCAGC	65b
CRISP-MY_ex23_F2	CACC GCTCCCACTGCACCGTGC	66b
CRISP-MY_ex23_R2	AAAC GCACGGTGCAGTGGGAGC	67b
CRISP-MY_ex23_F3	CACC GACTCCTGCACGGTGCAGT	68b
CRISP-MY_ex23_R3	AAAC ACTGCACCGTGCAGGAGTC	69b
CRISP-ERCC1_Ex10 F2	CACC GCTTTATTGTCACACTGG	31b
CRISP-ERCC1_Ex10 R2	AAAC CCAGTGTGACAATAAAGC	32b
CRISP-ERCC1_Ex10 F1 18	CACC TAATAATACGACTCACTATAG TCGGGACGCTTTCAAGAA	21b
CRISP-ERCC1_Ex10 R1 18	AAAC TTCTTGAAAGCGTCCCGA CTATAGTGAGTCGTATTATTA	22b
CRISP-ERCC1_Ex10 F2	CACC TAATAATACGACTCACTATAG GCTTTATTGTCACACTGG	23b
CRISP-ERCC1_Ex10 R2	AAAC CCAGTGTGACAATAAAGC CTATAGTGAGTCGTATTATTA	24b
CRISP-ERCC1_Ex10 F1	CACC ATCGGGACGCTTTCAAGA	29b
CRISP-ERCC1_Ex10 R1	AAAC TCTTGAAAGCGTCCCGAT	30b
CRISP-ERCC1_Ex10 F2	CACC GCTTTATTGTCACACTGG	31b
CRISP-ERCC1_Ex10 R2	AAAC CCAGTGTGACAATAAAGC	32b
CRISPR-ERCC1_Ex5 F1	CACC GCCGCTGGTGGATGTAGTCT	45b
CRISPR-ERCC1_Ex5 R1	AAAC AGACTACATCCACCAGCGGC	46b
CRISP-ER_In4_F2	CACC G AAGGGGTCTGGGGATGAC	70b
CRISP-ER_In4_R2	AAAC GTCATCCCCAGACCCCTTC	71b
CRISP-ER_In5_F1	CACC GTAAGCAGGGGTCACTCCCC	72b
CRISP-ER_In5_R1	AAAC GGGGAGTGACCCCTGCTTAC	73b
CRISPR-ERCC1_In4 F1	CACC GGTGTGACCCTAGGGCGT	52b
CRISPR-ERCC1_In4 R1	AAAC ACGCCCTAGGGTCACACC	53b

CRISPR-ERCC1_In3 F2	CACC GCCCTAGGTCTTCACTAA	54b
CRISPR-ERCC1_In3 R2	AAAC TTAGTGAAGACCTAGGGC	55b

2.1.8 ssODN donor templates

Table 6: ssODN donor templates
All ssODN were purchased from Biomers, Ulm, GER.

oligonucleotide	sequence (5`→ 3`)	No.
ERCC1_Ex10_STOP	tttctctcccctcccctccaggcccggagactctttgacgtcttacatgagTGATAA TAGGTCGACtcccgatgagcttagctgcccccca acgacacaagtaagcattttcctggtccaggctccggccg	43b
ERCC1_Ex10_STOP F	cgatgtagcgcacacacggctcatttaatgaccggttcctcttttctctcccctcccct ccaggcccggagactctttgacgtcttacatgagTGATAATAGGTCGACtcc cgatgagcttagctgcccccaacgacacaagta	51b

2.1.9 DNA-fragments

DNA-fragments were purchased from Integrated DNA Technologies, Leuven, BEL and sequences are attached in the supplementary part.

2.1.10 Ladders

Table 7: Ladders

ladder	company
1 kb DNA ladder	New England Biolabs, Frankfurt, GER
2-Log DNA ladder (0.1-10.0 kb)	New England Biolabs, Frankfurt, GER
100 bp DNA ladder	New England Biolabs, Frankfurt, GER
Gel loading dye, purple (6x)	New England Biolabs, Frankfurt, GER
Precision Plus Protein™ All Blue Standards	Biorad Laboratories, Munich, GER
Ribo Ruler High Range RNA Ladder 2x RNA Loading Dye	Thermo Fisher Scientific, Waltham, USA

2.1.11 Kits

CloneJET PCR Cloning Kit	Thermo Fisher Scientific, Waltham, USA
FirstChoice® RLM-RACE Kit	Ambion, Huntingdon, UK
Fisher BioReagents™ SurePrep™ RNA/DNA/Protein Purification Kit	Fisher Scientific, Hampton, USA
GenElute™ Mammalian Genomic DNA Miniprep Kit	Sigma-Aldrich, Steinheim, GER
innuSPEED Tissue RNA Kit	Analytik Jena, Jena, GER
Kapa HiFi PCR Kit	Peqlab Biotechnologie, Erlangen, GER

MEGAclear™ Kit	Ambion, Huntingdon, UK
MEGAshortscript™ T7 Kit	Ambion, Huntingdon, UK
Mix2Seq Kit	Eurofins, Ebersberg, GER
mMESSAGE mMachine® T7 Kit	Ambion, Huntingdon, UK
NucleoBond® Xtra Midi/Maxi Kit	Macherey-Nagel, Düren, GER
pGEM®-T Easy Vector System	Promega, Mannheim, GER
PlateSeq Kit DNA	Eurofins, Ebersberg, GER
Poly(A) Tailing Kit	Ambion, Austin, USA
Qubit™ Protein Assay Kit	Thermo Fisher Scientific, Waltham, USA
QuickExtract™ DNA extraction solution	Lucigen, Middleton, USA
Stemfect™ RNA Transfection Kit	Stemgent, Cambridge, UK
TransIT®- Oligo Transfection Reagent	Mirus Bio LLC., Madison, USA
TURBO DNA-*free*™ Kit	Invitrogen, Karlsruhe, GER
Wizard® SV *Gel and PCR Clean-Up* System	Promega, Mannheim, GER

2.1.12 Vectors and gene targeting constructs

Table 8: Vectors and gene targeting constructs

plasmid	source	No.
pBSK-loxP-IRES-Neo-pA-loxP	Chair of Livestock Biotechnology, Prof. A Schnieke, Freising, GER	723
pBSK-LSL-BS	Chair of Livestock Biotechnology, Prof. A Schnieke, Freising, GER	-
pBS-U6-chimaeric	Kindly provided by Dr. Oskar Ortiz Sanchez, IDG, Helmholtz Zentrum München, Oberschleißheim, GER	703
pCAG-Cas9-bpA	Kindly provided by Dr. Oskar Ortiz Sanchez, IDG, Helmholtz Zentrum München, Oberschleißheim, GER	-
pGEM®-T Easy	New England Biolabs, Frankfurt, GER	-
pJet1.2/blunt	Thermo Fisher Scientific, Waltham, USA	-
pSL1180	Amersham Bioscience, Freiburg, GER	-
pX330-U6-Chimeric_BB-CBh-hSpCas9	Addgene (Plasmid #42230), Cambridge, USA	704
pX459-Cas9-puro	Kindly provided by Prof. Benjamin Schusser, Chair of Reproductive Biotechnology, TUM, Freising GER	842
pZERO-mcs	Kindly provided by Prof. Dirk Haller, Chair of Nutrition and Immunology, Freising GER	844
pBS-ERCC1-E7-2xSTOP-E10 rev (Δ7)	generated during this work	758

pGE-ERCC1-E02-roxloxP-E6	generated during this work	757
pGE-ERCC1-F3-3-roxloxP	generated during this work	15
pJet-ERCC1-Δ7-gRNA-E10-2 (dc)	generated during this work	80
pJet-ERCC1-E7-3xSTOP-E10 (Δ7)	generated during this work	759
pJet-ERCC1-I3-loxP$_2$-I4	Stephan Rambichler, Master Thesis	843
pJet-ERCC1-I3-loxP$_2$-I4-gRNA-I4 (dc)	generated during this work	79
pJet-ERCC1-I4-loxP$_2$-I5	generated during this work	838
pJet-ERCC1-I4-loxP$_2$-I5-gRNA-E5 (dc)	generated during this work	77
pJet-ERCC1-I4-loxP$_2$-I5-gRNA-I5 (dc)	generated during this work	78
pSL1180 rev-U6-trac	generated during this work	756
pX330-MCS-Cas9	generated during this work	705
pX330-MCS-Cas9-puro	generated during this work	841

2.1.13 Media, supplements and reagents

Table 9: Media, supplements and reagents

name	company
bacterial	
Ampicillin	Carl Roth, Karlsruhe, GER
LB Agar, Miller (Luria-Bertani)	Difco BD, Sparks, USA
Luria Broth, Base, Miller	Difco BD, Sparks, USA
cell culture	
Accutase	Sigma-Aldrich, Steinheim, GER
Amphotericin B	Sigma-Aldrich, Steinheim, GER
Ala-Gln	Sigma-Aldrich, Steinheim, GER
Blasticidin S	InvivoGen, San Diego, USA
Cell culture water	Sigma-Aldrich, Steinheim, GER
Collagenase type IA (C2674)	Sigma-Aldrich, Steinheim, GER
DMEM- high glucose	Sigma-Aldrich, Steinheim, GER
DMSO	Sigma-Aldrich, Steinheim, GER
FBS Superior	Biochrom GmbH, Berlin, GER
G418	PAA, Pasching, AUT
Hypoosmolar buffer	Eppendorf, Hamburg, GER
Lipofectamine® 2000	Thermo Fisher Scientific, Waltham, USA
MEM non-essential amino acid solution (NEAA)	Sigma-Aldrich, Steinheim, GER
Nucleofector solution	Lonza, Basel, Sui
Opti-MEM®	Gibco by Life Technologies, Paisley, UK
Penicillin/Streptomycin	Sigma-Aldrich, Steinheim, GER
Phosphate-buffered saline (PBS)	Sigma-Aldrich, Steinheim, GER
Puromycin	InvivoGen, Toulouse, FRA

Sodium pyruvate solution	Sigma-Aldrich, Steinheim, GER
Trypan blue stain 0.4 %	Invitrogen, Karlsruhe, GER

2.1.14 Antibodies

Table 10: Antibodies

antibody	company	No.
primary antibodies		
Anti-MYBPC3	Abcam	Ab171153
Anti-MYBPC3	Santa Cruz	Sc-137181
Anti-MYBPC3	Custom made (Linke), kindly provided by Prof. Dr. Lucie Carrier, UKE, Hamburg	-
Anti-MYBPC3	Custom made (Gautel), kindly provided by Prof. Dr. Lucie Carrier, UKE, Hamburg	-
Anti-MYBPC3	Custom made (Winegard), kindly provided by Prof. Dr. Lucie Carrier, UKE, Hamburg	-
Anti-α-actinin	Sigma	A7811
Anti-CSQ	Dianova	ABR-01164
Anti-GAPDH	Sigma	Sto-1
secondary antibodies		
Anti-Mouse	Sigma	A9044
Anti-Rabbit	Sigma	A0545

2.1.15 Webtools and Software

Table 11: Webtools and Software

name	source	URL
webtools		
CRISPOR	Concordet and Haeussler 2018	http://crispor.tefor.net/
Genome database “Ensembl”	EMBL-EBI, Hinxton, UK	https://www.ensembl.org/index.html
Genome database “NCBI”	Bethesda, Rockville, USA	https://www.ncbi.nlm.nih.gov/
Optimised CRISPR Design	Zhang Lab, MIT, Cambridge, USA	http://crispr.mit.edu/
Primer design tool “Primer3”	Whitehead Institute for Biomedical Research, Cambridge, USA	http://primer3.ut.ee/
RepeatMasker	Institute for Systems Biology, Seattle, USA	http://www.repeatmasker.org/cgi-bin/WEBRepeatMasker
Reverse Complement	Paul Stothard, University of Alberta, Edmonton, CAN	https://www.bioinformatics.org/sms/rev_comp.html
Sequence alignment tool “BLAST®”	Bethesda, Rockville, USA	https://blast.ncbi.nlm.nih.gov/Blast.cgi

TIDE: Tracking of Indels by DEcomposition	Desktop Genetics, London UK	https://tide.deskgen.com/
Vector design software "Everyvector"	everyVECTOR Software Inc., Cambridge, USA	http://www.everyvector.com/
software		
Chromatogram viewer "Finch TV"	Geospiza, Denver, USA	-
Gel documentation "Quantum ST5 v16.15"	Vilber Lourmat, Eberhandzell, GER	-
Microscope software "Axio Vision"	Carl Zeiss, Göttingen, GER	-
Microsoft® office	Microsoft, Redmond, USA	-
qPCR software "7500 fast real time PCR system"	Life Technologies, Carlsbad, USA	-

2.2 Methods

2.2.1 Microbiological methods

2.2.1.1 Culturing bacterial cells

Depending on the experiment bacterial cells were either grown in LB-medium while shaking, or on agar plates supplemented with the appropriate amount of the required antibiotic. A single bacterial clone was picked from an agar plate and either put into LB-Medium or plated on a new agar plate and the culture incubated overnight at 37°C. For blue-white screening, plates were additionally coated with X-Gal and IPTG.

2.2.1.2 Cryoconservation of bacterial cells

For long-term storage of bacterial cells, 0.5 mL overnight culture and 0.5 mL 99 % glycerol were mixed and stored at -80°C.

2.2.1.3 Isolation of plasmid DNA from bacteria

Depending on the amount of required DNA different isolation methods were used. If small amounts were needed, the miniprep protocol was applied. To purify larger amounts of DNA with higher purity the midiprep protocol was used.

2.2.1.3.1 Miniprep

The miniprep of plasmid DNA is based on the alkaline lysis method and is a rapid, small-scale isolation method. 2 mL of an overnight culture were centrifuged 1 min at 13227xg, the pellet resuspended in 100 µL solution I (5 mM sucrose, 10 mM EDTA, 25 mM Tris, pH 8.0), 200 µL

alkaline solution II (0.2 M NaOH, 1 % SDS) were added, the mixture shaken, incubated 3 min at RT and 150 µL solution III (3 M sodium acetate, pH 4.8) were added. The mixture was shaken, incubated 30 min on ice, centrifuged 5 min at 13227xg, the supernatant was transferred into a new reaction tube, 1 mL 95 % Ethanol was added and the mixture shaken and centrifuged 15 min at 13227xg. The pellet was washed with 80 % and 95 % Ethanol, centrifugation of 10 min at 13227xg followed, Ethanol was removed, the pellet was air-dried at RT and dissolved in 50 µL H_2O supplemented with RNase A.

2.2.1.3.2 Midiprep

For larger amounts of DNA with higher purity the NucleoBond® Xtra Midi Kit was applied according to the manufacturer`s instructions. Plasmid DNA was isolated from 100 mL overnight bacterial suspension culture.

2.2.1.4 Electroporation

To introduce plasmid DNA into electrocompetent *E. coli,* 1-5 µL ligation reaction or 10-30 pg plasmid were mixed with 50 µL of thawed *E.coli* DH10b and electroporated using the Multiporator at 2.5 kV for 5 ms. Bacteria were incubated 30 min at 37°C in antibiotic-free LB medium, plated on LB plates containing antibiotics and incubated at 37°C overnight.

2.2.2 Molecular biological methods

2.2.2.1 Isolation of genomic DNA from mammalian tissue

DNA was extracted from mammalian tissue using phenol-chloroform extraction. About 1 mm^3 of tissue was mixed with 1 mL lysis buffer (83 mM Tris-HCl pH 7.4, 0.8 % SDS, 0.2 M EDTA, 0.2 M NaCl). After adding 100 µg/mL proteinase K, the mixture was incubated overnight at 55°C with shaking. To avoid contamination with RNA, samples were treated with 400 µg/mL RNase A solution and incubated 5 min at RT. An equal volume of phenol-chloroform-isoamyl alcohol (25:24:1) was then added, shaken, incubated at RT for 10 min, centrifugated for 10 min at 13227xg and the upper phase containing genomic DNA was transferred into a fresh 2 mL reaction tube. An equal volume of chloroform was added, the mixture was shaken rapidly, centrifuged for 10 min at 17970xg, the upper phase was transferred into a new 1.5 mL tube and 1/20 volume of 3 M sodium acetate and 0.7 volume of isopropanol added. The solution was shaken gently until the DNA precipitated, spun for

5 min at 13227xg, isopropanol was removed, the pellet was washed with 70 % ethanol, centrifuged for 5 min at 13227xg, air-dried and dissolved in water.

2.2.2.2 Isolation of genomic DNA from mammalian cells

Depending on the purity and amount of required DNA different isolation methods were used. To get DNA with higher purity the GenElute™ Mammalian Genomic DNA Miniprep Kit was used. To purify DNA from multiple different cell clones QuickExtract™ DNA extraction solution was applied.

2.2.2.2.1 GenElute™ Mammalian Genomic DNA Miniprep Kit

Cells were detached, spun down 5 min at 300 g and the GenElute™ Mammalian Genomic DNA Miniprep Kit was applied on the cell pellet according to the manufacturer`s instructions.

2.2.2.2.2 Quick extract

Cells were detached, centrifuged 5 min at 300 g, the pellet was resuspended in the appropriate amount of QuickExtract™ DNA extraction solution, the suspension was incubated 15 min at 65°C and the reaction was inactivated 8 min at 95°C. DNA was stored at -20°C.

2.2.2.3 Isolation of RNA from mammalian tissue

To isolate RNA from mammalian tissue, the SpeedMill PLUS was used in combination with the innuSPEED Tissue RNA Kit. The kit was used according to the manufacturer`s instructions.

2.2.2.4 Isolation of RNA from mammalian cells

For isolation of RNA from mammalian cells, the Fisher BioReagents™ SurePrep™ RNA/DNA/Protein Purification Kit was used according to the manufacturer`s instructions.

2.2.2.5 Purification and quality control of RNA

The TURBO DNA-*free*™ Kit was used to remove residual genomic DNA contamination from isolated RNA samples. The Kit was applied according to the manufacturer`s instructions.

To check the quality of isolated RNA the samples were loaded on a 0.8 % TBE gel (see 2.2.2.12) containing 0.3 % formaldehyde. Prior to loading, the samples were mixed with 2x loading dye, heated for 10 min at 70°C and cooled on ice for 5 min. RNA was successful isolated, if there were distinct bands of the 18S and 28S ribosomal RNA.

2.2.2.6 Measuring the concentration of DNA and RNA

For measuring DNA and RNA concentration the NanoDrop® Lite was used according to the manufacturer`s instructions.

2.2.2.7 Synthesis of cDNA

For analysis of gene expression levels RNA was reverse transcribed into cDNA by using SuperScript® III Reverse Transcriptase Kit and random hexamer primer. 500 ng of RNA were transcribed into cDNA according to the manufacturer`s instructions. RNaseOUT™ Recombinant RNase Inhibitor was not used.

2.2.2.8 Polymerase chain reaction (PCR)

For amplification of specific DNA sequences from genomic DNA, plasmid DNA and cDNA different polymerases were used. GoTaq Polymerase was used mostly for screening PCRs. For long-range PCR, or if a correct amplification was needed, e.g. to generate fragments of targeting vectors, polymerases with proofreading such as Q5 Polymerase and 5 Prime Taq DNA Polymerase were used. Table 12 shows the settings for different polymerases.

Table 12: Settings of PCRs with different polymerases

GoTaq® G2 Polymerase					
reaction mixture		**thermal cycling conditions**			
component	**final concentration**	**step**	**temperature**	**time**	**No. of cycles**
DNA cDNA	10-200 ng 2 µL	Initial Denaturation	95°C	2 min	1
5x Green GoTaq® Reaction Buffer	1x	Denaturation	95°C	30 sec	30-40
dNTPs	200 µM each	Annealing	57-65°C	30 sec	
Forward primer	0.5 µM	Extension	72°C	1 min/kb	
Reverse primer	0.5 µM	Final Extension	72°C	5 min	1
GoTaq® DNA Polymerase	1.25 U	Storage	8°C	Indefinite	
H_2O	To 50 µL				

Q5® Polymerase					
reaction mixture		**thermal cycling conditions**			
component	**final concentration**	**step**	**temperature**	**time**	**No. of cycles**
DNA cDNA	1 pg-1 µg 2 µL	Initial Denaturation	98°C	30 sec	1
5x Q5 Reaction	1x	Denaturation	98°C	10 sec	25-35

Buffer					
5x Q5 High GC Enhancer	1x	Annealing	55-65°C	30 sec	
dNTPs	200 µM each	Extension	72°C	30 sec/kb	
Forward primer	0.5 µM	Final Extension	72°C	2 min	1
Reverse primer	0.5 µM	Storage	8°C	Indefinite	
Q5 High-Fidelity DNA Polymerase	1 U				
H_2O	To 50 µL				

5 Prime Taq DNA Polymerase					
reaction mixture		**thermal cycling conditions**			
component	**final concentration**	**step**	**temperature**	**time**	**No. of cycles**
DNA cDNA	1-500 ng 2 µL	Initial Denaturation	93°C	3 min	1
10x Tuning or HighFidelity Buffer	1x	Denaturation	93°C	15 sec	25-35
dNTPs	200 µM each	Annealing	50-65°C	30 sec	
Forward primer	0.5 µM	Extension	68°C	1-8 min	
Reverse primer	0.5 µM	Final Extension	68°C	5 min	1
GoTaq^R DNA Polymerase	2 U	Storage	8°C	Indefinite	
H_2O	To 50 µL				

2.2.2.9 Colony PCR

Colony PCR was used for fast detection of successful cloning events. One primer binds to plasmid insert, the other to plasmid backbone and single bacterial colonies served as template. Clones were picked from an agar plate with a tip, resuspended in PCR reaction mix and transferred on a new agar plate.

2.2.2.10 Overlap extension PCR

Overlap extension PCR was used to introduce modifications during amplification of PCR-fragments. Two primers containing desired mutations and having an overlap at the 5` end were used separately with two flanking primers to get overlapping DNA-fragments. These fragments were employed together with the flanking primers as mega primers to amplify a full-length mutagenised DNA sequence. PCR reaction steps were performed with KAPA HiFi or Q5 Polymerase. Table 13 shows the settings for KAPA HiFi and Q5 DNA Polymerase. First PCR of Q5 polymerase was conducted as described in 2.2.2.8.

Table 13: Settings of Overlap extension PCR

1. PCR: KAPA HiFi DNA Polymerase					
reaction mixture		**Thermal cycling conditions**			
component	**final concentration**	**step**	**temperature**	**time**	**No. of cycles**
DNA	0.1-100 ng	Initial Denaturation	95°C	3 min	1
5x KAPA HiFi Fidelity Buffer	1x	Denaturation	98°C	20 sec	5
		Annealing	65°C	15 sec	
KAPA dNTP Mix	300 µM each	Extension	72°C	1 min	
		Denaturation	98°C	20 sec	5
Forward primer	0.3 µM	Annealing	62°C	15 sec	
		Extension	72°C	1 min	
Reverse primer	0.3 µM	Denaturation	98°C	20 sec	10
		Annealing	58°C	15 sec	
KAPA HiFi DNA Polymerase	1 U	Extension	72°C	1 min	
		Final Extension	72°C	90 sec	1
H_2O	To 50 µL				
		Storage	8°C	Indefinite	

2. PCR: KAPA HiFi DNA Polymerase					
reaction mixture		**thermal cycling conditions**			
component	**final concentration**	**step**	**temperature**	**time**	**No. of cycles**
PCR reaction	10 µL each	Initial Denaturation	95°C	3 min	1
5x KAPA HiFi Fidelity Buffer	1x	Denaturation	98°C	20 sec	10
		Annealing	62°C	15 sec	
KAPA dNTP Mix	300 µM each	Extension	72°C	2 min	
		Denaturation	98°C	20 sec	25
Forward primer	0.3 µM	Annealing	58°C	15 sec	
Reverse primer	0.3 µM	Extension	72°C	2 min	
KAPA HiFi DNA Polymerase	1 U	Final Extension	72°C	2 min	1
H_2O	To 50 µL	Storage	8°C	Indefinite	

2.PCR: Q5® DNA Polymerase					
reaction mixture		**thermal cycling conditions**			
component	**final concentration**	**step**	**temperature**	**time**	**No. of cycles**
PCR reaction	2-4 µL each	Initial Denaturation	95°C	30 sec	1
5x Q5 reaction buffer	1x	Denaturation	98°C	10 sec	15
		Annealing	65°C	30 sec	
5x Q5 high GC enhancer	1x	Extension	72°C	90 sec	
		Denaturation	98°C	10 sec	20
dNTPs	200 µM each	Annealing	58°C	30 sec	
Forward primer	0.5 µM	Extension	72°C	90 sec	
Reverse primer	0.5 µM	Final Extension	72°C	2 min	1
Q5 High-Fidelity DNA Polymerase	1 U	Storage	8°C	Indefinite	
H_2O	To 50 µL				

2.2.2.11 Rapid amplification of cDNA ends (RACE)

To amplify cDNA ends the FirstChoice® RLM-RACE Kit was used according to the manufacturer`s instructions with the exception that the reverse transcritption was done using the SuperScript® III Reverse Transcriptase Kit (see 2.2.2.7) instead of the included M-MLV Reverse Transcriptase solution. GoTaq Polymerase was used for all PCRs.

2.2.2.12 Agarose gel electrophoresis to separate DNA-fragments

The agarose gel electrophoresis was used to analyse the size of DNA-fragments. Therefore, the concentration of the agarose gel was adjusted to the size of the expected DNA-fragments. To analyse fragments between 20 bp up to 14 kb 0.8 % - 3 % agarose was dissolved in TBE (90 mM Trizma Base, 90 mM boric acid, 2 mM EDTA) and 0.4 µg/mL ethidium bromide (EtBr) was added. For preparative gels 0.8 % - 1,5 % agarose was dissolved in TAE (40 mM Trizma Base, 20 mM acetic acid, 1 mM EDTA, pH 8.0) with the same amount of EtBr. If necessary, samples were mixed with 5x gel loading buffer (50 % glycerol, 0.2 M EDTA, traces of bromphenol blue). The gels were run for one up to seven hours at 80 – 120 V and the separated DNA-fragments were visualised under UV light (254-366 nm) using the Bio Imaging System Quantum ST5.

2.2.2.13 Purification of DNA using the Wizard SV Gel and PCR Clean-Up System

For Purification of DNA-fragments the Wizard® SV *Gel and PCR Clean-Up* System was applied according to the manufacturer`s instructions.

2.2.2.14 Isolation of DNA-fragments from agarose gels

Separated DNA-fragments were isolated from agarose gels under UV-light with a clean scalpel. Afterwards they were purified using the Wizard® SV *Gel and PCR Clean-Up* System (see 2.2.2.13).

2.2.2.15 Ligation

T4 DNA Ligase was used for ligation of DNA-fragments and vector backbones. The reaction was carried out according to the manufacturer`s instructions. Ligation mixture was incubated 2 h at RT and afterwards overnight at 16°C.

For easy cloning of blunt end PCR products or DNA-fragments the vector system CloneJET PCR Cloning Kit and for sticky end ligation the pGEM®-T Easy Vector System was used according to the manufacturer`s instructions. For difficult samples the pGEM®-T Easy ligation mix was incubated at 4-16°C overnight.

2.2.2.16 Restriction digestion

Preparative digests were used for cloning steps or for linearisation of targeting vectors and analytical digests were used to verify plasmid size. All digests were performed according to the manufacturer`s instructions. Table 14 shows settings for restriction digestion.

Table 14: Settings of restriction digests

preparative digest		analytical digest	
component	**final conc.**	**component**	**final conc.**
DNA	7-40 µg	DNA	0.2-3 µg
10x NEBuffer	1x	10x NEBuffer	1x
Enzyme	5 U/µg	Enzyme	3-5 U/µg
H_2O	To 50 µL	H_2O	To 20-50 µL

2.2.2.17 Blunting of DNA-fragments

The DNA polymerase I Large Fragment (Klenow) was used to generate blunt ends of DNA-fragments. The enzyme is active in all NEB buffers and is filling 5` overhangs and removing 3` overhangs to form blunt ends. dNTPs were added to the reaction to inhibit 3`-5` exonuclease activity of the polymerase I. The reaction was performed according to the manufacturer`s instructions. Reaction settings are shown in Table 15.

Table 15: Settings of blunting reactions

component	final conc.
DNA	5 µg
10x NEBuffer	1x
dNTPs	50 µM each
Enzyme	1 U/µg
H_2O	To 50 µL

2.2.2.18 Dephosphorylation of DNA-fragments

By removing 5` phosphates using Calf Intestinal Alkaline Phosphatase (CIP), religation of vectors with blunt or compatible ends was prevented. One U CIP for every 1 pmol of DNA ends were added to a restriction digest and incubated at 37°C for 30-60 min. After purification, the fragments were used for ligation.

2.2.2.19 Gibson assembly

For easy joining of multiple DNA-fragments, Gibson assembly was used. For the isothermal reaction the 5x ISO buffer (500 mM Tris-HCl (pH 7.5), 50 mM $MgCl_2$, dNTPs 1 mM each, 50 mM DTT, 25 % PEG-8000, 5 mM NAD) was mixed with 80 U Taq ligase, 0.08 U T5 exonuclease, 0.5 U Phusion polymerase, 100 ng linearised vector backbone and equimolar amounts of DNA-fragments. The mixture was incubated at 50°C for 1 h and kept on ice until transformation of *E. coli*.

2.2.2.20 Sequencing of DNA-fragments

DNA sequencing was conducted by Eurofins Genomics (Ebersberg, GER). Therefore, PCR samples were purified by the Wizard® SV *Gel and PCR Clean-Up* System or by using Antarctic Phosphatase (AP) and Exonuclease I (ExoI). For the latter, 3.5 U AP, 4 U ExoI and 10 µL PCR sample were mixed and filled up to 11 µL with ddH_2O. After incubation at 37°C for 30 min the mixture was inactivated at 80°C for 15 min and sent for sequencing.

2.2.2.21 Generation of components of CRISPR/Cas9 system

2.2.2.21.1 Hybridisation of oligonucleotides

Synthesis of gRNA oligonucleotides was conducted by Eurofins Genomics (Ebersberg, GER). Lyophilised single-stranded oligos were solved in TE-buffer (10 mM Tris-HCl, 1 mM EDTA), 0.5 pmol of each of the two complementary oligos were added to 99 µL TE-buffer, heated at 100°C for 5 min and slowly cooled down at RT.

2.2.2.21.2 Ligation of hybridised oligonucleotides into vector backbones

Hybridised Oligos containing gRNA recognition sequences were cloned into different vector backbones (pBS-U6-chimaric, pX330-U6-MCS-Cas9 and pX330-U6-MCS-Cas9-Puro). Ligation mixture was incubated 2 h at RT and afterwards overnight at 16°C. Reaction settings are shown in Table 16.

Table 16: Settings of ligation reactions

component	final conc.
hybridised oligos	1.5 µL
10x T4 DNA Ligase Buffer	1x
digested vector backbone	100 ng
T4 DNA Ligase	1.5 µL
H_2O	To 15 µL

2.2.2.21.3 Template preparation for *in silico* transcription of gRNA

To generate templates for *in silico* transcription of RNAs, Nested PCR was performed using Q5® Polymerase (see 2.2.2.8). After first PCR, DNA-fragments were isolated from gel (see 2.2.2.13), used as template for same PCR again, enzymatic purification followed (see 2.2.2.20) and DNA-fragments were purified using phenol-chloroform extraction (see 2.2.2.21.4). Afterwards *in silico* transcription followed.

2.2.2.21.4 Phenol-Chloroform extraction

For purification of DNA-fragments solution was mixed with an equal volume of phenol-chloroform-isoamyl alcohol (25:24:1), shaken and incubated at RT for 10 min. After centrifugation for 10 min at 13227xg, the upper phase containing genomic DNA was transferred into a fresh 2 mL reaction tube, 1/10 volume of 5 M sodium acetate and 2-fold volume of 100 % Ethanol was added. The solution was shaken gently, incubated for at least 15 min at -20°C and spun for 15 min at 13227xg at 4°C. Supernatant was removed, the pellet air-dried and dissolved in water.

2.2.2.21.5 *In silico* transcription of gRNA

For *in silico* transcription of gRNA the MEGAshortscript™ T7 Kit was applied according to the manufacturer`s instructions. Reaction mixture was incubated for 4 h at 37°C.

For *in silico* transcription of Cas9 mRNA the mMESSAGE mMACHINE™ T7 Kit was applied according to the manufacturer`s instructions. Reaction mixture was incubated for 4 h at 37°C.

2.2.2.21.6 PolyA tailing

For polyA tailing of Cas9 mRNA the Poly(A) Tailing Kit was applied according to the manufacturer`s instructions.

2.2.2.21.7 RNA purification

For purification of *in silico* transcripted gRNA the MEGAclear™ Kit was used according to the manufacturer`s instructions. All centrifugation steps were carried out at 4°C except eluation step, which was conducted at RT.

2.2.2.21.8 Quality control of RNA

Quality of RNA was controlled by loading the samples on a 1.5 % TBE gel (see 2.2.2.5).

2.2.2.22 Quantitative real time PCR (Q-PCR)

To analyse exression levels of genes Fast SYBR® Green PCR Master Mix was used. First, primer specificity and cDNA dilutions were tested and analysed by amplification blots and melting curves. Second, expression levels were analysed in triplicates with the 7500 FastReal-Time PCR Cycler according to the following settings. Expression levels were normalised to endogenous *GAPDH* (Glycerinaldehyd-3-phosphat-Dehydrogenase) expression, the $\Delta\Delta C_T$ value was calculated and a fold-difference in expression levels was determined.

Table 17: Settings of Q-PCR reactions

Fast SYBR® Green PCR					
reaction mixture		**thermal cycling conditions**			
component	**final concentration**	**step**	**temperature**	**time**	**No. of cycles**
cDNA (1:5)	1 µL	Activation	95°C	20 sec	1
SYBR® Green Mix	4 µL/1x	Denaturation	95°C	3 sec	40
Forward primer	0.4 µM	Annealing/ Extension	60°C	30 sec	
Reverse primer	0.4 µM				
H_2O	To 10 µL				

2.2.2.23 Protein extraction from tissue samples

For protein isolation samples of different tissues were frozen in N_2, smashed, about 50 mg of powder was resuspended in an 8x volume of water supplemented with 1x PhosSTOP™ and frozen and thawed for 3 times. After adding steel balls the solution was shaken twice at 20 Hz for 30 sec in the SpeedMill PLUS tissue lyser. The mixture was centrifuged for 30 min at 16000xg at 4 °C, the supernatant containing cytosolic proteins was frozen at -80°C and the

pellet was dissolved in a 5x volume of Krania`s buffer (30 mM Tris pH 8.8, 5 mM EDTA, 30 mM NaF, 3 % SDS, 10 % glycerol) and 1 µM DTT. Lysation and centrifugation was repeated as described above and supernatant was kept at -80 °C.

2.2.2.24 Measuring of protein concentration

Protein concentration was determined by using a Qubit 4 Fluorometer (Thermo Fisher) according to the manufacturer`s instructions.

2.2.2.25 Western Blot

To separate proteins according to their sizes sodiumdodecylsulfate polyacrylamide gelelectrophoresis (SDS-PAGE) was conducted. The concentration of the polyacrylamide in the resolving gel was adjusted to the size of expected proteins. For bigger proteins 10 % and for smaller ones (about 50 kDa and smaller) 12 % was chosen. The stacking gel was prepared with 5 % polyacrylamide (see Table 18).

Table 18: SDS-PAGE gels

component	resolving		stacking
	10 %	12 %	5 %
H_2O	4.8 mL	4.3 mL	6.0 mL
40 % Acrylamide	2.5 mL	3.0 mL	1.3 mL
0.5 M Tris pH 8.8	2.5 mL	2.5 mL	-
0.5 M Tris pH 6.8	-	-	2.5 mL
10 % SDS	0.1 mL	0.1 mL	0.1 mL
10 % APS	0.1 mL	0.1 mL	0.1 mL
TEMED	4 µL	4 µL	10 µL

For denaturation 20 µg of protein solution was mixed with 4x Lämmli buffer (250 mM Tris-HCl pH 6.8, 1 % SDS, 1 M sucrose, 24 mM DTT, a trace of bromphenol blue), heated for 10 min at 95°C and kept on ice until loading. The gel was run for 10 min at 80°C and for 110 min at 120 V in running buffer (25 mM Tris, 200 mM glycine, 0.1 % SDS).

The blotting chamber for wet blots was assembled according to the manufacturer`s instructions and proteins were transferred for 70 min at 400 mA on a nitrocellulose membrane in blot buffer II (50 mM Tris, 400 mM glycine, 0.1 % SDS, 20 % (v/v) methanol).

The membrane was stained with ponceau S (0.5 % Ponceau S, 1 % (v/v) acetic acid) for confirmation of successful transfer, washed 2x with water, incubated 3x 5 min with TBS-Tween 0.1 % (100 mM Tris, 150 mM NaCl, 0.1 % Tween 20) and blocked 1 h in 5 % MLK-TBST solution under shaking. After washing the membrane 3x 5 min with TBS-Tween 0.1 %,

primary antibodies diluted in 10 mL TBS-Tween 0.1 % were added and incubated over night at 4°C (see Table 19).

Table 19: Used primary antibodies

antibody	company	source	binding site	dilution
Anti-MYBPC3	Abcam	rabbit	N-terminal	1:1000
Anti-MYBPC3	Santa Cruz	mouse	N-terminal (1-120 aa)	1:1000
Anti-MYBPC3	Custom made (Linke)	rabbit	M motif	1:1000
Anti-MYBPC3	Custom made (Gautel)	rabbit	C0-C1	1:5000
Anti-MYBPC3	Custom made (Winegard)	rabbit	C0-C2	1:1000
Anti-α-actinin	Sigma	mouse	-	1:1000
Anti-CSQ	Dianova	rabbit	-	1:2500
Anti-GAPDH	SIGMA	mouse	-	1:5000

The next day the membrane was washed 3x 5 min with TBS-Tween 0.1 %, the secondary antibody was diluted in 10 mL TBS-Tween 0.1 %, added (see Table 20), incubated under shaking for 1 h at room temperature and the membrane was washed 3x 5 min with TBS-Tween 0.1 %. To detect chemiluminescence the Clarity™ Western ECL Substrate was used according to the manufacturer`s instructions. The bands were visualised using the ChemiDoc™ Touch Imaging System.

Table 20: Used secondary antibodies

antibody	company	source	dilution
Anti-Mouse	Sigma	rabbit	1:6000
Anti-Rabbit	Sigma	goat	1:6000

2.2.3 Cell culture

All work was carried out in a class II laminar flow hood with sterilised material. Cells were cultured at 37°C in an incubator containing 5 % CO_2 and 95 % humidity. Antibiotic-free medium (DMEM, 1x NEAA, 1 mM sodium pyruvate, 2 mM Ala-Gln, 10 % FBS) was used and every second day medium was changed.

Passaging of cells was conducted at a confluence of about 80-95 %. For this purpose, medium was aspirated, cells were rinsed with PBS, incubated with Accutase for 5-10 min at 37°C, diluted in an accurate volume of medium and cultivated on a new flask.

For isolation of primary cells, pigs of the TUM facility for livestock were either sacrificed or the tissues were obtained from the slaughterhouse. In the first 3-5 days medium contained penicillin, streptomycin and amphotericin B and was changed every day.

2.2.3.1 Isolation of primary porcine mesenchymal stem cells (MSC)

Porcine MSCs were isolated from fat tissue of a slaughtered pig. The tissue was washed three times with 80 % Ethanol, skin and bristles were removed with a scalpel and a piece with the size of about 3x3x2 cm was cut out. After washing the tissue three times with PBS and 80 % Ethanol, it was placed in a Petri-dish, minced into small pieces with a scalpel, transferred into a flask containing Collagenase type IA and incubated 30 min at 37°C on a magnetic stirrer. About 40 mL medium was added, cells were centrifuged for 10 min at 300 g and supernatant was removed. The previous step was repeated until the supernatant was clear, the pellet was resuspended in medium and plated on three T150 flasks.

2.2.3.2 Isolation of primary porcine kidney fibroblasts (KDF)

For isolation of KDF the whole kidney was obtained and washed three times with 80 % Ethanol. After removing the skin and vessels, a piece with the size of about 2x2x2 cm was cut out. The tissue was washed three times with PBS and 80 % Ethanol, placed in a Petri-dish and mince into small pieces with a scalpel. The minced tissue was transferred into a flask containing Collagenase type IA and incubated 30 min at 37°C on a magnetic stirrer. Afterwards about 40 mL Medium was added and cells were centrifuged for 10 min at 300 g. The supernatant was removed and the previous step was repeated until the supernatant was clear. The pellet was resuspended in medium and plated on three T-150 flasks.

2.2.3.3 Cryoconservation and thawing of cells

Cells were detached, diluted with medium and spun down 5 min at 300xg. After resuspending the pellet in 1 mL cryo medium containing 70 % FCS and 10 % DMSO, suspension was transferred to a cryovial and cells were frozen at -80°C using a Mr. Frosty^{R} freezing container. The vial was kept at liquid nitrogen for long-term storage.

The vial with frozen cells was transferred to a water bath at 37°C until the cryo medium was almost completely liquid. Suspension was rapidly mixed with 5 mL prewarmed medium, cells were spun down for 5 min at 300 g, resuspended in fresh medium and cultured.

2.2.3.4 Counting of cells

For counting of cells the Countess^{TM} automated cell counter (Invitrogen) was used according to the manufacturer`s instructions

2.2.3.5 Transfection of mammal cells

2.2.3.5.1 Nucleofection

Cells were detached from the cell culture vessel using accutase. 0.5-1x10^6 cells were centrifuged for 5 min at 300xg and resuspended in 100 µL Nucleofector™ Solution (Lonza) containing up to 5 µg DNA. The solution was transferred to a nucleofection cuvette (Lonza), cells were pulsed using the correct program of the nucleofector and transferred to a T25 cell culture flask. Medium was changed the next day.

2.2.3.5.2 Electroporation

For Electroporation cells were detached from the cell culture vessel using accutase and 1x10^6 cells were centrifuged for 5 min at 300xg. The pellet was resuspended in 400 µL hypoosmolar buffer, 5 µg of linearised DNA was added, the suspension was transferred into a 4 mm cuvette, incubated for 5 min at room temperature and pulsed at 1200 V for 85 µs in an Eppendorf Multiporator. Suspension was incubated for 5 min and transferred to a T25 cell culture flask. Medium was changed the next day.

2.2.3.5.3 Lipofection

At a confluence of cells of about 60-70 %, Medium was aspired, cells were washed twice with PBS and kept in Opti-MEM® Medium until Lipofectamine® 2000 was used. Per 12-well, Opti-MEM® Medium was mixed with 0.2-3 µg of DNA and separately with 2 µL Lipofectamine® 2000 to a total volume of 50 µL of each dilution. After incubation of 5 min at room temperature, diluted DNA was added dropwise to diluted Lipofectamine® 2000 reagent, solutions were mixed briefly, incubated for 20 min at room temperature and DNA-lipid complex was added dropwise to cells. After 4 h of incubation, medium was added and changed the next day.

2.2.3.5.4 Stemfect Kit

Stemfect™ RNA Transfection Kit was used for transfection of RNA into mammalian cells. One day prior to transfection cells were plated on a 12-well plate at a density, that will yield a 50 % - 90 % confluence after 24 hours. On the next day medium was aspirated, 1 mL medium was added 2 hours prior to transfection. Per 12-well, 60 µL Stemfect Transfection Buffer was mixed with 200 ng RNA of gRNA and 400 ng RNA of Cas9 in one reaction tube and with 2 µL Stemfect RNA Transfection Reagent in another rection tube. Diluted transfection reagent

was added to diluted RNA, solutions were mixed briefly, incubated for 15 min at room temperature and the mixture was added dropwise to cells. Medium was changed the next day.

2.2.3.5.5 TransIT-Oligo Transfection

To transfect oligos into mammalian cells TransIT®-Oligo Transfection Reagent was used according to the manufacturer`s instructions.

2.2.3.6 Generation of single cell clones

2.2.3.6.1 Without selection

2.2.3.6.1.1 Cloning rings

24-48 h after transfection 600 to 1000 cells were split onto a 150 mm cell culture plate. Medium was changed at least every second day until single cell clones were visible. For picking clones, cells were washed with PBS, cloning rings were put in silicone and afterwards placed over single cell clone. Using accutase cells were transferred to 24-well plates and culture continued.

2.2.3.6.1.2 Dilution

24 h after transfection cells were diluted to a concentration of 5 cells/mL and 0.5 cells were transferred to a well of a 96-well plate and culture continued.

2.2.3.6.2 Selection of transient transfected cells

24 h after transfection cells were washed and selected using determined optimal concentration of puromycin. After 48 h of selection cells were cultured for 1-3 days without selection and single cell clones were generated as described above (see 2.2.3.6.1.1).

2.2.3.6.3 With selection of stably transfected cells

48 h after transfection cells were split onto 150 mm cell culture plates and selected using determined optimal concentration of Blasticidin S or G418. It was proceeded as described in 2.2.3.6.1.

2.2.3.7 Transduction of Cre recombinase into cells

To analyse functionality of loxP sites genetically modified cells containing loxP sites were transducted with Cre protein. Cells were washed, 5 µM of purified Cre recombinase was diluted with starvation medium (DMEM, 1x NEAA, 1 mM sodium pyruvate, 2 mM Ala-Gln,

0.5 % FBS), added to the cells, after 8 h of incubation cells were washed twice, medium was added and culture continued.

2.2.3.8 Preparing single cell clones for SCNT

To induce cell cycle synchronisation primary single cell clones were incubated with starvation medium (see 2.2.3.7) two days prior to SCNT.

3 Results

3.1 ERCC1

3.1.1 Characterisation of the porcine *ERCC1* gene

The purpose of the project was to modify the *ERCC1* gene to generate a porcine model that displays age-related heart diseases. The sequence of the porcine gene was not fully known and analysis of the *ERCC1* gene sequence was a necessary step towards gene manipulation. Only parts of the gene sequence were found in the National Center for Biotechnology Information (NCBI, https://www.ncbi.nlm.nih.gov/), which consisted of four exons. Blast comparison of these sequences with the human *ERCC1* gene sequence showed that these were exon six to exon ten of the pig. Consequently, further analysis of the gene was necessary.

3.1.1.1 Gap sequencing and gene annotation by comparison of human and porcine genome

The missing exon one to exon five were identified in a porcine working draft sequence (Sus scrofa clone RP44-9K15; GenBank: AC142092.2; https://www.ncbi.nlm.nih.gov/). As this sequence was still incomplete, missing parts were sequenced after PCR amplification. Boundaries of translated exons could be clarified due to information from NCBI and analysis of RNA. The porcine ERCC1 gene consists of 25399 bp and ten exons have been identified (see Figure 8 A).

In human, at least four transcript variants have been found, although only one isoform encodes functional ERCC1 protein and several exons within 5' untranslated region (5` UTR) undergo alternative splicing (van Duin et al. 1987, Manandhar et al. 2015). Comparison of the human and porcine sequences on the mRNA level showed identity of 87 %. Analysis of porcine RNA of heart tissue showed the same main transcript as it was found in humans and two other transcript variants that were alternative spliced in exons withtin 5` UTR (see Figure 8 B). Analysis of 3` UTR showed no alternative splicing of exon ten. Exon two to ten were verified by analysis of mRNA products of different cell types.

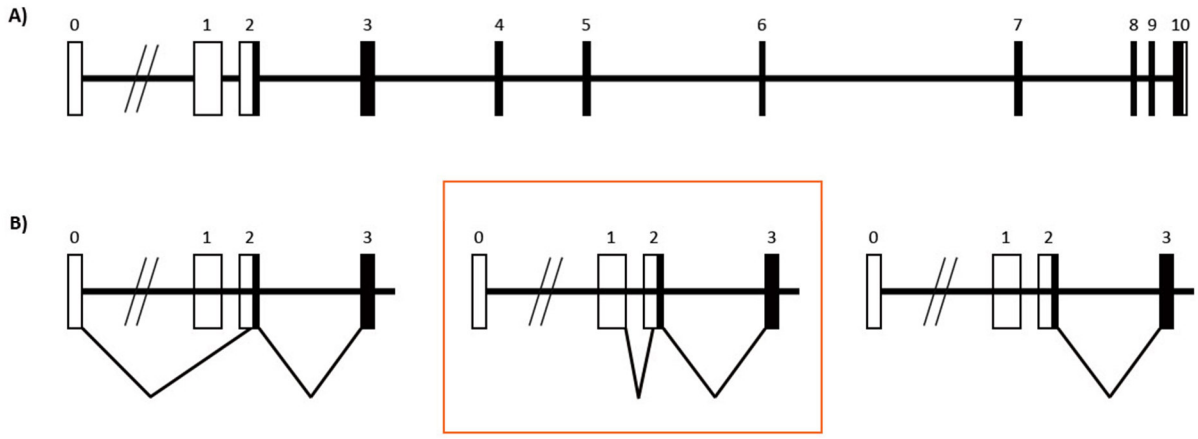

Figure 8: Structure of the *ERCC1* gene.
A) Overview of the porcine *ERCC1* gene locus. Translated exons are black, untranslated white. B) Overview of 5´ untranslated region (5` UTR) splicing. The splicing of the 5` UTR of the main transcript variant is marked with an orange frame.

3.1.1.2 ERCC1 expression level

Findings in mice indicate a low expression level of *ERCC1* throughout the whole body including the heart (van Duin et al. 1987, van Duin et al. 1988). The *ERCC1* expression level in porcine tissue and cell types was unknown, hence, expression was analysed. In several different tissue and cell types, such as kidney derived fibroblasts (KDFs), adipose derived mesenchymal stem cells (MSCs), colon, liver and heart tissue expression could be detected.

Quantitative real time PCR of different tissues (kidney cells, adipose derived MSCs and heart tissue) showed a similarily low expression level as in other species with the lowest value for heart tissue.

3.1.2 Strategy for introducing mutations in the *ERCC1* gene

Mouse models with the *ERCC1* gene knockouts showed progressive damage in the liver and mice died before weaning due to liver failure (Weeda et al. 1997, McWhir et al. 1993). To avoid a severe phenotype a strategy to achieve a double heterozygous pig was developed. An allele was designed to have a Δ7 mutation (deletion of the last seven amino acids) that was already introduced in mice and the homozygous form reduced lifespan less than complete null mutants (Weeda et al. 1997). The second allele was designed to carry loxP sites flanking exon two and three (conditional knockout) that can be inactivated in a tissue-, and time-specific manner by Cre recombinase and would otherwise remain fully functional. After generation of animals carrying these alleles they can be bred to obtain piglets from the

F1 generation carrying both mutations. The F1 animals can be used to introduce Cre in a heart-specific manner and the knockout of the floxed allele takes place only in heart tissue (see Figure 9).

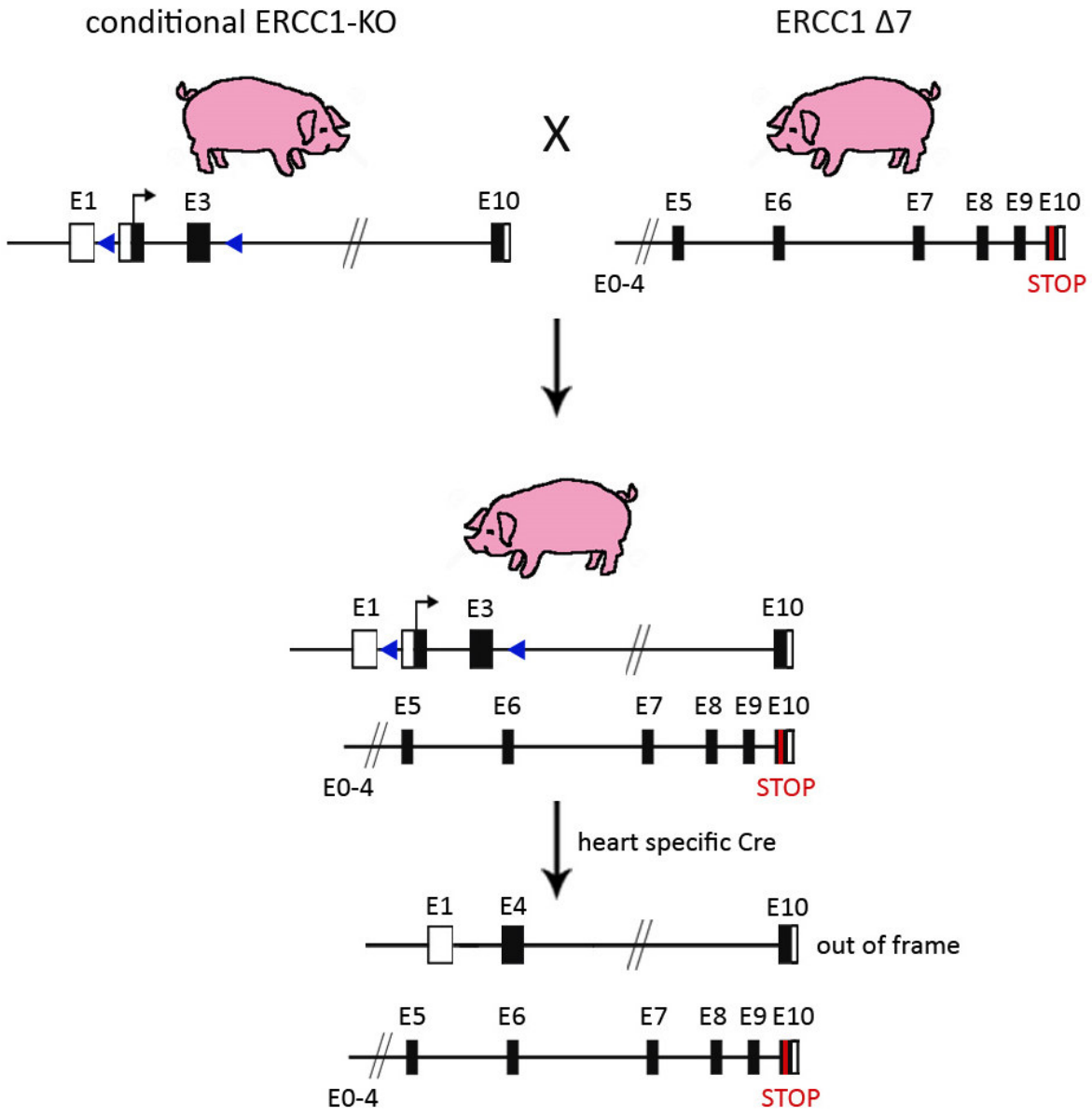

Figure 9: Strategy for generation of a porcine model with compound heterozygous mutations in the *ERCC1* gene.
After generation of a pig having parts of the gene flanked with loxP sites and another pig carrying a Δ7 mutation, these two animals can be bred. Piglets from the F1 generation carrying both mutations can be used to introduce Cre in a heart-specific manner and the knockout of the floxed allele takes place only in heart tissue.

As *Ercc1* plays an important role in the DSB repair, trying to mutate the gene by introducing DSBs and expecting HR to occur might be difficult if both alleles were affected. Indeed that manipulation of *ERCC1* might be problematic was indicated by generation of *Ercc1* knockout

mice, which was very inefficient, but nevertheless possible (personal communication, Prof. J.H. Hoeijmakers). For this reason, it was decided to design and follow several strategies to manipulate the porcine *ERCC1* gene.

3.1.3 Conventional gene targeting

Primary somatic stem cells and gene targeting via homologous recombination (HR) was used to introduce the desired changes in the porcine *ERCC1* gene. For that purpose, promotor trap targeting vectors were designed and transfected into somatic primary stem cells.

3.1.3.1 Introducing the Δ7 mutation by promotor trap strategy

The first step to introduce the Δ7 mutation was to generate a promotor trap targeting vector (No. 758). An integrated, functional and promotorless neomycin resistance gene (neo) was added to the targeting vector and was designed to be translated from the IRES as part of a bicistronic message RNA and thereby enables selection. The cassette was flanked with 1.5 kb homology arm at the 3` end and 2 kb homology arm at the 5` end (see Figure 10).

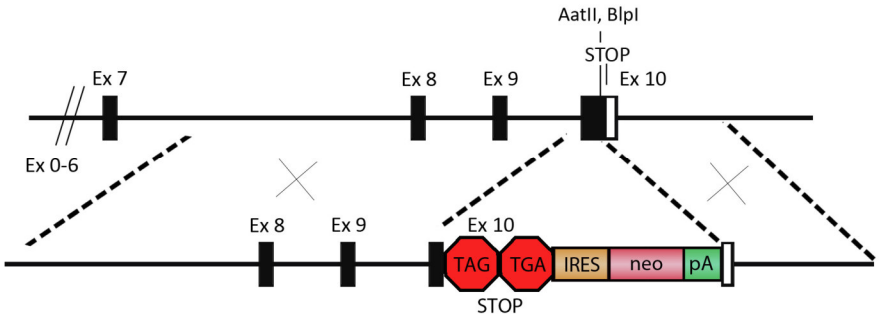

Figure 10: Targeting strategy for *ERCC1* gene locus to introduce Δ7 mutation by homologous recombination. **Top:** Overview of porcine *ERCC1* gene locus. Translated exons are black, untranslated white. **Below:** Promotor trap targeting vector (No. 758). Short and long homology arms are shown by black and white boxes. Yellow, red and green boxes represent internal ribosome entry site (IRES), neomycin resistance gene (neo) and poly A signal (pA). Two premature stop codons are located seven amino acids in front of the endogenous stop codon indicated with red stop signs.

After linearisation one to five µg of the Δ7 promotor trap targeting vector were transfected in MSCs and KDNFs, isolated from a black mini-pig (bmp 2506 MSC/KDF). After six rounds of transfection unfortunately no neo-resistant single cell clone positive for gene targeting could be identified.

3.1.3.2 Introducing loxP binding sites by promotor trap strategy

To introduce loxP sites in the *ERCC1* gene a promoter trap targeting vector (No. 757) was generated. It consisted of a 1 kb 5` short homology arm and a 6 kb 3` long homology arm. To

enable selection, the vector contained a promoterless blasticidin S resistance gene (BS). Two loxP sites, one at the end of the selection cassette and therefore in front of exon two and one after exon three, were added to obtain a conditional knockout. By using Cre recombinase in the living animal exon two and three can be cut out at any time and in a tissue-specific manner. Furthermore, the cassette was flanked by rox sites, because expression of selection gene leads to transcriptional termination and by the use of Dre recombinase these elements can be removed leaving one rox site and two loxP sites (see Figure 11).

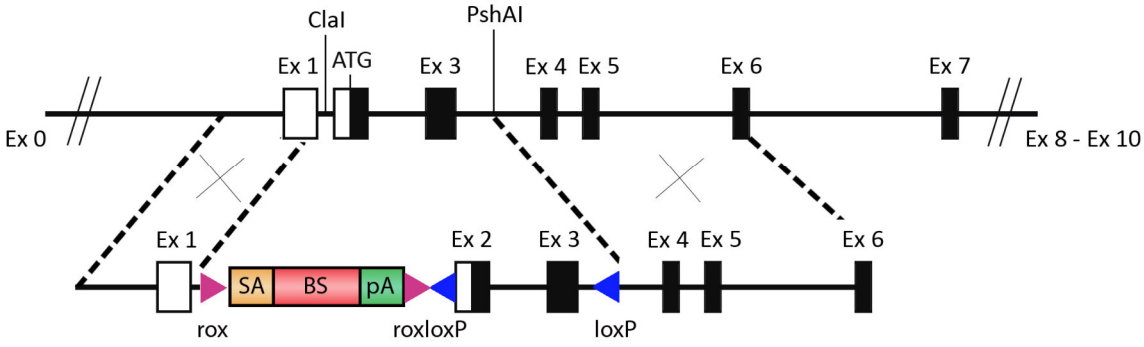

Figure 11: Schematic overview of *ERCC1* gene locus and promotor trap targeting vector for homologous recombination.
Top: Organisation of porcine *ERCC1* gene locus. Translated exons are black, untranslated white. **Below:** Promotor trap targeting vector (No. 757). Short and long homology arm are shown by black and white boxes. Yellow, red and green boxes represent splice acceptor (SA), blasticidin S resistance gene (BS) and poly A signal (pA). The selection cassette is flanked by rox sites, indicated with purple triangles. Blue triangles show positions of loxP sites.

To introduce loxP sites into the *ERCC1* gene locus, the promotor trap targeting vector was linearised and 5 µg were electroporated in MSCs of different isolates (bpm MSC 2506, LR MSC 110111). To verify correct targeting events BS-resistant cell pools and single cell clones were screened by PCR. Primers were designed to bind upstream of the short arm of the targeting vector (ERCC1_In1F3) and in the splice acceptor or the beginning of the BS resistance gene (ERCC1_SA_R, ERCC1_BS_R). After five rounds of transfection unfortunately no positive clone could be identified and all isolated cell pools were negative for successful targeting events.

3.1.4 CRISPR/Cas9-mediated gene targeting

It was difficult to get positive clones with promotor trap strategy (based on HR), thus a new strategy was designed. It is known that HR of a targeting vector into a genomic locus can be inefficient especially in primary somatic cells (Porteus 2007). However, the targeting event

can be stimulated by introducing double-strand breaks (DSBs) into the genomic locus of interest. It was shown that combination of designed endonucleases and donor templates can increase gene targeting frequencies four-, to eight-fold in mouse embryos and in *D. melanogaster* even ten-fold (Bibikova et al. 2003, Panda et al. 2013). Therefore, the CRISPR/Cas9 system was used to mediate gene targeting.

3.1.4.1 Introducing the Δ7 mutation

In order to use HDR for gene editing the DNA repair template containing the desired modification has to be delivered to the cells together with gRNA and Cas9 endonuclease. gRNAs were designed in exon ten of the *ERCC1* gene and used to introduce the Δ7 mutation. Furthermore, two different repair templates – a targeting vector (double-stranded plasmid DNA) and single-stranded oligodeoxyribonucleotide (ssODN) - were designed.

3.1.4.1.1 Homology directed repair with targeting vector

Efficient HDR requires that the DNA repair template contains homologous regions immediately upstream and downstream of the gRNA site. Thus, to avoid long parts without sequence homology a vector (No. 759) without selection system and only containing three times stop codons at the correct position was used (see Figure 12). Homologous arms were designed with about one kb length each site (Zhang et al. 2017). A suitable gRNA (CRISP-ERCC1_Ex10-2) was cloned in the pX330-MCS-Cas9 vector (No. 705) for DNA transfection.

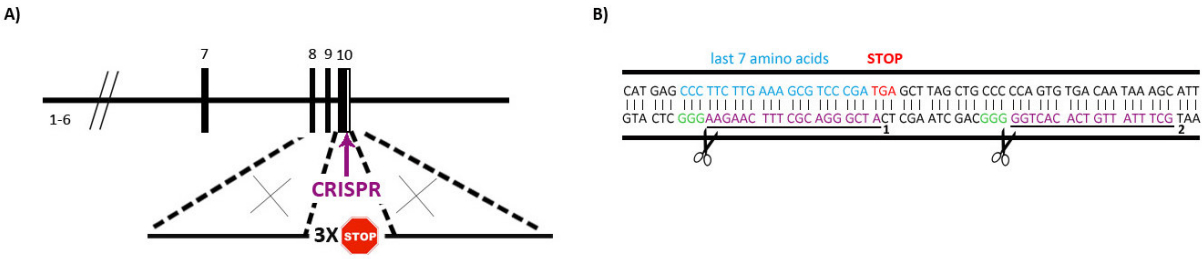

Figure 12: Strategy for CRISPR/Cas9-mediated introduction of the Δ7 mutation.
A) schematic overview of the CRISPR cutting site and the donor template (No. 759). The gRNA introduces a DSB in exon ten and the cotransfected targeting vector can be used for HDR. B) part of the sequence of exon ten. The gRNA recognises a sequence only few base pair downstream of the last seven amino acids and the stop codon of the *ERCC1* gene. gRNA recognition sites are marked in violet and protospacer adjacent motive (PAM) in green.

As a first step, the most efficient method of delivering vectors containing Cas9 and gRNA together with DNA repair template into the cells was tested. For this both lipofection and nucleofection have been used. For lipofection 200-600 ng and for nucleofection 1.2-5 µg of linearised targeting vector (NotI) were transfected. Since NHEJ with the use of CRISPR/Cas9

system occurs more often compared to HDR the plasmid containing the CRISPR/Cas9 system was conducted in lower amounts, only 100-300 ng were used for lipofection and 600 ng for nucleofection. Correct targeting events were analysed by screening PCR with the use of forward primer designed to bind to the modified sequence (ERCC1_D7_STOP_F) and a reverse primer binding downstream of the 3` homology arm in exon ten of the *ERCC1* gene (ERCC1_Ex10_R5) giving a fragment of 1354 bp (see Figure 14).

Only if screening of transfected cell pool showed a signal by PCR single cell clones were isolated and analysed. Several transfections were performed and ten out of eleven cell pools (91 %) had a positive signal. In total 156 single cell clones resulting from lipofection and 390 from nucleofection were tested. Only four positive clones were found after nucleofection, but they failed to grow. Targeting efficiency was about 1 % for nucleofection (see Table 21).

Table 21: Targeting efficiencies after transfection of different cell types.

	transfection method	No. of screened clones	No. of clones with mutations	No. of viable clones	percentage	total
bmp m KDF 280515	lipofection	104	0	-	0 %	0 %
bmp m MSC 250614	lipofection	52	0	-	0 %	
bmp m KDF 250614	nucleofection	79	4	0	5.1 %	1 %
bmp m KDF 230715	nucleofection	104	0	-	0 %	
LR m KDF R26 F4	nucleofection	79	0	-	0 %	
LR m KDF 266	nucleofection	128	0	-	0 %	
Total	nucleof./lipof.	546	4	0	0.73 %	0.73 %

One drawback of this approach is the lack of a selection system for positive targeting events. Nevertheless, having a targeting vector containing a selection cassette means working with a much larger plasmid. To maintain the small size of the targeting vector a vector containing CRISPR/Cas9 components and additionally a puromycin resistance gene (puro) was used (No. 842). After 48 h of selection only cells containing at least the CRISPR/Cas9 components survive. Due to shorter selection time it is possible to enrich for cells expressing Cas9, but the probability of stable integrations is reduced compared to other selection systems that take up to 14 days. gRNA Ex10-2 (CRISP-ERCC1_Ex10-2) was cloned into the pX459-Cas9-

puro vector and nucleofection and screening PCR was conducted as mentioned above (see 3.1.4.1.1; see Figure 14).

Although, stable transfections are more efficient when using linear DNA a circular donor vector was used, because donor topology can have an influence on HDR and circular, supercoiled donors are more stable and can be used for efficient gene targeting (Orlando et al. 2010, McLenachan et al. 2007). The circular vector was nucleofected as mentioned above into different cell isolates and screening of all pools showed a posititve signal by PCR. Three positive clones were found and frozen. Using a circular vector in combination with a selection system increased targeting efficiency from about 1 % to 3 % (see Table 22). The frozen positive clones have been used for further analysis (see 3.1.4.1.3).

Table 22: Targeting efficiencies using a circular donor vector and puromycin selection.

	transfection method	No. of screened clones	No. of clones with mutations	No. of viable clones	percentage	total
bmp m KDF 230715	nucleofection	56	0	-	0 %	2.9 %
Hyb f KDF 200416	nucleofection	48	3	3	6.2 %	
Total	nucleofection	104	3	3	2.9 %	2.9 %

3.1.4.1.2 Transfection of single-stranded oligodeoxyribonucleotides (ssODN)

It was shown that combining the CRISPR/Cas9 system and a single-stranded oligodeoxyribonucletiode (ssODN) can have higher targeting efficiencies than those obtained with a dsDNA donor plasmid of the same length. Furthermore, synthesis of a ssODN is much easier than generation of most of the dsDNA donor plasmids (Yang et al. 2013, Richardson et al. 2016). The desired sequence modifications are small – only 9 bp three times STOP codon and 6 bp exchanged sequence afterwards – and 60 bp of homology arms each site are sufficient for HDR with a ssODN. Hence, it was designed with 51 bp 5` homology arm and 64 bp 3` homology arm (ERCC1_Ex10_STOP, No. 43b) and was used together with two different gRNAs (see Figure 13). Different transfection methods were tried to optimise the simultaneous delivery of ssODN and CRISPR/Cas9 components. Since some kits were specified for delivery of small molecules it was decided to avoid vectors containing the CRISPR/Cas9 plasmid system but using RNA in these cases. Therefore, two different gRNAs (CRISP-ERCC1_Ex10-2, CRISP-ERCC1_Ex10-1) were cloned in the pBS-U6-chimaric vector and

it was used for transcription of RNA *in silico.* For nucleofection the pX330-MCS-Cas9 vector (No. 705) containing gRNA CRISP-ERCC1_Ex10-2 was used.

Figure 13: Gene targeting using CRISPR/Cas9 system and a ssODN.
A) A combination of CRISPR/Cas9 and donor ssODN can be used for HDR. B) Two different gRNAs have been tested. The gRNAs recognise a sequence near the position of the last seven amino acids of the *ERCC1* gene. gRNA recognition sites are marked in violet and PAM in green.

Two different kits, one specialised for transfection of oligos (TransIT®-Oligo Transfection Reagent) and the other for transfection of RNA (Stemfect™ RNA Transfection Kit) were used. But, none of the kits showed a better or even similar efficiency compared to nucleofection. Since the pools and eGFP controls already showed a very low transfection efficiency no single cell clones were generated and further experiments were conducted with nucleofection.

For nucleofection 3-5 µg of ssODN was transfected together with 200-600 ng of the pX459-Cas9-Puro-gRNA-ERCC1-E10-2 vector (No. 68). Correct targeting events were analysed by screening PCR mentioned above (see 3.1.4.1.1; see Figure 14). Only if the cell pool showed the 1354 bp fragment indicating a positive targeting event single cell clones were generated and analysed.

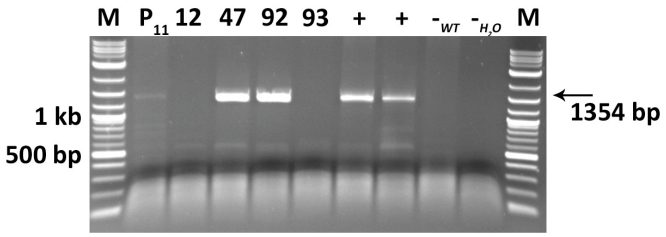

Figure 14: Examples for screening of pools and single cell clones.
Screening PCR of pools and single cell clones. M: 2-Log DNA ladder; P_{11}: cell pool; 12,47,92,93: single cell clones; +: positive control; $-_{WT}$: wildtype control; $-_{H2O}$: water control. The forward primer can only bind if a targeting event took place. Therefore, only positive clones show the expected band of 1354 bp. Wildtype and water control show no band.

All pools showed a posititve signal by screening PCR and a total of 312 single cell clones were screened for a positive targeting event. Five positive clones were found, but only one could

be expanded enough for cryoconservation. Targeting efficiency was about 1.6 % (see Table 23).

Table 23: Targeting efficiencies for CRISPR-Cas9-mediated gene targeting using ssODN.

	transfection method	No. of screened clones	No. of clones with mutations	No. of viable clones	percentage	total
bmp m KDF 250614	nucleofection	41	0	-	0 %	1.6 %
bmp m KDF 230715	nucleofection	216	4	1	2 %	
LR m KDF R26 F4	nucleofection	55	1	-	2 %	
Total	nucleofection	312	5	1	1.6 %	1.6 %

Since efficiency was still not very high an asymmetric oligo was considered to be used. It was shown that Cas9 asymmetrically releases the 3` end of the nontarget DNA strand and by designing the ssODN complementary to the strand that is released first the rate of HDR increases (Richardson et al. 2016). However, using an asymmetric oligo did not improve the targeting efficiency and after transfection no positive single cell clones were found.

The gRNA CRISP-ERCC1_Ex10-2 was cloned in the pX459-Cas9-puro vector (No. 842), which contains a puromycin resistance gene (puro) and allows enrichement of Cas9 expressing cells. Nucleofection and screening PCR was conducted as mentioned above (see 3.1.4.1.1; see Figure 14). Transfections have been done in three different cell isolates, 75 % of screened cell pools showed a positive signal by PCR and using selection increased targeting efficiency three-fold. Out of 149 cell clones seven positive clones were identified and frozen (see Table 24).

Table 24: Targeting efficiencies using a ssODN donor template and puromycin selection.

	transfection method	No. of screened clones	No. of clones with mutations	No. of viable clones	percentage	total
Hyb f KDF 200416	nucleofection	95	6	6	6.3 %	4.7 %
Hyb f KDF 130617	nucleofection	35	0	-	0 %	
Hyb m KDF 040717 (915)	nucleofection	19	1	1	5.2 %	
Total	nucleofection	149	7	7	4.7 %	4.7 %

Frozen clones have been further analysed (see 3.1.4.1.3).

3.1.4.1.3 Characterisation of positive clones (*ERCC1* Δ7)

As mentioned above several clones were positive for a targeting event according to 3` junction PCR and were frozen. Before using these clones for SCNT (somatic cell nuclear transfer) further analysis was necessary. Since the CRISPR/Cas9 system was used the second allele should be tested for unwanted indels. For this, primers binding 384 bp upstream (ERCC1_Ex9F) and 314 bp downstream (ERCC1_Ex10R8 156) of the introduced stop codons were designed that give an amplicon of 713 bp. As they bind both targeted and wt alleles it was necessary to sequence the PCR product to exclude editing of the second allele (see Figure 15). Only two clones after transfection of a ssODN and two clones after transfection of a double cut donor plasmid showed fragments with the correct size. Some clones showed only one band of a wrong size and others a double band. These results indicate a targeting event at the correct position but wrong recombination. To analyse the fragments more in detail the DNA sequence was determined. Only one clone (No. 3) showed correct sequence, all others had unwanted indels either in the targeted or the second allele (see Figure 15).

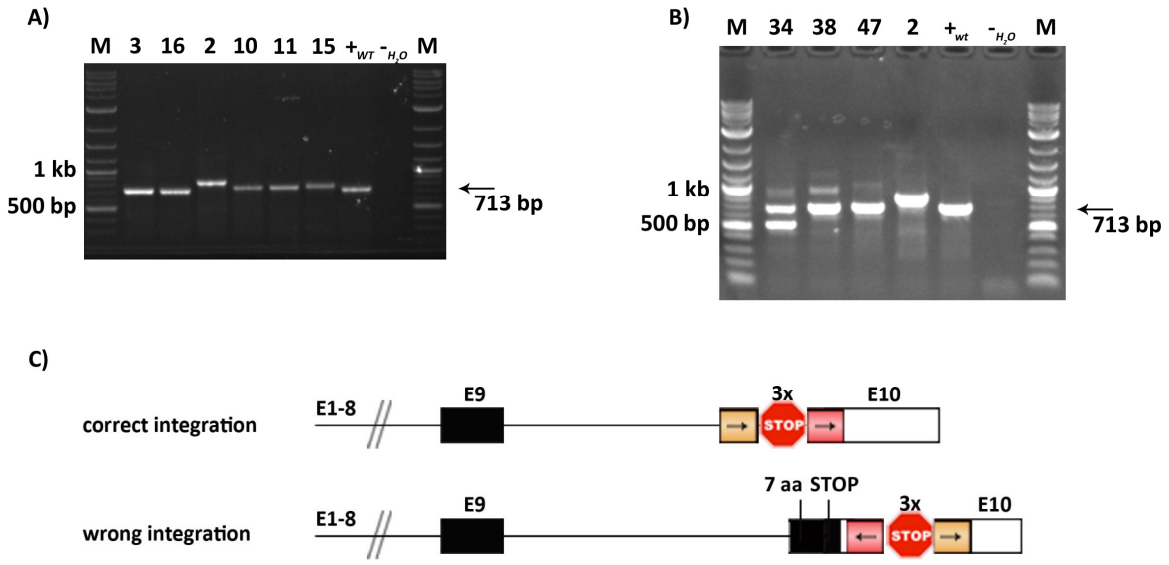

Figure 15: Analysis of the second allele after a positive targeting event.
M: 2-Log DNA ladder; 3,16,2,10,11,15,34,38,47: single cell clones; $+_{WT}$: wildtype control; $-_{H2O}$: water control. A) Screening PCR of the second allele of positive clones after transfection of CRISPR/Cas9 and ssODN. Only two cell clones, 3 and 16, showed a 713 bp fragment. B) Screening of the second allele after transfection of CRISPR/Cas9 and double cut donor vector (34,38,37) or ssODN (2). Only two clones, 38 and 47 showed a band with the correct size. C) Example of an unwanted recombination within the targeted allele. Red and orange indicate the homologous regions of the ssODN, arrows show the orientation. The premature stop codons are indicated with red stop signs.

3.1.4.2 Introducing loxP sites

Introducing the Δ7 mutation and working with a promotor trap targeting vector for introducing loxP sites showed that modifiying the ERCC1 gene is challenging. These strategies had the main drawback that the coding sequence of the gene itself is disrupted and clones correctly modified might lack DNA repair function. The hope was that this problem could be solved by using gRNAs for intronic or exonic regions combined with vectors or ssODN containing loxP sites and homologous regions. For better efficiencies a combination of donor templates and CRISPR/Cas9 system was conducted and several locations and strategies have been tried out (see Figure 16). Deletion of either exon four, five or six leads to a frameshift and premature stop codon. These locations have been chosen for targeting. Further details can be found in the next sections.

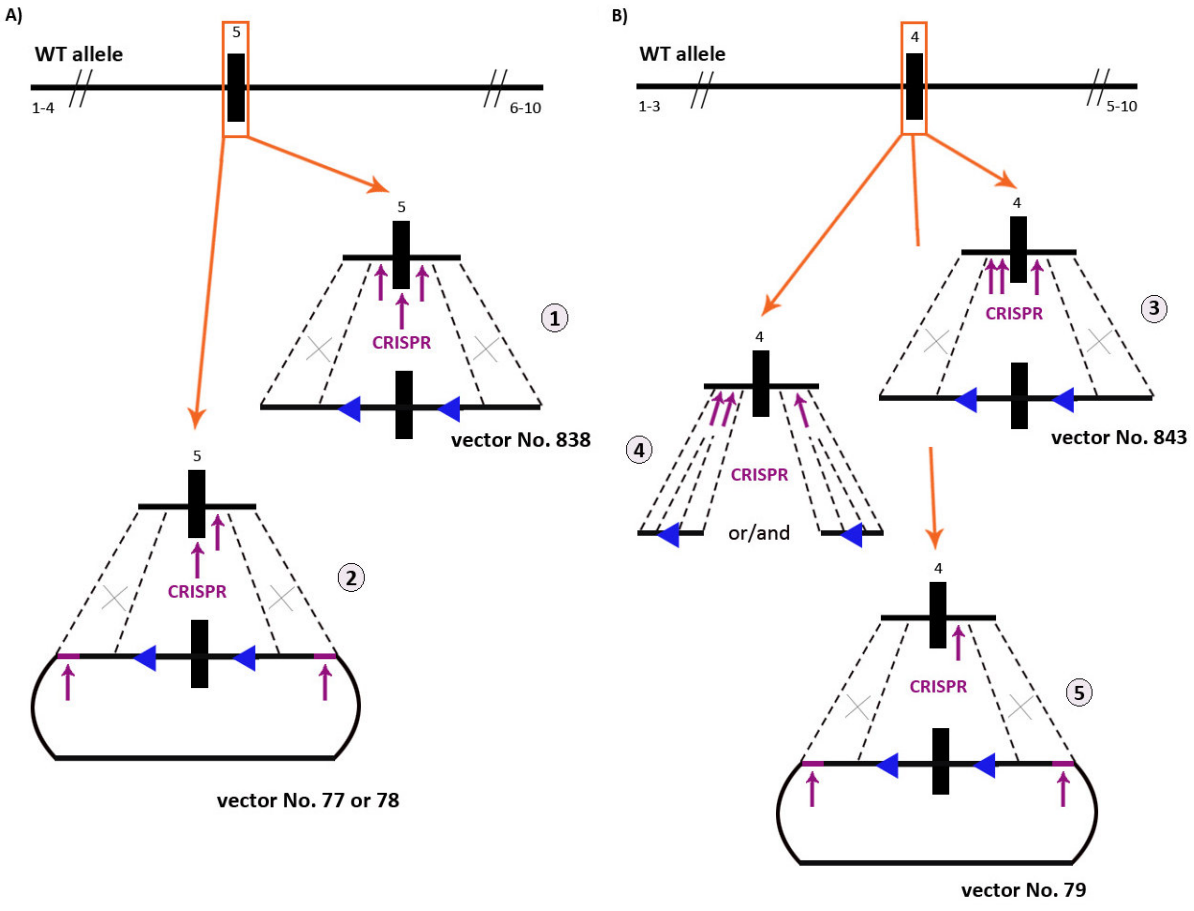

Figure 16: Strategies for introducing loxP sites on different target sites.
Different strategies to introduce loxP sites with the help of the CRISPR/Cas9 system and donor templates. gRNA recognition sites are indicated with violet arrows, loxP sites with blue triangles. A) Strategy for introducing loxP sites around exon five. Different gRNAs were combined with (1) a targeting vector (No. 838), or (2) a double cut vector (No. 77, 78). B) To introduce loxP sites around exon four (3) a targeting vector (No. 843), or (4) ssODNs or (5) a double cut vector (No. 79) was used.

3.1.4.2.1 Flanking exon 5 (**A**)

Exon five is 100 bp in length and critical to *ERCC1* function. Work in mice has shown that disruption of exon five causes functional inactivation of the gene (McWhir et al. 1993). To target porcine *ERCC1* exon five, three different gRNAs (CRISPR-ERCC1_Ex5-1, CRISP-ER_In4-2, CRISP-ER_In5-1) in combination with a targeting vector (strategy 1) or double cut vectors (strategy 2) were used. gRNAs were eiter cloned into the pX330-MCS-Cas9 vector (No. 705 see 2.1.12) or in a vector containing the Cas9 enrichment system (No. 842 see 2.1.12). The following strategies (see Figure 16) were used to introduce loxP sites flanking exon 5.

Strategy 1: The donor DNA (No. 838 see 2.1.12) consisted of exon five flanked by loxP sites and 1 kb of intron three, exon four and intron four and 0.2 kb intron 5. For nucleofection, 5 μg linearised (NotI) targeting vector was cotransfected with 400-600 ng of the plasmids containing gRNA Ex5-1 or In4-2 or In5-1 (No. 40, 52 and 53; with selection No. 63, 64 and 65 see 10.2).

Strategy 2: gRNA binding sites for either gRNA Ex5-1 or gRNA In5-1 were added to the same donor template as used for strategy 1 resulting in double cut vectors (No. 77 and 78 see 2.1.12). For nucleofection, 5 μg double cut donor template was cotransfected with 400-600 ng of plasmids containing gRNAs Ex5-1 or In5-1 and Cas9 enrichment system (No. 63, and 65).

Positive targeting events were screened by PCR using a forward primer (ERCC1_loxP5F 137) binding partly in loxP sequence and a reverse primer (ERCC1_Sq49_496R) binding 244 bp downstream of the 3` end of the targeting vector generating a 720 bp fragment (see Figure 17 and Figure 18 C).

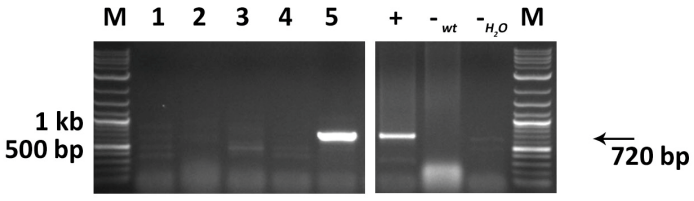

Figure 17: Examples for screening PCR of single cell clones.
Screening PCR of single cell clones after targeting of exon 5. M: 2-Log DNA ladder; 1,2,3,4,5: single cell clones; +: positive control; -WT: wildtype control; -H2O: water control. The forward primer can only bind if a targeting event took place. Therefore, only positive clones show the expected band of 720 bp. Wildtype and water control show no band.

Several different cell types were transfected and screened and 57 % of screened cell pools had a positive signal by PCR. 4 clones showed positive 3` junction PCR for strategy 1 and the best targeting efficiency of screened cell clones showed gRNA In5-1 with 2.5 %, whereas gRNA In4-2 did not work and gRNA Ex5-1 gave efficiencies between 0 % and 2.9 % depending on the cell type (see Table 25). With 14 cell clones positive for 3` junction PCR strategy 2 was more successful and the targeting efficiency increased from 0.5 % to 1 % for gRNA Ex5-1 and from 2.5 % to 15 % for gRNA In5-1 (see Table 25).

Table 25: Targeting efficiencies after transfection of different gRNAs.

targeting vector (No. 838)	gRNA	puromycin selection	No. of screened clones	No. of clones with loxP	No. of viable clones	percentage	total
bmp m KDF 230715	Ex5-1	NO	307	1	0	0.3 %	0.3 %
	Ex5-1	YES	34	1	1	2.9 %	0.5 %
Hyb f KDF 200416	Ex5-1	YES	320	1	1	0.3 %	
Hyb f KDF 130617	Ex5-1	YES	51	0	-	0 %	
Hyb f KDF 200416	In5-1	YES	29	0	-	0 %	2.5 %
bmp m KDF 230715	In5-1	YES	11	1	1	9 %	
Hyb f KDF 200416	In4-2	YES	43	0	-	0 %	0 %
Total	-	-	795	4	3	0.5 %	0.5 %

dc targeting vectors (No. 77 and 78)	gRNA	puromycin selection	No. of screened clones	No. of clones with mutations	No. of viable clones	percentage	total
Hyb f KDF 200416	Ex5-1	YES	58	0	-	0 %	1 %
Hyb f KDF 130617	Ex5-1	YES	46	1	1	2.2 %	
Hyb f KDF 200416	In5-1	YES	87	13	13	15 %	15 %
Total	-	-	191	14	14	7.3 %	7.3 %

DSBs get repaired either by HDR or NHEJ, thus blocking the latter with an inhibitor such as SCR7 (5,6-bis((E)-benzylideneamino)-2-mercaptopyrimidin-4-ol) can increase efficiency of HDR-mediated gene targeting. SCR7 is a small molecule inhibitor that mediates degradation of DNA ligase IV, a key player in the NHEJ pathway (Maruyama et al. 2015). To analyse the effect of a NHEJ blocker different cell isolates were nucleofected with 5 µg linearised (NotI) targeting vector (No. 838 see 2.1.12) and 500 ng of the plasmid containing gRNA Ex5-1

(No. 63 see 10.2). Cells expressing CRISPR/Cas9 have been enriched by a puromycin selection and simultanously 10 µM SCR7 was added to the medium. To analyse positive targeting events PCR was conducted as mentioned above (see 3.1.4.2.1) Cell pools were screened and 67 % had a positive signal by PCR. Adding SCR7 showed no clear effect on targeting efficiency (see Table 26).

Table 26: Targeting efficiencies after addition of SCR7.

SCR7	gRNA	puromycin selection	No. of screened clones	No. of clones with mutations	No. of viable clones	percentage	total
bmp m KDF 230715	Ex5-1	YES	26	0	-	0 %	1.7 %
Hyb f KDF 200416	Ex5-1	YES	89	2	2	2.2 %	
Total	-	-	115	2	2	1.7 %	1.7 %

3.1.4.2.2 Flanking exon 4 (**B**)

Exon 4 has a length of 104 bp, and deletion of it leads to a frameshift and premature stop codon. To combine a targeting vector (strategy 3) or ssODNs (strategy 4) or a double cut targeting vector (strategy 5) with gRNAs, two different gRNAs (CRISPR-ERCC1_In4-1, CRISPR-ERCC1_In3-2) were cloned into the vector pX330-MCS-Cas9-puro (No. 841 see 2.1.12) by Stephan Rambichler (Master student, 2016). Another gRNA (CRISP-ER_In3-3) was cloned into the vector pX330-MCS-Cas9-puro (No. 841 see 2.1.12) and added to the vector pX330-Cas9-puro-gRNA-ERCC1-I4-1 (No. 61 see 10.2) by Melanie Manyet (Master student, 2017). The following strategies (see Figure 16) were used to place loxP sites flanking exon 4.

Strategy 3: A donor template (No. 843 see 2.1.12) consisting of exon 4 flanked by loxP sites and 1.5 kb of intron 3 and 1 kb intron 4, exon 5 and intron 5 was generated by Stephan Rambichler. Transfections of the donor plasmid combined with gRNAs and analysis of single cell clones were conducted by Stephan Rambichler and Melanie Manyet. Additional nucleofections of 5 µg linearised (NotI) targeting vector and 400-600 ng of the plasmids carrying gRNA In3-2 or In4-1 (No. 60 and 61 see 10.2) were carried out.

Strategy 4: Asymmetric ssODNs, each containing loxP sites flanked with 36 bp 5` homology region and 91 bp 3` homology region, were cotransfected with the same gRNAs used in strategy 3. Transfection and screening of cell clones were conducted by Stephan Rambichler.

Strategy 5: To generate a double cut vector (No. 79 see 2.1.12), gRNA In4-1 binding site was added to the same donor template as used for strategy 3. For nucleofection 400-600 ng of plasmids containing gRNA In4-1 and Cas9 enrichment system (No. 61 see 10.2) and 5 μg of the double cut donor template were cotransfected.

For the screening PCR, a forward primer was used that bound to part of intron three and the loxP site (ERCC1_LoxPIn3F2) with a reverse primer that bound 244 bp downstream of the 3` end of the targeting vector (ERCC1_Sq49_496R) resulting in an 1840 bp fragment (data not shown). Positive clones were further analysed for correct integration of both loxP sites by another screening PCR using primers that bound to part of intron four and the loxP site (ERCC1_In4F_loxP) and the same reverse primer as above (ERCC1_Sq49_496R) (data not shown).

After several transfections of different combinations of gRNAs and donor templates in total seven viable clones having both loxP sites were generated, frozen and a detailed analysis was carried out (see 3.1.4.2.3). HDR-mediated targeting with the use of a ssODN donor template for intron three or four (strategy 4) did not generate any positive single cell clones. Using a targeting vector and different gRNA combinations (strategy 3) resulted in a targeting efficiency between 0-3.1 %. Using only gRNA In4-1 instead of two gRNAs increased the efficiency no matter if a normal or a double cut vector was used. The use of a double cut donor vector (strategy 5) did not increase targeting efficiency (see Table 27).

Adding the NHEJ blocker SCR7 (see 3.1.4.2.1) to the medium showed no clear effect (work was carried out by Melanie Manyet).

Table 27: Targeting efficiencies after transfection of ssODN or targeting vectors in combination with gRNAs.

ssODN	gRNA	donor template	puromycin selection	No. of screened clones	No. of clones with loxP	No. of viable clones	percentage
bmp m KDF 230715[*1]	In4-1	ssODN In4	YES	17	0	-	0 %
bmp m KDF 230715[*1]	In3-2 In4-1	ssODN In3, In4	YES	2	0	-	0 %
Hyb f KDF 200416[*1]	In3-2	ssODN In3	YES	45	0	-	0 %
Hyb f KDF 200416[*1]	In4-1	ssODN In4	YES	50	0	-	0 %
Total	-	-	Yes	114	0	-	0 %

targeting vector (No. 838)	gRNA	donor template	puromycin selection	No. of screened clones	No. of clones with both loxP	No. of viable clones	percentage
Hyb f KDF 200416[*1]	In3-2 In4-1	TV loxP$_2$ ex4	YES	43	0	-	0 %
Hyb f KDF 200416[*2]	In3-2 In4-1	TV loxP$_2$ ex4	YES	126	3	3	2.4 %
Hyb f KDF 200416[*2]	In3/4	TV loxP$_2$ ex4	YES	79	2	2	2.5 %
Hyb f KDF 200416[*2]	In3-3	TV loxP$_2$ ex4	YES	48	0	-	0 %
Hyb f KDF 200416[*2]	In4-1	TV loxP$_2$ ex4	YES	65	2	1	3.1 %
bmp m KDF 230715[*2]	In3-2 In4-1	TV loxP$_2$ ex4	YES	33	0	-	0 %
Hyb f KDF 200416	In3-2 In4-1	TV loxP$_2$ ex4	YES	28	0	-	0 %
bmp m KDF 230715	In3-2 In4-1	TV loxP$_2$ ex4	YES	11	0	-	0 %
Total	-	-	Yes	433	7	6	1.6 %

dc targeting vector (No. 79)	gRNA	donor template	puromycin selection	No. of screened clones	No. of clones with both loxP	No. of viable clones	percentage
Hyb f KDF 200416	In4-1	TV loxP$_2$ ex4 dc	YES	29	1	1	3.4 %
Hyb f KDF 200416	In3-2 In4-1	TV loxP$_2$ ex4 dc	YES	32	0	-	0 %
Total	-	-	Yes	61	1	1	1.6 %

[*1] Transfections and screening of cell clones were conducted by Stephan Rambichler
[*2] Transfections and screening of cell clones were conducted by Melanie Manyet

3.1.4.2.3 Characterisation of positive clones (*ERCC1* loxP)

All clones that showed a positive 3` junction PCR were characterised in more detail. First, the screening PCR containing both loxP sites (see Figure 18 C) was sequenced to verify correct integration. For flanking exon five, 12 out of 19 analysed cell clones were positive for the presence of correct loxP sites (see Figure 19 A). It was not possible to verify correct integration of loxP sites flanking exon four for any of the 7 clones analysed (work was carried out by Melanie Manyet). Further analysis by other PCRs can be found in the next sections (see Figure 18).

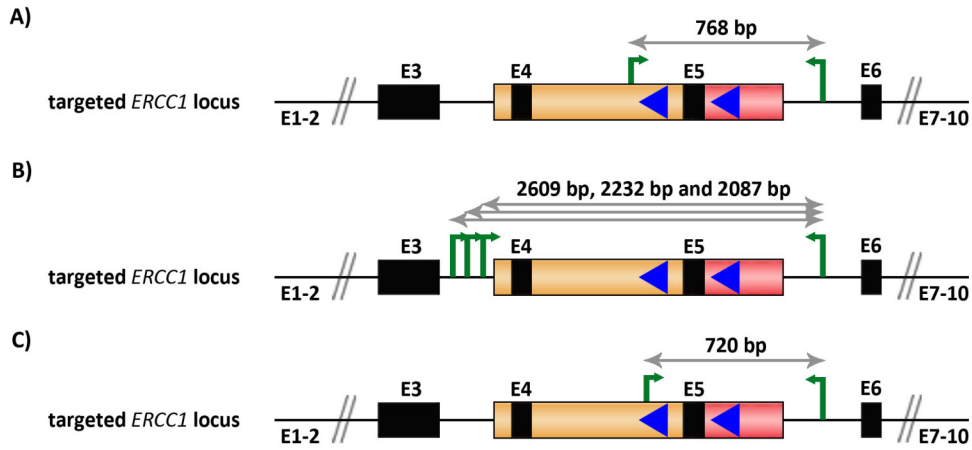

Figure 18: Strategy for PCRs used to characterise single cell clones.
Single cell clones with a positive 5` junction PCR were further characterised by different PCRs. Red and orange boxes indicate the homologous regions of the targeting vector. Black boxes show the exons, primer binding sites are indicated with green arrows, loxP sites with blue triangles. A) PCR to analyse the genotype of the cell clones generating a 768 bp for the targeted allele (700 bp for wildtype). B) PCR analysis to characterise the 5' and 3' junction regions of the targeted *ERCC1* locus. Different primer pairs were used resulting in 2087 bp, 2609 bp and 2232 bp amplified fragments for wildtype alleles, and 2155 bp, 2677 bp and 2300 bp fragments for targeted alleles. C) Screening PCR of single cell clones after targeting of exon 5. The forward primer can only bind if a targeting event took place. Therefore, only positive clones show the expected band of 720 bp.

Second, another PCR analysis was conducted using primers ERCC1_In4F3 136 and ERCC1_Sq49_496R, which generated a 700 bp fragment for the wildtype allele and a 768 bp fragment for a targeted allele, to investigate the genotype of the cells and to test the second allele for the presence of unwanted indels introduced by the CRISPR/Cas9 system (see Figure 18 A and Figure 19 B). Most clones showed either a heterozygous or even a homozygous genotype.

Third, PCR analysis was carried out to characterise the 5' and 3' junction regions of the targeted *ERCC1* locus (see Figure 18 B). For this, different primer pairs were used (ERCC1_In4F and ERCC1_Sq49_496R; ERCC1_In3_F3 and ERCC1_Sq49_496R; ERCC1_In3_F6 and ERCC1_Sq49_496R), but all primer combinations generated only very faint bands for the wildtype allele (2087 bp, 2609 bp and 2232 bp depending on the used primer pair) and no band for the floxed allele (68 bp bigger than the wildtype band). Interestingly, clones with a homozygous genotype showed no band at all (for example clone No. 4 and 11) independent of the primer pairs used (see Figure 19 C). As the PCR analysis across the 5' and 3' junction regions showed unclear results, loxP sites were tested for functionality and RNA was analysed.

To test the functionality of the loxP sites, Cre protein was transduced into the cells identified as having loxP sites flanking exon five (see 2.2.3.7). After transduction, clones were screened with the same screening PCR as above (see 3.1.4.2.1 and Figure 18 C). Since transduction of Cre is not 100 % efficient two fragments were expected, one from the intact sequence (720 bp) and a shorter fragment indicating that recombination took place (530 bp). Some of the clones showed both bands consistant with successful recombination. However, these results could not be repeated and sequence analysis of the bands recovered from agarose gel failed due to poor sample quality (see Figure 19 D).

RNA was also isolated from cells with loxP sites flanking exon five and from cells treated with Cre recombinase. RT-PCR was conducted using primers that bound within exons two (ERCC1_Ex2F) and six (ERCC1_Ex6R). Amplification was expected to produce 577 bp fragments for both wild type and floxed alleles, since the loxP sites were integrated in introns. Surprisingly, only heterozygous clones and wildtype samples showed the expected band at 577 bp originating from the functional transcript variant. Another fragment, approximately 380 bp, was found in all samples, even the wildtype, and seems to indicate an unknown transcript variant of the *ERCC1* gene. Unfortunately, homozygous clones (No. 4 and 11) showed no correct band for the wildtype transcript (see Figure 19 E) and it was assumed that the transcription of the edited gene is somehow altered, but the exact underlying mechanism is unknown. Unfortunately sequencing of recovered fragments was again not possible due to poor sample quality.

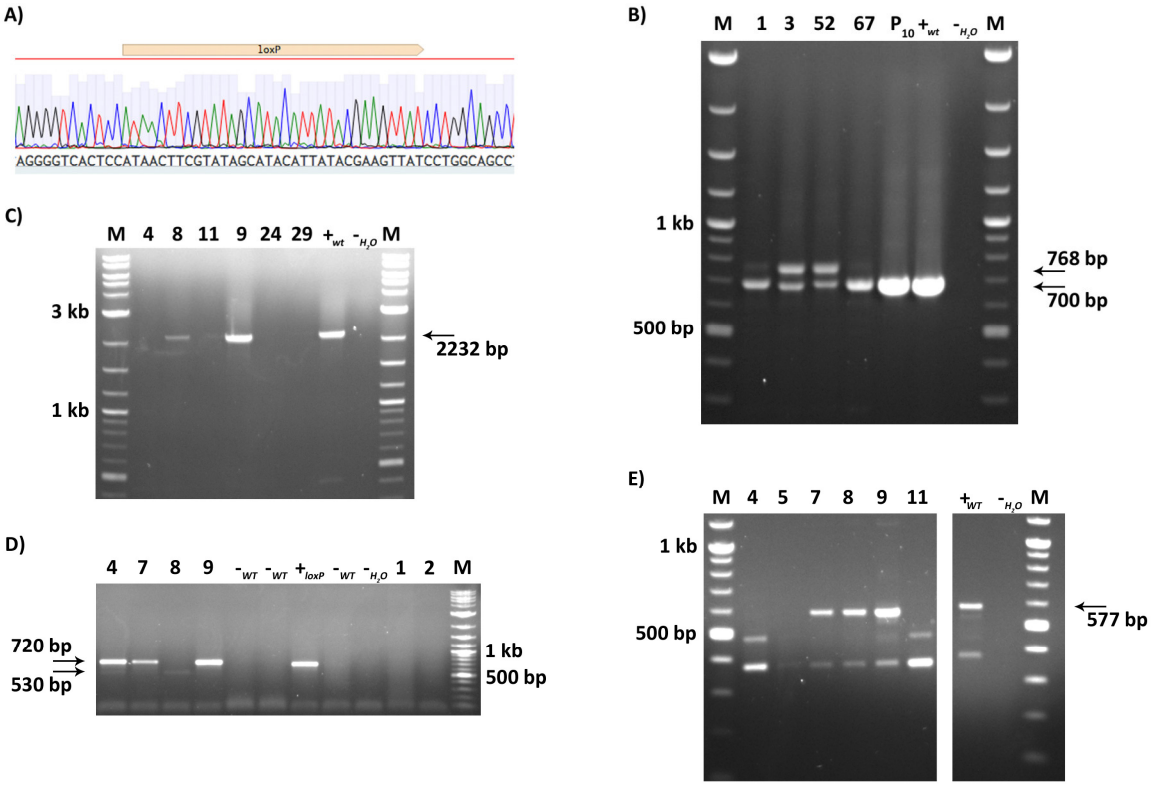

Figure 19: Characterisation of positive targeted clones.
A) Example of a sequencing result of one of the loxP sites flanking exon five. B-E) Further PCR analysis of single cell clones that showed a positive screening PCR. M: 2-Log DNA ladder; 1,3,52,67,4,8,11,9,24,29,7,2,5: single cell clones; P_{10}: cell pool; $+_{WT}$: wildtype control; $-_{H2O}$: water control; $-_{WT}$: negative/wildtype control; $+_{loxP}$: positive control. B) PCR for analysis of the zygosity. For wiltype allele a 700 bp and for a floxed allele a 768 bp fragment was expected. Only two clones (No. 3 and 52) show both bands, two other clones, the pool and the wildtype sample show only one band at 700 bp. C) PCR for generating and analysing the whole targeting vector and parts of the endogenous 3` and 5` regions. None of the clones show the expected band at 2300 bp for floxed alleles. Only heterozygous clones (No. 8 and 9) and wildtype sample show a band at 2232 bp originating from the wildtype allele. Homozygous clones (No. 4 and 11) show no band at all. D) PCR analysis of single cell clones after transduction with Cre recombinase. Only single cell clone No. 8 shows a faint band at 530 bp, indicating a successful recombination. Clone 4, 7 and 9 show a band at 720 bp, expected for floxed alleles before recombination. E) RNA analysis of positive single cell clones. Heterozygous clones (No. 7, 8 and 9) and wildtype samples show the expected band at 577 bp and an unexpected band about 220 bp smaller. Surprisingly homozygous clones (No. 4, 5 and 11) show also the latter band but unfortunately no band at 577 bp but one at about 500 bp.

3.1.5 Conclusion

Although a total of almost 2000 clones for introducing loxP sites and more than 1000 clones for introducing the Δ7 mutation were screened, it was not possible to derive cell clones carrying correct modifications on the *ERCC1* locus. Positive results for the screening of the 3` junction showed that modifications were introduced at the correct position. But, screening on RNA level of clones with loxP sites showed that the targeting was influencing transcription of the gene and some unwanted changes must have taken place upstream of the loxP sites. Positive clones for the Δ7 mutation showed similar results. Most of the clones

had unwanted rearrangements of the ssODN or targeting vector and the gene was not changed as it was desired. Furthermore, viability of targeted clones was low. The conclusion is that the function of this gene is important for cell survival of porcine cells and gene targeting and manipulation in this way is not recommended.

3.1.6 Alternative strategy – *ERCC1* Minigene in *ROSA26* locus

As introducing precise genetic modifications into the endogenous *ERCC1* locus was not successful an alternative strategy was designed. A plan was devised in which a porcine *ERCC1* minigene is introduced into the porcine *ROSA26* locus (see Figure 20). Targeting this locus allows ubiquitous and consistent expression of a transgene without interrupting the function of essential endogenous genes (Fischer et al. 2016, Li et al. 2014a, Li et al. 2014b). The integrated minigene will carry the desired modifications, such as the Δ7 mutation or flanking loxP sites while the endogenous *ERCC1* gene remains fully functional. In a second step one can inactivate the endogenous genes using CRISPR/Cas9, in which case cells will express only the *ERCC1* transgene. gRNAs can be delivered either in the living animal with organ-specific AAVs or in cell culture after successful integration of the minigene. To avoid that the minigene is inactivated by the CRISPR/Cas9 system, silent mutations were introduced in the gRNA binding sites. With this method introduced modifications can be activated more flexible and if negative effects are observed, e.g. in cell culture, timepoint of inactivation can be shifted, e.g. in the living animal.

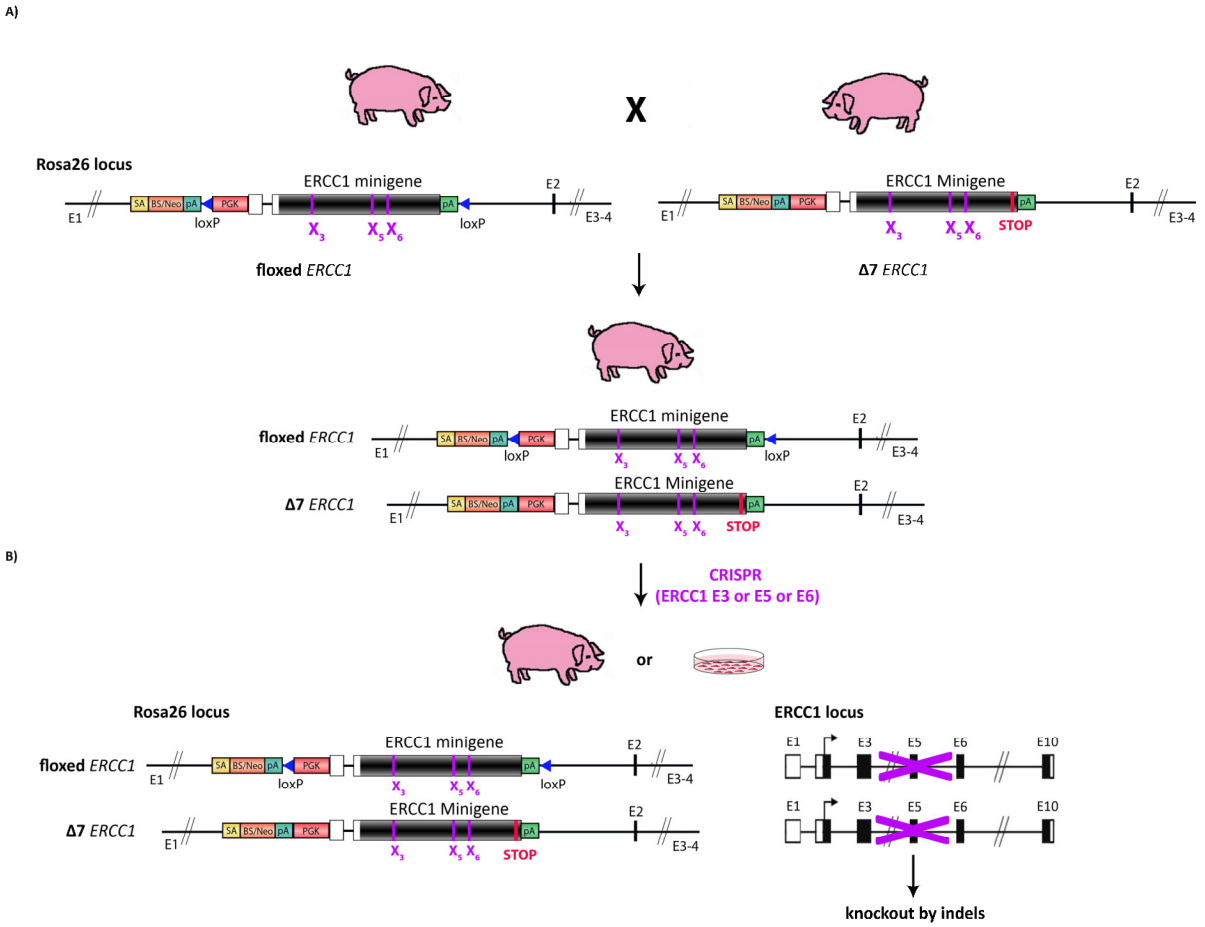

Figure 20: New strategy for generation of a porcine model with an *ERCC1* minigene at the *ROSA26* locus and a knockout of the endogenous *ERCC1* gene.
Yellow, orange, green and red boxes represent splice acceptor (SA), blasticidin S or neomycin resistance gene (BS/neo), poly A signal (pA) and PGK promotor. Blue triangles show positions of loxP sites, mutated gRNA binding sites are highlighted in violet (x_3/x_5/x_6: binding site in exon 3/5/6). A) Pigs having different *ERCC1* minigenes can be bred to generate an animal with *ERCC1* minigenes in both alleles. B) Piglets from the F1 generation and their cells carrying both minigenes can be used to mutate the endogenous *ERCC1* alleles by CRISPR/Cas9. One functional floxed minigene and one minigene carrying the Δ7 mutation would be left. The floxed part can be deleted by introduction of Cre rombinase in a heart-specific manner and the knockout of the floxed allele takes place only in heart.

3.1.6.1 Design of the minigene and gRNAs

gRNAs binding in one of the first six exons were designed, cloned into the vector pX330-MCS-Cas9-puro (No. 841 see 2.1.12), transfected into KDFs isolated from a female hybrid pig (KDF 200416, LRxbmp) and analysed by the webtool TIDE (https://tide.deskgen.com/). Two out of ten gRNAs showed targeting efficiencies higher than 30 % (54 % for Ex3-2 and 31 % for Ex6-2) and have been chosen for further experiments. Sequences of the minigene were changed accordingly to avoid binding and cutting of the two gRNAs and additionally binding site for gRNA Ex5-1, which already showed good results in previous experiments (see 3.1.4.2.1), was modified (see Figure 22). A fragment spanning exon two to exon ten of *ERCC1*

and containing the silent mutations was synthesised by a commercial provider (Integrated DNA Technologies). Exon one to two were added by overlap extension PCR and conventional cloning, as was the Δ7 mutation.

3.1.6.2 Generation of the targeting vector

Since the *ERCC1* gene shows low expression levels in different cell types and tissues a PGK promotor was chosen to ensure moderate expression level of the *ERCC1* minigene. The promotor, a poly A signal and loxP sites have been added by conventional cloning methods (see Figure 22). 5 µg of the vector was nucleofected into KDFs isolated from a female hybrid pig (KDF 200416, LRxbmp) and RNA was isolated from cell pools to test the functionality of the minigene. Sequencing of screening PCR revealed that a transcript containing the introduced mutations in exon 3 exists and therefore minigene is functional (see Figure 21) .

Figure 21: Analysis of functionality of *ERCC1* minigene.
Sequencing of screening PCR for RNA showed that a transcript with mutations in exon 3 exists and the minigene is functional.

A strategy to add 5` and 3` homologous regions to enable targeted insertions into the *Rosa26* locus with a promoter trap targeting vector was designed (see Figure 22), but this work was carried out at the very end of the project period and is still incomlete.

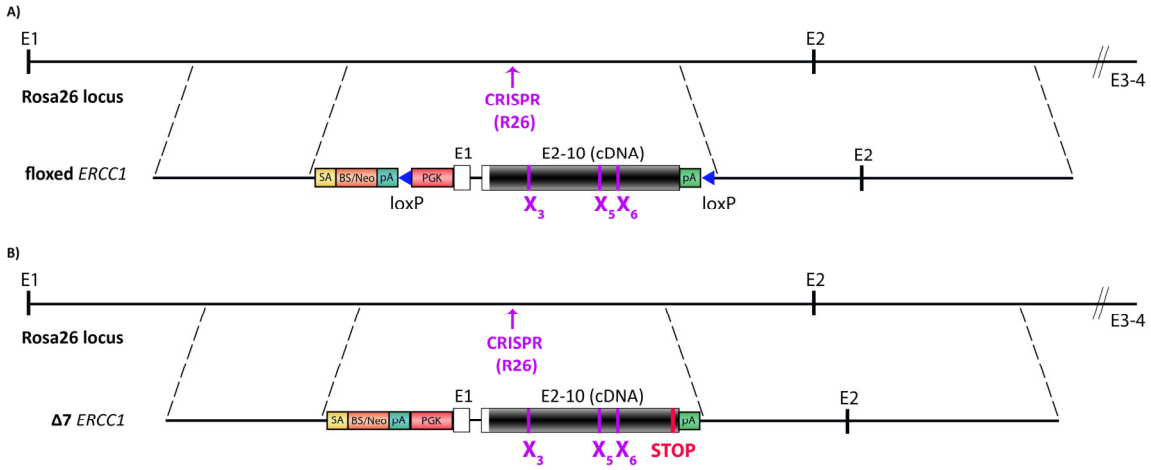

Figure 22: Targeting strategy for *ROSA26* gene locus to introduce *ERCC1* minigenes by homologous recombination.
Top: Overview of porcine *ROSA26* gene locus. **Below**: Promotor trap targeting vector. Yellow, orange, green and red boxes represent splice acceptor (SA), blasticidin S or neomycin resistance gene (BS/Neo), poly A signal (pA) and PGK promotor. Mutated gRNA binding sites are highlighted in violet (x_3/x_5/x_6: binding site in exon 3/5/6). A) Targeting vector to introduce loxP sites, blue triangles show positions of loxP sites. B) Targeting vector to introduce the Δ7 mutation. Three premature stop codons are located seven amino acids in front of the endogenous stop codon, highlited in red.

3.2 MYBPC3

In some pediatric cases, truncating *MYBPC3* mutations have been found to cause a rare but severe form of HCM that leads to premature death. Gene therapy could be a realistic option to effectively treat these patients. To establish *MYBPC3* gene therapy, several tests *in vitro* and *in vivo* are necessary. Some have already been successful *in vitro* and in homozygous *Mybpc3*-targeted knockin mice carrying a G>A transition of the last nucleotide of exon six (Gedicke-Hornung et al. 2013, Mearini et al. 2013, Mearini et al. 2014). The next step towards a clinical trial is to generate a large animal model that would enable pre-clinical translational studies of gene therapy. To develop a porcine model, two of the most common human founder *MYBPC3* mutations were to be replicated in the porcine genome using CRISPR/Cas9.

3.2.1 Introduction of indels in exon 6

A *MYBPC3* founder mutation of the last nucleotide of exon six (c.772G>A) occurred in 14 % of an HCM population in Tuscany, Italy (Girolami et al. 2006). Mouse models carrying this mutation have been generated and novel gene terapy has been tested in these (see above). To further test mRNA-based therapies porcine models mimicking the phenotype of this founder mutation would be helpful.

Comparison of the porcine and human sequence revealed that the porcine *MYBPC3* gene consists of 34 exons in contrast to the human *MYBPC3* gene, which consists of 35 exons (https://www.ncbi.nlm.nih.gov/, accessed on 26 January 2018). The sequence of human and procine exon six share 86 % identical nucleotides and it was confirmed that the last nucleotide is also a G in pigs (see Figure 23). Since it was planned to introduce indels that result in a premature stop codon in exon six or the next three exons leading to truncated protein, different gRNAs cutting in this region were designed. No suitable gRNA for the end of exon six could be identified using the Optimised CRISPR Design webtool (http://crispr.mit.edu/), but two of the suggested ones were binding in the second half of the exon and were chosen (see Figure 23).

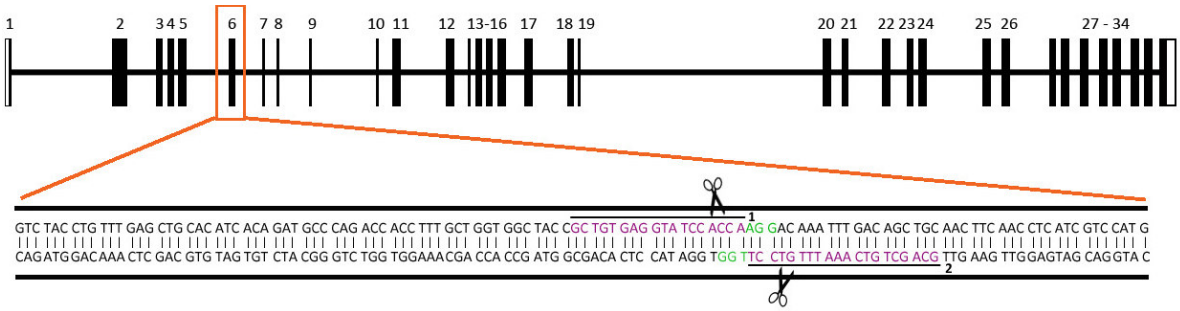

Figure 23: Strategy for genome editing in exon six of the *MYBPC3* gene using CRISPR/Cas9 system.
Top: schematic overview of porcine *MYBPC3* gene locus. Translated exons are black, untranslated white boxes. **Below**: Position of gRNA sequence is underlined, indicated as violet letters and numbered (1=Ex6-1, 2=Ex6-2). PAM is shown as green letters. Scissors indicate preffered position of DSBs.

3.2.1.1 Generation of gRNAs

The gRNAs Ex6-1 (CRISP18-MYBPC3) and Ex6-2 (CRISP20-MYBPC3) were cloned in the pBS-U6-chimaric vector (No. 703 see 2.1.12), which enabled generation of RNA, and gRNA Ex6-1 (CRISP18-MYBPC3) was cloned in the pX330-MCS-Cas9-puro (No. 841 see 2.1.12) vector, which contained the Cas9 enrichment system and was used for transfections. After *in vitro* transcription of gRNA Ex6-1 and gRNA Ex6-2 the quality of RNA was controlled by agarose gel electrophorese.

3.2.1.2 Generation of porcine cell clones

3.2.1.2.1 RNA Tranfection

RNA of gRNA Ex6-1 or Ex6-2 and Cas9 protein was transfected via Stemfect Kit into porcine KDFs and MSCs to test their functionality. 58 clones were screened for desired mutations in exon six of the *MYBPC3* gene by PCR using primers (MYBPC3_In5_F2, MYBPC3_In6_R3) amplifying a 723 bp fragment from intron five to intron six (see Figure 24 B). Sequencing of the screening PCR revealed that in total eight out of 58 clones were positive (14 %), whereas gRNA Ex6-1 generated more clones (6 out of 8) with desired mutations. It was planned to use correctly modified single cell clones for SCNT and reprogramming is dependent on the quality of donor cells. Hence, various cell isolates of different breeds were used for transfections to avoid that the cells used are not fully competent for the procedure. Single cell clones were screened by sequencing of the screening PCR, which amplified a 206 bp fragment from intron five to intron six (Primers: MYBPC3_In5_F, MYBPC3_In6_R2) (see Figure 24 A) or using primers mentioned above (MYBPC3_In5_F2, MYBPC3_In6_R3) (see Figure 24 B).

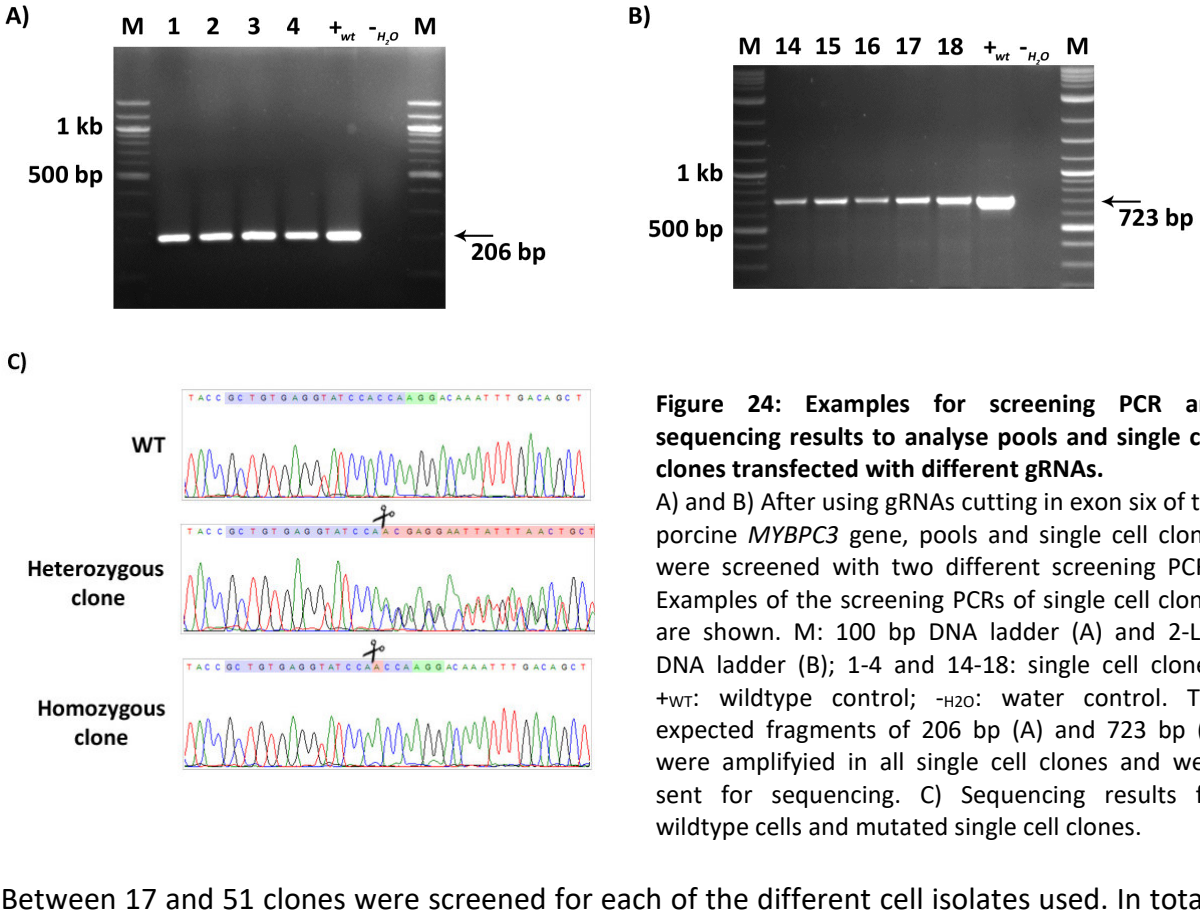

Figure 24: Examples for screening PCR and sequencing results to analyse pools and single cell clones transfected with different gRNAs.
A) and B) After using gRNAs cutting in exon six of the porcine *MYBPC3* gene, pools and single cell clones were screened with two different screening PCRs. Examples of the screening PCRs of single cell clones are shown. M: 100 bp DNA ladder (A) and 2-Log DNA ladder (B); 1-4 and 14-18: single cell clones; $+_{WT}$: wildtype control; $-_{H2O}$: water control. The expected fragments of 206 bp (A) and 723 bp (B) were amplifyied in all single cell clones and were sent for sequencing. C) Sequencing results for wildtype cells and mutated single cell clones.

Between 17 and 51 clones were screened for each of the different cell isolates used. In total 23 clones were identified with mutations in exon six and genome editing efficiency was between 20-27 % (see Table 28).

Table 28: Generation of single cell clones with mutations in exon six and genome editing efficiency of gRNAs.

exon 6	generation of single cell clones	No. of clones analysed	No. of clones with mutations	percentage
bmp m KDF 2506	cloning rings	17	4	24 %
bmp m KDF 2307	cloning rings	51	14	27 %
bmp m KDF 2307 (96)	dilution	25	5	20 %

Analysing the sequencing results showed that mutated clones had insertions of 1-3 bp or deletions of 1-3, 8 or 12 bp. Most of the mutations led to a premature stop in exon six (insertion of 1 bp, deletion of 2 or 8 bp), or in exon nine (insertion of 2 bp, deletion of 1 bp), or resulted in a deletion or insertion of one or four amino acids (deletion of 3 or 12 bp, insertion of 3 bp) (see Figure 25).

In total ten clones were heterozygous, two homozygous and five compound heterozygous for mutations in exon six (see Table 29). The genotype of six clones could not be determined, because base pair substitutions occurred and made exact analysis impossible. Three

heterozygous, one homozygous and three compound heterozygous clones were viable and frozen for other experiments and somatic stem cell nuclear transfer.

Table 29: Genotypes of the generated single cell clones.

exon 6	heterozygous				homozygous				compound heterozygous				
	total	type of mut.	No. of clones	No. of viable clones	total	type of mut.	No. of clones	No. of viable clones	total	type of mut. 1st allele	type of mut. 2nd allele	No. of clones	No. of viable clones
bmp m KDF 2506	1	Stop E6	1	1	0	-	-	-	1	Stop E6	1 AA del	1	1
bmp m KDF 2307	6	1 AA del	2	1	2	1 AA del	1	1	3	Stop E6	1 AA del	2	1
		STOP E6	3	1		STOP E6	1	0		Stop E9	1 AA del	1	0
		STOP E9	1	0		-	-	-		-	-	-	-
bmp m KDF 2307 (96)	3	1 AA del	1	0	0	-	-	-	1	STOP E6	4 AA del	1	1
		4 AA del	1	0									
		STOP E9	1	0									

3.2.1.2.2 DNA Tranfection

Using RNA for transfection of gRNAs can be ineffective since two components, the gRNA and Cas9, must be delivered in the same cell. Transfecting a plasmid containing both components at once eliminates this problem. Furthermore, working with a plasmid makes it possible to add a functional puromycin resistance gene and enrich cells positive for the CRISPR/Cas9 system. A plasmid containing gRNA Ex6-1, Cas9 and puromycin resistence gene sequence (No. 66) was transfected by nucleofection into KDFs and puromycin-resistant single cell clones were screened by sequencing of the screening PCR using primers amplifying the 723 bp fragment from intron five to intron six (MYBPC3_In5_F2, MYBPC3_In6_R3). Out of 54 clones screened for KDFs isolated from a female hybrid pig (KDF 200416, LRxbmp) 49 showed indel mutations in exon six. All 28 clones derived from KDFs from a male hybrid pig (KDF 040717, LRxbmp) showed indel mutations. Gene editing efficiency was between 91-100 % (see Table 30), which is 64-80 % higher than after RNA transfection.

Table 30: Genome editing efficiencies of gRNAs.

exon 6	No. of clones analysed	No. of clones with mutations	percentage	selection (puromycin)
Hyb f KDF 2004	54	49	91 %	Yes
Hyb m KDF 0407 (912)	28	28	100 %	Yes

Mutated clones showed several different mutations, such as insertions of 1-2 bp or deletions of 1- 45 bp, but only mutations leading to a premature stop codon were of interest. Fortunately, most of the indels led to a premature stop in exon six or nine (see Figure 25).

No. of alleles RNA transfection	No. of alleles DNA transfection	R	C	E	V	S	T	K	D	K	F	D	S	
10	-	CGC	TGT	GAG	GTA	TCC	ACC	AAG	GAC	AAA	TTT	GAC	AGC	wt
9	60	CGC	TGT	GAG	GTA	TCC	AAC	CAA	GGA	CAA	ATT	TGA*		STOP exon 6
-	1	CGC	TGT	GAG	GTA	TCC	CAC	CAA	GGA	CAA	ATT	TGA*		STOP exon 6
-	1	CGC	TGT	GAG	GTA	TCC	ACC	CAA	GGA	CAA	ATT	TGA*		STOP exon 6
1	-	CGC	TGT	GAG	GTA	TCC	AGA	CCA	AGG	ACA	AAT	TTG	ACA	GC STOP exon 9
-	1	CGC	TGT	GAG	GTA	TCC	AAA	CCA	AGG	ACA	AAT	TTG	ACA	GC STOP exon 9
3	-	CGC	TGT	GAG	GTA	TCC	ACC	AAC	AAG	GAC	AAA	TTT	GAC	AGC 1 AA inserted
1	56	CGC	TGT	GAG	GTA	TCC	-CC	A	AG	G	AC	A	AA	T TT G AC A GC STOP exon 9
-	2	CGC	TGT	GAG	GTA	TCC	AC-	A	AG	G	AC	A	AA	T TT G AC A GC STOP exon 9
-	3	CGC	TGT	GAG	GTA	TC-A	CC	A	AG	G	AC	A	AA	T TT G AC A GC STOP exon 9
1	-	CGC	TGT	GAG	GTA	T--	AC	CAA	GGA	CAA	ATT	TGA*		STOP exon 6
-	1	CGC	TGT	GAG	GTA	TC-	-C	CAA	GGA	CAA	ATT	TGA*		STOP exon 6
-	10	CGC	TGT	GAG	GTA	TCC	--CAA	GGA	CAA	ATT	TGA*			STOP exon 6
-	1	CGC	TGT	GAG	GTA	TCC	A--	AA	GGA	CAA	ATT	TGA*		STOP exon 6
6	3	CGC	TGT	GAG	GTA	TCC	---	AAG	GAC	AAA	TTT	GAC	AGC	1 AA missing
2	2	CGC	TGT	GAG	---	---	---	---	GAC	AAA	TTT	GAC	AGC	4 AA missing
-	1	CGC	TGT	---	---	---	---	---	GAC	AAA	TTT	GAC	AGC	5 AA missing
-	2	CGC	TGT	GAG	GTA	---	---	---	---	---	TTT	GAC	AGC	5 AA missing
-	1	CGC	TGT	---	---	---	---	---	---	---	---	GAC	AGC	8 AA missing
-	2	---	---	---	---	---	---	---	---	---	---	---	---	15 AA missing
-	1	CGC	TGT	GAG	GTA	---	-CCA	AGG	ACA	AAT	TTG	ACA	GC	STOP exon 9
-	1	CGC	TGT	G--	---	---	AC	CAA	GGA	CAA	ATT	TGA*		STOP exon 6
-	1	CGC	TGT	GAG	GTA	---	---	--G	GA	CAA	ATT	TGA*		STOP exon 6
1	-	CGC	TGT	GAG	GTA	TCC	A--	---	---	AA	ATT	TGA*		STOP exon 6
-	2	CGC	T--	---	---	---	---	--G	G	ACA	AAT	TTG	ACA	GC STOP exon 9
-	2	CGC	TGT	---	---	---	---	---	--C	AA	ATT	TGA*		STOP exon 6

Figure 25: Partial sequence of exon six of wildtype cells and single cell clones.
Every line shows observed mutations occurring in single cell clones after transfection with gRNA. Single letters indicate standard amino acid abbreviation. gRNA sequence is indicated as violet and PAM as green letters. Red letters or dashes indicate insertions or deletions and red background shows amino acid exchanges. Premature stop codons in exon six are marked with an asterisk.

No single cell clone was obtained that carried a heterozygous mutation in exon six of the *MYBPC3* gene, neither for KDFs isolated from a female nor male hybrid pig. 23 clones were homozygous and 26 compound heterozygous for female (KDF 200416, LRxbmp) and 20 homozygous and eight compound heterozygous for male cells (KDF 040717, LRxbmp) (see Table 31). In total 32 homozygous and 32 compound heterozygous clones were viable and frozen for further analysis and for somatic stem cell nuclear transfer to generate *MYBPC3* mutant piglets.

Table 31: Genotypes of generated single cell clones.

exon 6	heterozygous				homozygous				compound heterozygous				
	total	type of mut.	No. of clones	No. of viable clones	total	type of mut.	No. of clones	No. of viable clones	total	type of mut. 1st allele	type of mut. 2nd allele	No. of clones	No. of viable clones
Hyb f KDF 2004	0	-	-	-	23	STOP E6	13	7	26	Stop E6	Stop E9	16	15
										Stop E6	Stop E6	4	4
										Stop E9	Stop E9	1	1
										Stop E9	4 AA del	1	1
						STOP E9	10	6		Stop E6	1 AA del	1	1
										Stop E6	4 AA del	1	1
										Stop E6	8 AA del	1	1
										1 AA del	5 AA del	1	0
Hyb m KDF 0407 (912)	0	-	-	-	20	STOP E6	8	7	8	Stop E6	Stop E9	6	6
		-	-	-		STOP E9	10	10		Stop E6	Stop E6	1	1
		-	-	-		5 AA del	1	1		Stop E6	1 AA del	1	1
		-	-	-		15 AA del	1	1		-	-	-	-

3.2.2 Introduction of indels in exon 23

A Dutch study has shown that about 17 % of HCM cases in the Netherlands are caused by a mutation (c.2373-2374insG) in exon 24 of the human *MYBPC3* gene (Alders 2003, Niimura 1989) (Alders et al. 2003, Niimura et al. 1998). The insertion of guanine results in a newly created splice donor site. The following loss of 40 bp at the 3` end of exon 24 leads to a frameshift in exon 25 and ends in a premature stop codon (Moolman 2000) (Moolman et al. 2000). Since this is the most common human mutation in the Netherlands, it was decided to base the porcine model on this mutation. Breeding these pigs with those carrying a mutation in exon six would generate a novel model with compound heterozygous *MYBPC3* mutations. This could be a more valuable model than simple homozygous knockout pigs.

Since the porcine *MYBPC3* gene consists of one exon less than the human, the porcine exon 23 corresponds to the human exon 24. For introducing indels in exon 23, several gRNAs were

designed using the webtool Optimised CRISPR Design (http://crispr.mit.edu/) and three of them were used for generating single cell clones (see Figure 26).

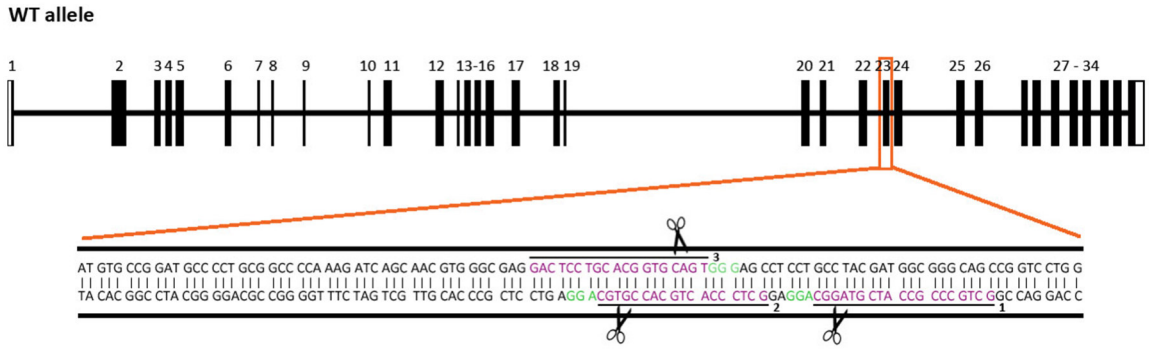

Figure 26: Strategy for generating indels in exon 23 of the MYBPC3 gene using CRISPR/Cas9 system.
Top: schematic overview of porcine *MYBPC3* gene locus**.** Translated exons are black, untranslated white boxes. **Below**: Position of gRNA sequence is underlined, indicated as violet letters and numbered (1=Ex23-1, 2=Ex23-2, 3=Ex23-3). PAM is shown as green letters. Scissors indicate preferred position of DSBs.

3.2.2.1 Generation of gRNAs

For easy generation of various clones having mutations in exon 23 of the *MYBPC3* gene the CRISPR/Cas9 system in combination with puromycin selection was used. The selection marker was either cotransfected with a plasmid containing the gRNA and Cas9 or a plasmid containing all three elements was transfected into KDFs. Above mentioned gRNAs (CRISP-MY_ex23-1, CRISP-MY_ex23-2, CRISP-MY_ex23-3) were cloned into the pX330-MCS-Cas9 (No. 705 see 2.1.12) vector for cotransfection or in the pX459-Cas9-puro (No. 842 see 2.1.12) vector.

3.2.2.2 Generation of porcine cell clones

For cotransfection 5 µg of the vector containing gRNA and Cas9 (No. 49, 50 or 51 see 10.2) and 0.5 µg of a vector carrying factors for puromycin resistance (No. 844 see 2.1.12) were nucleofected into KDFs 200416. Cell pools and single cell clones were analysed by sequencing of the screening PCR using primers amplifying an 812 bp fragment from exon 22 to exon 24 (MYBPC3_Ex22F 5M, MYBPC3_Ex24R 56M). Sequencing of the cell pools was analysed by the webtool TIDE (https://tide.deskgen.com/). The highest efficiency with 52.1 % was obtained for gRNA Ex23-1, whereas gRNA Ex23-2 had a genome editing efficiency of 47.6 %. Unfortunately, sequencing results of pools treated with gRNA Ex23-3 were of poor quality and could not be evaluated by the webtool.

Screening of single cell clones revealed that out of 31 clones 25 showed indel mutations in exon 23 after transfection with gRNA Ex23-3. For cells treated with gRNA Ex23-1 21 clones

were screened and seven showed mutations. 33 clones were screened after treatment with gRNA Ex23-2 and 19 were positive for genome editing. Therefore, gRNA Ex23-3 is the most efficient with 81 % and gRNA Ex23-1 and -2 showed genome editing efficiencies of 33 % and 58 % respectively (see Table 32).

Since gRNA Ex23-3 showed the highest genome editing efficieny (81 %) transfections were repeated with the vector containing the CRISPR/Cas9 system and the selection marker. For nucleofection 5 µg of the pX459-Cas9-Puro-gRNA-MYBPC3-E23-3 (No. 67 see 10.2) were used and transfected into male cells (KDF 040717, LRxbmp). The same screening PCR as mentioned above was conducted on single cell clones and indels were analysed by sequencing. In total, 17 cell clones were screened and ten showed mutations. The genome editing efficiency was 59 % (see Table 32).

Table 32: Gene edited clones and efficiencies of gRNAs after transfection of plasmid and selection.

exon 23	gRNA	No. of clones analysed	No. of clones with mutations	percentage	selection (puromycin)
Hyb f KDF 2004	Ex23-1	21	7	33 %	Yes/Cotransfection
	Ex23-2	33	19	58 %	Yes/Cotransfection
	Ex23-3	31	25	81 %	Yes/Cotransfection
Hyb m KDF 0407 (928)	Ex23-3	17	10	59 %	Yes

The exact genotype of above mentioned clones was determined if possible and several different indels were found. gRNA Ex23-1 resulted in indels such as 1 bp deletions, insertions or substitution and deletions of 3 bp. All mutations led to a premature stop in exon 24 (deletion, insertion of 1 bp) or to a deletion or substitution of 1 amino acid (deletion of 3 bp, substitution of 1 bp) (see Figure 27).

No. of alleles	Q	W	E	P	P	A	Y	D	G	G	Q	P	
2	CAG	TGG	GAG	CCT	CCT	GCC	TAC	GAT	GGC	GGG	CAG	CCG	wt
2	CAG	TGG	GAG	CCT	CCT	GCC	NTA	CGA	TGG	CGG	GCA	GCC G	STOP exon 24
1	CAG	TGG	GAG	CCT	CCT	GCC	T-CG	ATG	GCG	GGC	AGC	CG	STOP exon 24
2	CAG	TGG	GAG	CCT	CCT	GCC	TA-G	ATG	GCG	GGC	AGC	CG	STOP exon 24
1	CAG	TGG	GAG	CCT	CCT	GCC	-AC	--T	GGC	GGG	CAG	CCG	1 AA missing
2	CAG	TGG	GAG	CCT	CCT	GCC	---	GAT	GGC	GGG	CAG	CCG	1 AA missing
2	CAG	TGG	GAG	CCT	CCT	GCC	GAC	GAT	GGC	GGG	CAG	CCG	1 AA exchanged

Figure 27: Partial sequence of exon 23 of wildtype cells and single cell clones.
After using gRNA Ex23-1 for genome editing, several mutations were observed in single cell clones and are listed. Single letters indicate standard amino acid abbreviation. gRNA sequence is indicated as violet and PAM as green letters. Red letters or dashes indicate insertions or deletions and red background shows amino acid exchanges.

After transfection of gRNA Ex23-2 mutated clones showed insertions of 1-2 bp or deletions of 1, 2, 5, 7 or 103 bp. One mutation (deletion of 103 bp) resulted in the loss of the last 16 amino acids of exon 23 and the splice donor. All other indels generated a premature stop in exon 24 (see Figure 28).

No. of alleles	G	E	D	S	C	T	V	Q	W	E	P	P	
5	GGC	GAG	GAC	TCC	TGC	ACG	GTG	CAG	TGG	GAG	CCT	CCT	wt
2	GGC	GAG	GAC	TCC	TGC	AAC	GGT	GCA	GTG	GGA	GCC	TCC T	STOP exon 24
1	GGC	GAG	GAC	TCC	TGC	ACG	CGG	TGC	AGT	GGG	AGC	CTC CT	STOP exon 24
17	GGC	GAG	GAC	TCC	TGC	A-GG	TGC	AGT	GGG	AGC	CTC	CT	STOP exon 24
2	GGC	GAG	GAC	TCC	TGC	A--GT	GCA	GTG	GGA	GCC	TCC	T	STOP exon 24
2	GGC	GAG	GAC	TCC	---	--GGT	GCA	GTG	GGA	GCC	TCC	T	STOP exon 24
2	GGC	GAG	GAC	TCC	TGC	---	---	-AGT	GGG	AGC	CTC	CT	STOP exon 24
1	GGC	GAG	GAC	TCC	TGC	---	---	---	---	---	---	---	AA missing/splicing

Figure 28: Partial sequence of exon 23 of wildtype cells and single cell clones after treatment with gRNA Ex23-2.
Observed mutations occurring in single cell clones after treatment with gRNA Ex23-2 are listed. Single letters indicate standard amino acid abbreviation. gRNA sequence is indicated as violet and PAM as green letters. Red letters or dashes indicate insertions or deletions and red background shows amino acid exchanges.

Clones treated with gRNA Ex23-3 showed insertions of 1 bp or 361 bp (not shown in figure; cell clone No. 5-T6) or deletions of 1-7, 9-11, 14, 26 or 84 bp. The insertion of 361 bp was assumed to lead to 24 additional amino acids, whereas the last 13 amino acids of exon 23 and the splice donor were lost. Deletions of 3, 6 or 9 bp resulted in the deletion of 1-3 amino acids. All other mutations led to a premature stop in exon 24 (see Figure 29).

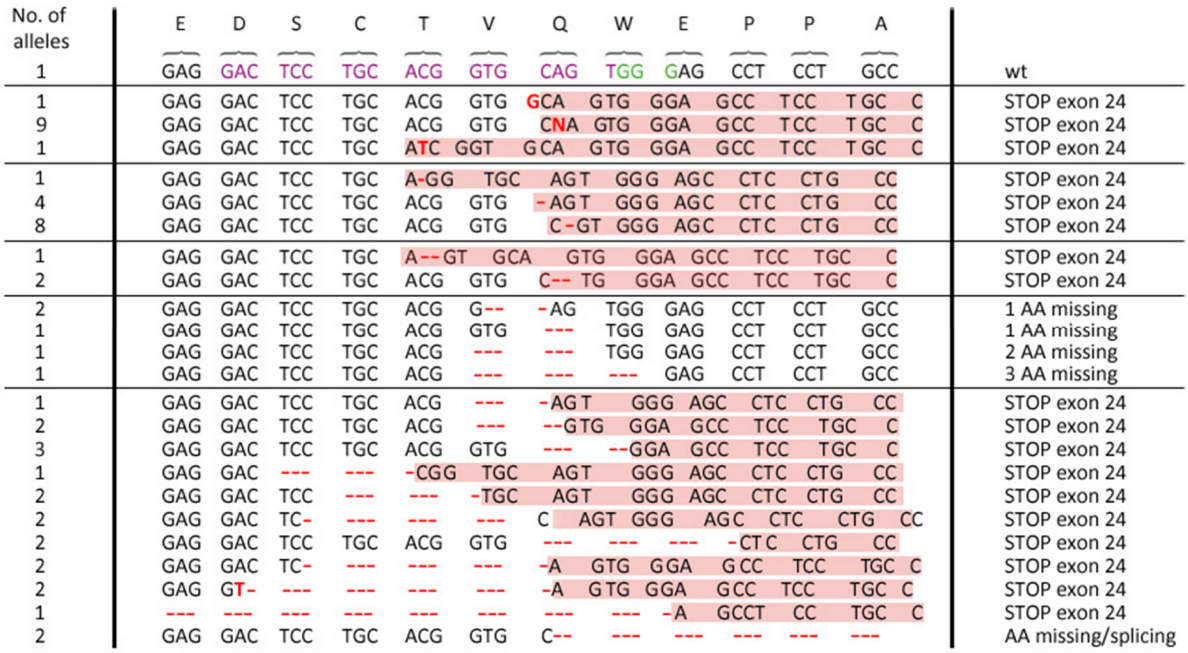

No. of alleles	E	D	S	C	T	V	Q	W	E	P	P	A	
1	GAG	GAC	TCC	TGC	ACG	GTG	CAG	TGG	GAG	CCT	CCT	GCC	wt
1	GAG	GAC	TCC	TGC	ACG	GTG	GCA	GTG	GGA	GCC	TCC	TGC C	STOP exon 24
9	GAG	GAC	TCC	TGC	ACG	GTG	CNA	GTG	GGA	GCC	TCC	TGC C	STOP exon 24
1	GAG	GAC	TCC	TGC	ATC	GGT	GCA	GTG	GGA	GCC	TCC	TGC C	STOP exon 24
1	GAG	GAC	TCC	TGC	A-GG	TGC	AGT	GGG	AGC	CTC	CTG	CC	STOP exon 24
4	GAG	GAC	TCC	TGC	ACG	GTG	-AGT	GGG	AGC	CTC	CTG	CC	STOP exon 24
8	GAG	GAC	TCC	TGC	ACG	GTG	C-GT	GGG	AGC	CTC	CTG	CC	STOP exon 24
1	GAG	GAC	TCC	TGC	A--GT	GCA	GTG	GGA	GCC	TCC	TGC	C	STOP exon 24
2	GAG	GAC	TCC	TGC	ACG	GTG	C-- TG	GGA	GCC	TCC	TGC	C	STOP exon 24
2	GAG	GAC	TCC	TGC	ACG	G--	-AG	TGG	GAG	CCT	CCT	GCC	1 AA missing
1	GAG	GAC	TCC	TGC	ACG	GTG	---	TGG	GAG	CCT	CCT	GCC	1 AA missing
1	GAG	GAC	TCC	TGC	ACG	---	---	TGG	GAG	CCT	CCT	GCC	2 AA missing
1	GAG	GAC	TCC	TGC	ACG	---	---	---	GAG	CCT	CCT	GCC	3 AA missing
1	GAG	GAC	TCC	TGC	ACG	---	-AGT	GGG	AGC	CTC	CTG	CC	STOP exon 24
2	GAG	GAC	TCC	TGC	ACG	---	--GTG	GGA	GCC	TCC	TGC	C	STOP exon 24
3	GAG	GAC	TCC	TGC	ACG	GTG	---	--GGA	GCC	TCC	TGC	C	STOP exon 24
1	GAG	GAC	---	---	-CGG	TGC	AGT	GGG	AGC	CTC	CTG	CC	STOP exon 24
2	GAG	GAC	TCC	---	---	-TGC	AGT	GGG	AGC	CTC	CTG	CC	STOP exon 24
2	GAG	GAC	TC-	---	---	---	C AGT	GGG	AGC	CTC	CTG	CC	STOP exon 24
2	GAG	GAC	TCC	TGC	ACG	GTG	---	---	---	-CTC	CTG	CC	STOP exon 24
2	GAG	GAC	TC-	---	---	---	-A	GTG	GGA	GCC	TCC	TGC C	STOP exon 24
2	GAG	GT-	---	---	---	---	-A	GTG	GGA	GCC	TCC	TGC C	STOP exon 24
1	---	---	---	---	---	---	---	---	-A	GCCT	CC	TGC C	STOP exon 24
2	GAG	GAC	TCC	TGC	ACG	GTG	C--	---	---	---	---	---	AA missing/splicing

Figure 29: Partial sequence of exon 23 of wildtype cells and single cell clones after treatment with gRNA Ex23-3.
Single letters indicate standard amino acid abbreviation. gRNA sequence is indicated as violet and PAM as green letters. Red letters or dashes indicate insertions or deletions and red background shows amino acid exchanges.

Six clones of which two were heterozygous, two homozygous and two compound heterozygous were mutated after treatment with gRNA Ex23-1. Treatment with gRNA Ex23-2 resulted in five heterozygous, seven homozygous and four compound heterozygous clones. Using gRNA Ex23-3 did not lead to a heterozygous single cell clone for female cells (KDF 200416, LRxbmp) and only one heterozygous single cell clone was found for male cells (KDF 040717, LRxbmp). Homozygous mutations in exon 23 occurred in ten female and three male single cell clones whereas eight female and five male single cell clones were compound heterozygous (see Table 33).

In total, eight heterozygous, 19 homozygous and 15 compound heterozygous clones were viable and frozen for further analysis and somatic stem cell nuclear transfer.

Table 33: Occurring genotypes in single cell clones.

exon 23	heterozygous				homozygous				compound heterozygous				
	total	type of mut.	No. of clones	No. of viable clones	total	type of mut.	No. of clones	No. of viable clones	total	type of mut. 1st allele	type of mut. 2nd allele	No. of clones	No. of viable clones
Hyb f KDF 2004 C1	2	Stop E24	1	1	2	STOP E24	1	0	2	Stop E24	1 AA del	2	2
		1 AA del	1	1		1 AA sub.	1	0					
Hyb f KDF 2004 C2	5	Stop E24	5	5	7	STOP E24	7	7	4	Stop E24	Stop E24	3	2
										Stop E24	16 AA del	1	1
Hyb f KDF 2004 C3	0	-	-	-	10	STOP E24	10	10	8	Stop E24	Stop E24	5	3
										Stop E24	1 AA del	2	1
										Stop E24	24 AA ins	1	1
Hyb m KDF 0407 (928) C3	1	Stop E24	1	1	3	Stop E24	2	1	5	Stop E24	Stop E24	2	2
										Stop E24	1 AA del	1	1
						13 AA del	1	1		Stop E24	2 AA del	1	1
										Stop E24	3 AA del	1	1

3.2.3 Generation of a piglet

After generation and analysis of single cell clones a set of them were used in the first two rounds of somatic cell nuclear transfer and embryo transfer in collaboration with the group of Prof. Wolf, LMU to obtain genetically modified pigs. Three cell clones with mutations in exon six and two cell clones with indels in exon 23 were used. Up to now two pregnancies were obtained. One pregnancy resulted in a late abortion and from the other eight mummified and one stillborn (#10064) piglets were obtained. Since quality of samples from mummified piglets is not sufficient for expression analysis, samples of different tissues were only taken from the stillborn animal.

3.2.3.1 Genotype of the piglet - Exon 23

To analyse the genotype of the piglet a part of the tail and kidney cells were used for DNA isolation by phenol-chloroform extraction and quick extract. Screening PCR was performed

with primers amplifying an 812 bp fragment from exon 22 to exon 24 (MYBPC3_Ex22F 5M, MYBPC3_Ex24R 56M, see 3.2.2.2). The expected band at 812 bp, a higher band at about 1.2 kb and some unspecific bands at about 1.1 kb were visible indicating a heterozygous or compound heterozygous genotype of the piglet (see Figure 30 A). Sequencing of the screening PCR confirmed that the piglet originated from clone No. 5-T6 (see 3.2.2.2) meaning that the fragment with a size of 812 bp was positive for a single base pair deletion in Exon 23 resulting in a frameshift and premature stop in exon 24 (see Figure 30 B). Whereas the bigger fragment originated from the other allele, where a duplication of 361 bp consisting of parts of the *MYBPC3* gene took place. Parts of exon 22, intron 22 and exon 23 were duplicated and some parts of exon 23 were deleted. In total 72 bp of exons were duplicated leading to an insertion of 24 amino acids and several other amino acids were exchanged due to deletion and duplication (see Figure 30 C).

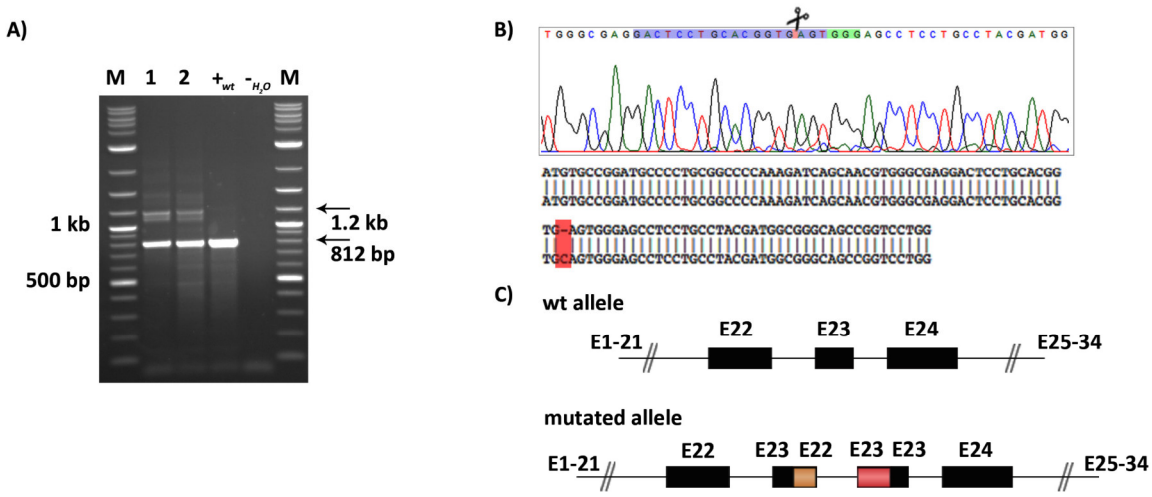

Figure 30: Analysis of the genotype of the stillborn piglet.
A) Screening PCR with genomic DNA of the stillborn piglet. M: 2-Log DNA ladder; 1: tail; 2: kidney cells; $+_{wt}$: wildtype KDF; $-H_2O$: water control. The expected fragment of 812 bp and a second fragment of 1.2 kb were amplified. Additionally, some unspecific band at about 1.1 kb was visible. B) Sequencing results of the PCR and sequence alignment with exon 23 of the wildtype *MYBPC3.* gRNA binding site is highlighted in blue, PAM sequence in green and mutations in red. Sequencing result and alignment show both a deletion of 1 bp at the cutting site of gRNA Ex23-3. C) Structure of the second allele compared to wildtype allele. Parts of exon 23 are deleted and duplication of parts of exon 22, intron 22 and exon 23 took place.

Analysis of the genotype of the stillborn piglet showed that exon 23 was compound heterozygous mutated. To verify the functionality of the mutations analysis of RNA and protein expression followed.

3.2.3.2 Expression of MYBPC3 mRNA and of genes indicating HCM

Mouse models showed that mutant RNA of the *MYBPC3* gene is often degraded by nonsense-mediated mRNA decay (Vignier et al. 2009). To analyse the level of total RNA Q-PCR was conducted on RNA samples of heart tissue. Expression values were calculated and showed that MYBPC3 was expressed 0.6-fold lower than in wt cells.

Some genes such as Natriuretic peptide A and B (*NPPA* and *NPPB*), actin isoform sceletal muscle α-actin (*ACTA1*) and beta heavy chain subunit of cardiac myosin (*MYH7*) are normally expressed in the fetal stage and get replaced by other isoforms in adulthood. Upon cardiac stress, those are strongly upregulated in the myocardium and therefore these genes are indicators for heart diseases such as HCM (Man et al. 2018). Natriuretic peptide A and B (*NPPA* and *NPPB*) are hormone peptides that are produced in cardiac cells and have a huge range of actions contributing to cardiovascular homeostasis (Baxter 2004, Saito 2010). The actin isoform sceletal muscle α-actin (*ACTA1*) is the major protein component of the skeletal muscle thin filament and is essential for muscle contraction (Nowak et al. 2013). *MYH7* encodes the beta heavy chain subunit of cardiac myosin. It is part of the thick filament and plays an important role in cardiac muscle contraction (van Rooij et al. 2009).

NPPA showed a 10-fold and *NPPB* a more than 300-fold greater expression in the stillborn piglet than in wildtype samples indicating a heart disease (see Figure 31). Whereas, ACTA1 and MYH7 showed normal expression patterns.

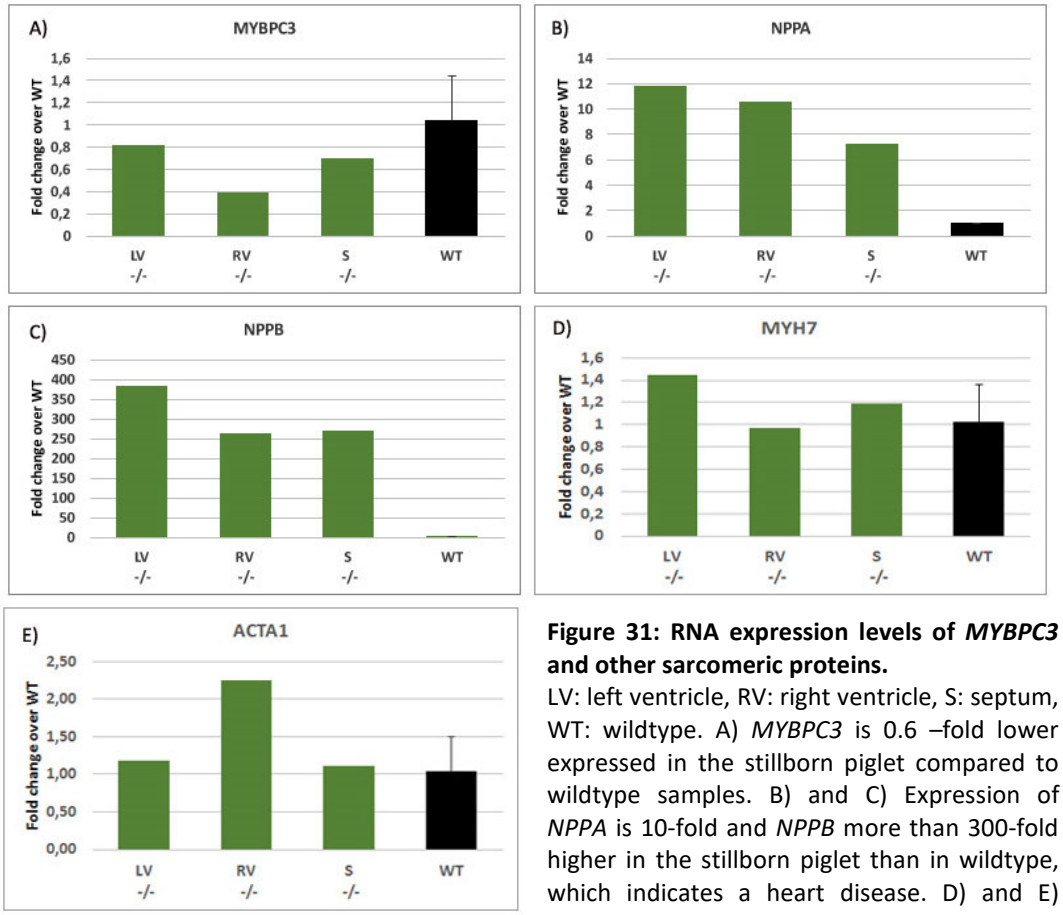

Figure 31: RNA expression levels of *MYBPC3* and other sarcomeric proteins.
LV: left ventricle, RV: right ventricle, S: septum, WT: wildtype. A) *MYBPC3* is 0.6 –fold lower expressed in the stillborn piglet compared to wildtype samples. B) and C) Expression of *NPPA* is 10-fold and *NPPB* more than 300-fold higher in the stillborn piglet than in wildtype, which indicates a heart disease. D) and E) MYH7 and ACTA1 showed normal expression.

3.2.3.3 Analysis of MYBPC3 and other sarcomeric proteins

Heart tissue of the stillborn piglet showed abnormalities regarding RNA levels of *MYBPC3*, *NPPA* and *NPPB*. To examine *MYBPC3* expression on protein level western blot analysis was performed. Very low levels of cMyBP-C protein were detectable in the heart of the piglet.

To see if sarcomeric proteins, such as α-actinin, were normally expressed in the heart of the stillborn piglet western blot analysis was performed. α-actinin is a sarcomeric protein binding to actin, forming a mechanical link between antiparallel actin filaments and anchoring them to the Z-line (Gautel and Djinovic-Carugo 2016). Calsequestrin is a calcium-binding protein, plays a role in cardiac regulation (Faggioni and Knollmann 2012) and is used for loading control. These sarcomeric proteins showed normal protein expression (see Figure 32).

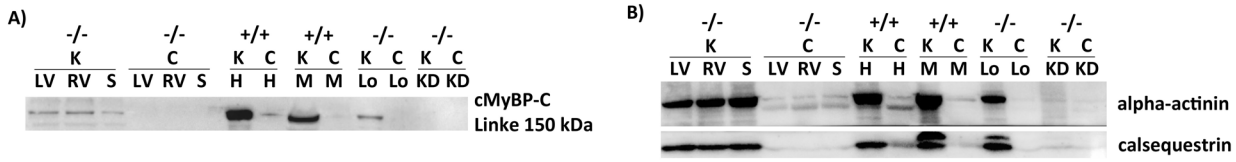

Figure 32:Protein analysis of different tissues of the stillborn piglet.
-/-: tissue from knockout piglet; **+/+**: tissue from wildtype; **K**: Isolation with Kranias buffer; **C**: Cytosolic proteins; **LV**: left ventricle; **RV**: right ventricle; **S**: septum; **H**: heart tissue; **M**: muscle; **Lo**: Longissimus; **KD**: kidney. A) Only very low levels of cMyBP-C were detectable in the heart tissue of the stillborn piglet. B) α-actinin and calsequestrin showed normal expression in knockout and wildtype cardiac tissues.

3.2.4 Summary

Several cell clones of different isolates with mutations in either exon six or 23 were obtained by the use of CRISPR/Cas9. Two pregnancies were established, one resulted in a late abortion and one led to eight mummified and one stillborn piglets. The stillborn piglet originated from a compound heterozygous cell clone with mutations in exon 23 of the *MYBPC3* gene, showed absence of cMyBP-C and had upregulation of markers of HCM.

4 Discussion

In this work, two loci, *ERCC1* and *MYBPC3*, were chosen to generate porcine models of cardiovascular diseases. Genome editing was used for both to obtain the desired genome modifications. It was highly efficient for the *MYBPC3* gene locus, but prooved problematic for *ERCC1* gene locus (see below). Although there was the possibility to conduct genome editing in pig embryos, I decided to generate the modifications in cell culture followed by production of animals by somatic cell nuclear transfer for three reasons. The first important advantage of cell culture is that single cell clones can be analysed after manipulation prior to generation of animals. Since both alleles of both genes were planned to have different mutations - integrated loxP sites and Δ7 mutation for *ERCC1* and indels in exon six and 23 leading to premature stop for *MYBPC3* -, it was important to choose clones with exactly the intended mutations. If genome editing would have been conducted in embryos, it would have been difficult to generate animals with the desired modifications and analysis would have been only possible after birth. The second reason to choose cell culture was the possibility to utilise selection systems to enrich cells either carrying the transfected vetor or having correct targeting events (Campbell 2002). Third, animals obtained after SCNT will have the same genotype in all cells since they originate from a single cell nucleus. If genome editing is conducted in embryos mosaicism can occur when modification of the target sequence takes place after the zygote stage (Burdon and Wall 1992, Campbell 2002).

Mouse models or human patients with similar mutations as planned for both genes exist or were identified. There are founder mutations in exon six and 24 of the human *MYBPC3* gene and for the former a mouse model has been generated (Carrier et al. 2015, Vignier et al. 2009). The Δ7 mutation of the *Ercc1* gene was analysed in a mouse model (*Ercc1*^{*292} or *Ercc1*$^{\Delta 7}$). Another mouse strain (*Ercc1*$^{flox/-}$) carries a Cre-lox system for skin-specific knockouts and most important mice with full knockouts (*Ercc1*$^{-/-}$) exist (Weeda et al. 1997, Doig et al. 2006, McWhir et al. 1993). Although mice with a full knockout died before weaning, viability of animals with skin-specific knockouts was normal (McWhir et al. 1993, Doig et al. 2006). For these reasons, it was assumed that generation of porcine cells and animal models with similar mutations would be possible. This was true for the *MYBPC3* gene, but proved difficult for the *ERCC1* gene, which will be discussed in the next chapter.

4.1 Structure of *ERCC1*

At the beginning of this thesis only parts of the porcine *ERCC1* gene were available in NCBI (https://www.ncbi.nlm.nih.gov/) and gene annotation was necessary. This was in contrast to the *MYBPC3* gene, which was already completely annotated. Most sequences missing in NCBI were found via a swine BAC library that contained a working draft of the *ERCC1* gene. Remaining gaps had to be filled by PCR and sequencing.

Furthermore, RNA analysis was necessary since boundaries of translated exons were not defined. Also, the number of transcript variants was unclear. At least four variants have been found in humans, but only one encodes functional ERCC1 protein (van Duin et al. 1986, van Duin et al. 1987). Analysis of 5` UTR and 3` UTR of the porcine *ERCC1* gene revealed that the same main transcript as in humans exists in porcine cells, plus two additional isoforms, which are the results of alternative splicing between exons zero, one and two within 5` UTR. The Swine Genome Sequencing Consortium released the whole genomic sequence for the ERCC1 gene, which confirmed my annotation, on 2017/02/07 (https://www.ncbi.nlm.nih.gov/).

4.2 Cloning of targeting vectors

Difficulties regarding amplification and cloning of some parts of the *ERCC1* gene occurred during several steps indicating that the repetitive elements of the gene disturb amplification and/or DNA is difficult to access. Two different promotor trap targeting vectors were designed (see 3.1.3). The transfection with Δ7 promotor trap targeting vector was used in six rounds of transfection in different cell types, but no positive clones were generated. As large regions of homology might be preferential (Lu et al. 2003, Hasty et al. 1991, Deng and Capecchi 1992), the original plan was to use a Δ7 targeting vector with about nine kb homology arm at the 5` end. But, all strategies for amplification of regions in intron six failed. The same problem occurred at the conditional promotor trap targeting vector, which was planned to contain the same region. Hence, a shorter version, spanning six kb of 3` homology arm, was used instead of the originally planned 10-12 kb (see 3.1.3). When designing strategies for CRISPR/Cas9-mediated gene targeting, a targeting vector for flanking exon six was considered, since exon six is besides exon eight and nine the smallest and

deletion leads to a frameshift. Nevertheless, this strategy was abandoned as no screening PCR could be established. For screening PCR, several primers were designed and more than ten different combinations were tried out with different polymerases and parameters, but none resulted in amplification of intron five to intron six region of *ERCC1* (data not shown). One possible explanation are structural elements such as GC-contents higher than 65 %, stretches of AT-repeats or repetitive sequences that can disturb PCR reactions (Sahdev et al. 2007, Dhatterwal et al. 2017, Hommelsheim et al. 2014, Riet et al. 2017). Although about 700 bp of the sequence upstream of exon six have a slightly increased GC-content (about 60 %) and an influence on PCR efficiency is plausible, it is unlikely that it should cause the PCR reaction to fail. Two stretches of more that 20 bp AT-repeats were found in the first one kb of intron six and this may have impacted the outcome of the PCR.

Other repetitive elements, such as long interspersed repetitive elements (LINEs) and short interspersed repetitive elements (SINEs) are originally derived from transposons. LINEs are about six kb long, harbour an internal polymerase II promotor, encode two proteins and insert in the genome after translation and reverse transcription. Reverse transcription often fails and many truncated, non-functional insertions occur, e.g. LINE1 copies have an average size of 900 bp and LINE1 elements (L1Hs) consist of about one kb. SINEs are retroposons with a repetitive sequence of 80-400 bp, which harbour an internal polymerase III, encode no proteins and transposition into new parts of the genome takes place after proliferation via transcription and reverse transcription (Lander et al. 2001, Okada 1991). Regions, which were amplified in the screening PCRs was analysed by a webtool for repetitive elements (RepeatMasker: http://www.repeatmasker.org/cgi-bin/WEBRepeatMasker, accessed on 13 July 2018). The sequence consists of 33 % LINEs and of 26 % short SINEs. This represents a higher proportion of repeat units compared to the rest of the porcine genome. LINEs comprise on average about 20 % and SINEs about 13 % of the porcine genome and the relative content of repetitive elements (40 %) is lower than reported for other mammalian species (Groenen et al. 2012). Analysis of the whole porcine *ERCC1* gene sequence showed that the gene consists of about 52 % total interspersed repeats, which again is very high compared to other genes, e.g. the whole *MYBPC3* gene consist of 31 % repetitive elements (http://www.repeatmasker.org/cgi-bin/WEBRepeatMasker, accessed on 13 July 2018). The high content of repetitive elements in the *ERCC1* gene and especially in the region around

exon six can have an impact on the efficiency of PCR and cloning steps and is a possible explanation for the occurred problems.

4.3 Targeting of *ERCC1* affects cell viability

It was not possible to generate cell clones with a positive targeting event by using one of the promotor trap vectors. One problem was that both vectors only contained relatively short lengths of homology arms, which can lead to low efficiency. Furthermore, the selection system can be problematic since the efficiency of a promotorless resistance gene depends on the expression level of the targeted gene (Friedel et al. 2005). The *ERCC1* gene is expressed very low in the cell lines used and it is possible that correct targeted clones are not able to resist the selection pressure. Another problem can be the toxicity of the vectors. If the vectors are integrated correctly the *ERCC1* gene has either the Δ7 mutation or is completely knocked out as long as the resistance cassette is not cut out with the Cre/lox system. This means that correctly targeted single cell clones not only have to survive selection pressure, but negative effects due to less functional ERCC1 protein additionally can occur.

To avoid drawbacks of the promotor trap vectors other strategies were conducted (see 3.1.4). To increase targeting efficiencies the CRISPR/Cas9 system was used parallel to newly designed targeting vectors. Selection systems were only used for a short time (48h) for enrichment of cells containing the CRISPR/Cas9 system. The new targeting vectors had no selection system and in case of the conditional targeting vector the ERCC1 gene was not disturbed and expression of a positive targeted allele where one exon is flanked by loxP sites should be possible. Single cell clones were only generated if cell pools showed positive screening PCR. It was therefore surprising that after more than 1000 clones were screened for the Δ7 mutation and about 1700 for the conditional mutation only few clones (19 for Δ7 mutation and 28 for loxP) were found with a positive screening PCR at the 5` junction. Moreover, expansion of cell clones was difficult, many of the single cell clones stopped growing after passage six to eight and freezing was often not possible or cells died after thawing, especially for clones containing the Δ7 mutation (11/19 clones could be cryoconserved for Δ7 mutation and 26/28 for loxP). This was unexpected, because even if the CRISPR/Cas9 system introduces indels in the second, non-targeted allele, at least one

allele should have been capable to produce a functional ERCC1 protein for both strategies. In case of the ∆7 mutation the gRNA binding site is located in the 3` UTR and non-targeted alleles can be expressed correctly, even after introduction of indels. In case of the loxP vector it is possible to have disturbing indels in exon five leading to a premature stop codon. Nevertheless, this is only true for the strategy with gRNA cutting in exon five, other strategies used gRNAs in introns and besides, the targeted allele can give rise to a correct protein. One explanation for the mortality of the cells is that important regulatory elements positioned in introns were disturbed either by cutting with CRISPR or by introduced elements, e.g. loxP sites. Introns can have direct functional roles, e.g. regulation of splicing, enhancement of gene expression, control of mRNA transport, chromatin assembly and the 5` and 3` UTR can affect mRNA stability and nonsense-mediated decay (Jo and Choi 2015). If these functions are impaired by the introduced changes, lack of a fully functional protein would lead to a high mortality. Another possible explanation is that porcine cells are more sensitive than murine cells and do not survive with one functional *ERCC1* allele.

The results are in contrast to findings in mouse models. Several different mutations have been introduced in the mouse *ERCC1* gene and living animals having a knockout have been generated (see 1.1.1.2.3). Furthermore, heterozygous mouse embryonic fibroblasts (MEFs) showed no altered proliferation rate and only homozygous *Ercc1*-mutant cells grew three times slower as wildtype fibroblasts and stopped dividing at passage 6-7 (Weeda et al. 1997). Nevertheless, any porcine targeted cell clone treated with CRISPR/Cas9 and/or targeting vectors for both modification types, the Δ7 mutation or the loxP sites, showed growth characteristics as homozygous MEFs. A gRNA cutting in exon five (CRISPR-ERCC1_Ex5) was used to generate clones carrying truncating mutations in the *ERCC1* gene, which are expected to result in a non-functional protein, because half of the protein and the XPF binding site are missing. Although several heterozygous and even homozygous mutated clones could be frozen at passage five to six, all of them stopped growing at later passages or after thawing (data not shown). One possible explanation for a different outcome of the experiments compared to mouse is the cell types used, because all my work was conducted in primary KDFs or MSCs. These differ from murine ES cells, e.g. HR frequency is 100-fold lower and the number of cell divisions is limited (Polejaeva and Campbell 2000). Another possible explanation is that experiments in mouse models are not exactly reproducible in pigs. The extremely rare occurrence of mutations of the *ERCC1* gene in humans and the

associated severe phenotype - three known human patients were found in the last thirty years suffering from a severe phenotype leading to an early death (see 1.1.1.2.2) - indicate that mutations in the *ERCC1* gene are presumably lethal. This leads to the probable conclusion that introduction of a knockout or even mutations causing a mild impairment of the *ERCC1* gene is very difficult in larger animals.

Furthermore, personal communication (Prof. J.H. Hoeijmakers) revealed that generation of murine ES cells containing a mutation in the *ERCC1* gene was challenging as well. Therefore, I tried to improve gene targeting, which will be discussed in the next sections.

4.4 Improvement of gene targeting and limitations of the strategies used

The physiological oxygen level ranges between 4 to 14 % in organs such as lung, liver and kidney. Nevertheless, traditional cultivation of cells is performed at about 21 % oxygen, which is the oxygen level in ambient atmospheric air. Thus, the oxygen level is 1.5-, to 5-fold higher in cell culture than under physiological conditions and it is believed that resulting abundant reactive oxygen species and associated oxidative stress affects the condition and viability of the cultured cells (Jagannathan et al. 2016, Halliwell 2003). For this reason and after personal communications (Prof. J.H. Hoeijmakers), cells were cultivated under 3 % oxygen in the hope that mortality of *ERCC1*-deficient cells decreases. But, viability of cells was still low and there was no significant difference in growth between the standard and the lower oxygen level (data not shown).

The integration of the Δ7 mutation and the loxP sites could be achieved with the usage of simple targeting vectors or ssODN in combination with a CRISPR/Cas9 plasmid (without selection; see 3.1.4). However, targeting efficiency was still very low in screened cell clones, since four clones out of 390 were positive for the Δ7 TV (1 %), five out of 312 for the Δ7 ssODN (1.6 %) and one out 307 for the loxP integration (0.3 %). Methods to increase targeting efficiency were using of a double cut donor vector instead of a simple targeting vector and adding a selection system to the CRISPR/Cas9 plasmids. It was assumed that *in vivo* donor linearisation might assist in DSB recognition, donor recruitment and protects from degradation by exonucleases, e.g. degradation can take place while a pre-cleaved template has to wait for the chromosome to be cut (Cristea et al. 2013). Using only selection system did increase targeting efficiency 1.5-fold for loxP integration (2 out of 405 screened

clones were positive resulting in an efficiency of 0.5 %) and 2.9-fold for the Δ7 mutation (ssODN: 7 out of 149, 4.7 %), whereas combination of both methods gave inconsistent results. Using a combined system generated a decrease in efficiency from 1.2 % to 0 % for combination of gRNA In3-2 and In4-1 (Selection and TV: 3 out of 241, Selection and dc TV: 0 out of 32) and a slight increase from 3.1 % to 3.4 % for gRNA In4-1 (Selection and TV: 2 out of 65, Selection and dc TV: 1 out of 29, 1.1-fold change). Nevertheless, compared to the usage of only selection combination of both methods increased targeting efficiency 2-fold for gRNA Ex5-1 (Selection and TV: 2 out of 405, 0.5 %, Selection and dc TV: 1 out of 104, 1 %) and 6-fold for gRNA In5-1 (Selection and TV: 1 out of 40, 2.5 %, Selection and dc TV: 13 out of 87, 15 %).

Inconsistent results regarding the double cut vector can be explained by low sample sizes and experiments need to be repeated for a more reliable statistic. Using a combination of selection system and a circular donor vector for the Δ7 mutation did not increase efficiency (3 out of 104, 2.9 %) compared to the use of only selection and ssODN and it is likely that the 2.9-fold increase for both was due to the selection system. However, it was clearly shown that using a double cut vector and especially a selection system can increase targeting efficiency notably (see Table 34).

Table 34: Improvement of targeting efficiencies via different strategies.

improvement via selection									
			w.o. selection			**with selection**			**fold change**
project	**gRNA**	**donor template**	**No. of clones**		**efficiency**	**No. of clones**		**efficiency**	
			screened	**targeted**		**screened**	**targeted**		
loxP Ex5	Ex5-1	TV	307	1	0.3 %	405	2	0.5 %	1.5
Δ7	Ex10-2	ssODN	312	5	1.6 %	149	7	4.7 %	2.9
improvement via selection and circular vector									
			w.o. selection			**with selection**			**fold change**
project	**gRNA**	**donor template**	**No. of clones**		**efficiency**	**No. of clones**		**efficiency**	
			screened	**targeted**		**screened**	**targeted**		
Δ7	Ex10-2	TV	390	4	1 %	104	3	2.9 %	2.9
improvement via selection and double cut vector									
			with selection			**with selection and dc vector**			**fold change**
project	**gRNA**	**donor template**	**No. of clones**		**efficiency**	**No. of clones**		**efficiency**	
			screened	**targeted**		**screened**	**targeted**		
loxP Ex5	Ex5-1	TV	405	2	0.5 %	104	1	1 %	2
	In5-1	TV	40	1	2.5 %	87	13	15 %	6
loxP Ex4	In3-2 In4-1	TV	241	3	1.2 %	32	0	0 %	-
	In4-1	TV	65	2	3.1 %	29	1	3.4 %	1.1

Using a ssODN was more efficient for introducing the Δ7 mutation, whereas integration of loxP sites could not be achieved with this method. This indicates that there is no optimal method and components for transfections have to be evaluated empirically and combined individually for each purpose and locus.

Two different mechanisms, the HDR and NHEJ, are used to repair DSBs. Findings indicate that HDR and NHEJ occur not sequentially, but can be alternative pathways for repair and moreover, compete for the repair of the same DSB (Pierce et al. 2001). Since *ERCC1* is involved in DSB repair and homologous recombination (Manandhar et al. 2015, Wood 2010), targeting the gene using CRISPR/Cas9 can already shift the balance to NHEJ. To compensate this effect and therefore promote the occurrence of HDR, SCR7 was used. It has been shown that inhibition of essential factors of the NHEJ pathway, e.g. by small molecules such as SCR7, L755507 and resveratrol (Maruyama et al. 2015, Yu et al. 2015, Li et al. 2017), or enhancement of HDR, e.g. via the use of RS-1 (Song et al. 2016), can lead to a higher occurrence of HDR. Using SCR7 showed inconsistent results because, depending on the cell type, either an increased or decreased efficiency was observed (see 3.1.4.2). Certainly, determination of the effective concentration of SCR7 was an issue. The amount of the molecule used was based on publications (Maruyama et al. 2015, Chu et al. 2015) and on various experiments with different concentrations (see Master Thesis Melanie Manyet, 2017). Nevertheless, the lack of a suitable reporter system and time limitations leading to small sample sizes were problems influencing the outcome of the experiments. To solve this problem the generation of a reporter system and repeated experiments with SCR7 would be necessary. Another solution would be the use of other, above mentioned molecules to increase gene targeting efficiency. Nevertheless, as it is unknown how treatment of primary cells with SCR7 might later also affect nuclear transfer efficiency, it was deemed rational not to persue it any further.

The CRISPR/Cas9-mediated gene targeting was much more efficient compared to the promotor trap systems. Nevertheless, this system has limitations leading to a relatively low targeting efficiency. Since HDR is dependent on donor templates it presumably only occurs in cell cycle phases S and G2 when the needed sister chromatid and by this a homologous template is available, whereas NHEJ occurs throughout the cell cycle and is favoured for DSB repair (Davis and Chen 2013, Maruyama et al. 2015). A possible solution to shift the balance

to HDR is synchronisation of cells in the G2/M phase of the cell cycle. Inhibitors of the microtubule polymerisation, such as Nocodazole and ABT-751, have been used in human pluripotent stem cells and synchronisation led to an increase in HDR events (Yang et al. 2016). Another group generated a Cas9 fusion protein that had low expression levels in G1 but high in S/G2/M resulting in increased site-specific integration events in human cell lines (Gutschner et al. 2016).

Screening of positive targeted single cell clones was another limitation of the strategies used. In contrast to the promotor trap vectors, the new vectors contained only minimal changes compared to wildtype sequences, e.g. the vector or ssODN for integration of the $\Delta 7$ mutation had only an exchange of 15 bp and no change in size resulted after correct incorporation of the mutations. This meant that either primers can be found that can target the 15 bp for screening PCR or sequencing of the PCR is necessary to reveal the changes. Methods such as Southern blot, which would have depended on the presence of a unique restriction site in the inserted modifications, were not possible. To avoid such problems in future projects, vectors should be designed with the addition of a unique primer sequence and restriction site. For screening of loxP sites problems can occur due to the loxP sites, which were present twice in the sequence and are composed of two recombinase binding elements with palindromic sequences surrounding a core of an asymmetric crossover sequence (Van Duyne 2001).

Furthermore, using the CRISPR/Cas9 system for better efficiencies can have negative effects, such as low viability as mentioned above due to unwanted indels in the targeted gene and offtarget effects. Although, possible off-target sites can be predicted by several webtools, e.g. Optimised CRISPR Design and CRISPOR (http://crispr.mit.edu/ and http://crispor.tefor.net/), and analysis can be conducted by targeted sequencing, the appropriate number of potential off-target sites remains unclear, because the accuracy of *in silico* prediction can vary (Tycko et al. 2016). Several predicted off-target sites have been screened for different gRNAs and no indels were found (data not shown), but only whole genome sequencing would give clear results about off-target effects. Furthermore, a Cas9 nickase – the Cas9-D10A mutant nickase that induces a nick instead of a DSB - and one or two different gRNAs can be used to facilitate HDR with minimal mutagenic activity and avoid off-target effects (Cong et al. 2013, Fujii et al. 2014).

Other possible drawbacks of the CRISPR/cas9 system will be discussed in the following chapter.

4.5 Recombination

3` Screening PCRs of single cell clones carrying the Δ7 mutation or loxP sites clearly showed targeting at the correct position and results indicate that the locus was genome edited. However, further screenings revealed that all of the clones except one (Clone No. 3 for Δ7 mutation, cryoconservation but stopped growing after passage six) had undesired recombinations and indels. When the Δ7 ssODN was used, several different rearrangements of regions of exon ten were observed. Clones, which were positive for loxP sites, showed additional transcripts with wrong sizes and homozygous clones had no wildtype transcripts at all. Furthermore, all performed PCR analysis of the sequence upstream of the 3` end of the targeting vector failed possibly due to repetitive sequences of intron three (35 % SINE and 23 % LINE, http://www.repeatmasker.org/cgi-bin/WEBRepeatMasker, accessed on 27 April 2018).

Although the CRISPR/Cas9 is a versatile method for genome editing and has valuable applications, not all negative effects associated with its use are known. Hence, it might be responsible for the observed recombinations and rearrangements. In fact, other groups have noticed similar problems, e.g. deletions or insertions were observed in the loxP sites after the usage of gRNA and ssODN, and findings suggested that the mutations occurred during the recombination process (Bishop et al. 2016). Another group corrected a mutated allele by the use of CRISPR/Cas9 and ssODN and found erroneous alleles (“illegitimate repair”), that resulted from incorrect repair through HDR, next to correctly repaired alleles (Mianne et al. 2016). Furthermore, a group observed that the 5` junction had a high tendency to be joined correctly using microhomology-mediated end-joining and CRISPR/Cas9 or TALENS for gene knockin, whereas the 3` junction contained nucleotide substitutions, insertions or deletions (Nakade et al. 2014). Additionally, microinjection of two pairs of gRNAs in combination with a ssODN, which can bridge the breackpoints, led to deletions or inversions of up to 1.15 Mb in mouse zygotes. But further analysis showed that an unexpected level of complex rearrangements occurred, e.g. duplications of gene fragments in different orientations, local re-integration of the excised DNA-fragments and other unclear structural changes (Boroviak

et al. 2016, Boroviak et al. 2017). These examples show that after the usage of CRISPR/Cas9 unexpected events can happen and underlying mechanisms are not fully elucidated.

Although, the usage of a double cut donor vetor resulted in more targeted single cell clones several clones with an incorrect insertion of the donor plasmid were observed. In fact, the sequence was not correctly integrated via homologous recombination, but completely inserted in the *ERCC1* locus. Similar findings were also made from another group, which used double cut vectors and 3 % NHEJ-mediated insertions of large pieces from donor plasmid were detected (Zhang et al. 2017).

All findings indicate that CRISPR/Cas9 can result in unpredictable rearrangements. But in contrast to other groups that observed errors only in a small proportion of their genetically modified organisms or cells, not one of the *ERCC1* targeted cell clones showed the desired modifications without additional rearrangements. As no targeting experiment of the porcine *ERCC1* gene had been conducted the outcome was unknown. Only one correct targeted single cell clone for the Δ7 mutation (Clone No. 3) and none for loxP were obtained. This illustrates that additional to the CRISPR/Cas9 system the targeted locus has an impact on the outcome of the experiments. It is very likely that the role of the gene in genome integrity interferes with the desired modifications and that the functionality of the *ERCC1* gene is necessary for survival and hence disruption and loss of function is cytotoxic. Therefore, spontaneous genetic rearrangements might have happened in the porcine cells during gene editing experiments to maintain functional *ERCC1* gene. This phenomenon has already been shown in some Fanconi anemia patients, in which a mutation was reverted as a consequence of recombination of two mutated alleles that yielded an affected allele (Soulier et al. 2005). Furthermore, a progressive loss of *Ercc1*-deleted cells was observed in living animals. Newborn mice, which carried one knockout and one floxed *Ercc1* allele and expressed Cre recombinase from the Tie2 promotor, had a deleted floxed allele in about 50 % of spleen cells. At the age of one year hardly any cells with a recombined allele were found, indicating that *Ercc1*-deleted cells are outcompeted by cells in which the floxed allele was not recombined (Verhagen-Oldenampsen et al. 2012).

4.6 New strategies

Generation of single cell clones with a modification in the endogenous *ERCC1* gene was not achieved and consequently, generation of a porcine model with the methods used was not possible. Therefore, further strategies were designed to obtain an animal model with the phenotype of an old heart.

First, heart-specific AAVs can deliver the CRISPR/Cas9 system specifically into cardiac cells. These AAVs can be applied in the living animal at any time and by the generation of indels a knockout of the *ERCC1* gene could be achieved in the heart. Since the mutations would occur only in the heart, the effect on the whole organism would not be as dramatic as shown in mouse models. Nevertheless, this method has several drawbacks, e.g. not all cells would be transduced, cells containing the CRISPR/Cas9 could have mutations with no effect on the functionality of the gene or even keep their wildtype genotype and moreover cells with indels would be heterogenous since every cell will carry a different modification.

For these reasons, a second alternative strategy was designed (see 3.1.6). By introducing a modified *ERCC1* minigene in the *ROSA26* locus, integration of the desired modifications is shifted to another locus and both endogenous *ERCC1* alleles keep their full functionality. The intention is that viability of cells will not be influenced and unwanted recombinations during the integration process will be avoided. By the use of gRNAs the endogenous alleles can be destroyed at any timepoint. The advantage of this method is the possibility to react flexibly to negative effects. If the destruction of the endogenous alleles is too harmful in cell culture, living animals with functional *ERCC1* alleles can be generated and the $\Delta 7$ mutation or a floxed allele can be activated in a chosen tissue at a particular time.

4.7 MYBPC3

In contrast to the *ERCC1* project the *MYBPC3* project was straightforward and generation of clones showed no difficulties. The generation of a truncation of the *MYBPC3* was achieved very efficiently by the use of the CRISPR/Cas9 system. Compared to the *ERCC1* gene it was much easier to work with the *MYBPC3* gene. The porcine gene was already annotated and no sequences with high GC-contents or repetitive elements were found. PCRs of all necessary regions were possible and generation and use of gRNAs was straightforward.

Generation of a gene edited animal by nuclear transfer was achieved but the piglet was not viable.

Analysis of the stillborn piglet indicated that the animal had died due to heart failure. This could be a result of either problems during SCNT or due to the introduced mutations, since the piglet was compound heterozygous for the *MYBPC3* gene and protein expression was well below normal. Data from other species indicate that stillbirth can occur due to HCM, e.g. severe forms of HCM lead to death within the first year in infants (Lekanne Deprez et al. 2006, Marziliano et al. 2012). Furthermore, a group generated genetically modified pigs with a point mutation (R723G) in the porcine *MYH7* gene, which is mutated in 30 % of HCM patients. In humans, the mutation causes a severe form of HCM, clinical symptoms become manifest at an age of >12 years and perinatal death was not reported. Whereas, all piglets, even heterozygotes, died perinatally or within 24 h after birth and it stands to reason that the animals displayed an early stage of HCM (Montag et al. 2018). But, findings in other species are in contradiction. Although, stillborn kittens were observed in an inbred of Maine Coon cats that carry mutations in the MYBPC3 gene and develop HCM, it was shown that the mutations were not the cause of death (Wess et al. 2010, Kittleson et al. 2015). Additionally, homozygous knockout mice were obtained with Mendelian ratios of wildtype and embryonic lethality was not observed (Carrier et al. 2004, McConnell et al. 1999).

Somatic cell nuclear transfer is a complex multistep procedure that can be challenging and many biological and technical factors influence its efficiency. For example, the quality of the oocyte is very important since it has to survive removal of the metaphase plate and undergo cell culture conditions that may not be as *in vivo*. Another important factor is the reprogramming of transferred nucleus, which is in fact believed to be the main reason for cloning failure. The donor genome has to be reprogrammed before cell-fate decisions are made, especially regarding trophoblast differentiation, because malfunctions of it lead to placental insufficiency, which is a significant complication of SCNT leading to abortions (Arnold et al. 2006, Mullins et al. 2004, Akagi et al. 2014). Certainly, reprogramming is dependent on the quality of donor cells and to avoid that the cells used are not fully competent for the procedure various cell isolates of different breeds were used. While it cannot be excluded that the cells used were not suitable, it is unlikely that this will apply to all isolates and both mutations.

As the *MYH7* mutated piglets were also generated by SCNT, it is possible that the cloning procedure itself may have caused or contributed to the observed mortality (Montag et al. 2018). The nuclear transfer has long been associated with reduced viability. In general, a higher rate of stillbirths can be observed after nuclear transfer although the precise cause varies (Estrada et al. 2007, Watanabe and Nagai 2009, Kurome et al. 2013). Cardiovascular abnormalities have been found in patients with Beckwith-Wiedemann syndrome, which is a genetic overgrowth disorder and is mostly caused by imprinting defects (Greenwood et al. 1977, Brioude et al. 2018, Chen et al. 2013). A similar disorder, the large offspring syndrome, is a common problem occurring in animals generated by nuclear transfer since reprogramming and imprinting is a critical step during nuclear transfer (Chen et al. 2013, Young et al. 1998).

In conclusion, an influence of the cloning procedure on observed mortality in pigs is plausible, but pigs might also be more sensitive than mice and cats and even more sensitive than humans since even the heterozygous mutation in *MYH7* was lethal and pregnancy of two sows ended in late abortion and a stillbirth piglet combined with mummified fetuses for mutations in *MYBPC3*. Also, mouse and cat models show not the same manifestations of HCM as observed in humans.

The stillborn piglet had a heartbeat shortly before birth, therefore heart failure occurred during birth stress. The occurrence of the mummified piglets and also of the abortion indicates problems during gestation and the mummified fetuses may have had a negative effect on the stillborn piglet as well as delaying birth (more than 12 h). The cause of mummification and abortion is difficult to ascertain and although systemic maternal pathogens have been reported to cause this, no health problems were reported for this sow (Christianson 1992). Additionally, an impact of factors caused by SCNT cannot be excluded since mummified piglets and abortions are not uncommon after SCNT, but the exact connection could not be clarified (Estrada et al. 2007, Kolber-Simonds et al. 2004).

Analysis of the stillborn piglet showed decreased mRNA levels of the *MYBPC3* gene and protein was only detected in very low amounts indicating that the introduced mutations are functional and led to reduced amounts of the cMyBP-C protein. Furthermore, expression of genes associated with heart failure and disease was altered as it was expected in animals with the introduced mutations (see 3.2.3). Although, a connection of the altered gene

expression and the modification of the gene is very likely, it cannot be excluded that the piglet suffered from heart failure due to unknown factors independent of the mutations and it is very difficult to draw firm conclusions from a single animal. Manifestation of other diseases connected with SCNT, such as large offspring syndrome, is a possible cause for the heart failure in the stillborn piglet, although it showed no typical symptoms, such as abnormalities regarding growth or an enlarged tongue.

In summary, there are three different conclusions possible. Either the development failure and the heart failure occurred due to the missing cMyBP-C protein and the introduced mutations led to a very severe phenotype. Or, the heart failure occurred due to other reasons such as imperfect imprint after SCNT and the mutations in the *MYBPC3* gene do not lead to an early phenotype. Or, third a combined effect occurred. In the first case the use of homozygous or compound heterozygous clones is not recommended for SCNT. In my opinion, a combination of the induced *MYBPC3* defect and other unknown factors led to the loss of pregnancy and resulted in the stillborn piglet.

5 Outlook

Although, it was expected that targeting of the *ERCC1* gene would be difficult, nevertheless one allele should be possible according to results in mice. Several different strategies were used to generate gene targeted cells, but all failed. Still, a porcine model with conditional mutations in the *ERCC1* gene would be a valuable tool to provide important insights into many mammalian pathologies, not only regarding the heart. Such animals would have a broad field for usage, e.g. neurodegenerative disorders or cancer development. Recent findings indicate that several neurodenerative disorders, such as Parkinson`s disease, are linked to deficiency in repair of DNA damage and *Ercc1*-deficient mice have been used to study neurodenerative abnormalities (Sepe et al. 2016, Borgesius et al. 2011, de Waard et al. 2010). Furthermore, mice with a skin-specific *Ercc1* knockout developed epidermal skin tumors much more rapidly than controls after UV-irradiation (Doig et al. 2006). Additionally, a defect in the NER pathway leads to accumulation of DNA damage and there is a large amount of data supporting the view that DNA mutation is a typical feature of carcinogenesis (Lee and Chan 2015, Kidane et al. 2014). Hence, porcine models with a conditional *ERCC1* defect are worth pursuing, even though working with the gene is challenging. New strategies

for the generation of such animals have been designed and first steps carried out. AAVs carrying gRNA targeting exon five were designed and parts of the targeting vector containing the ERCC1 minigene for insertion into the Rosa26 locus have been generated. The latter strategy might also be applied for other genes that are difficult to target.

First experiments to generate a living animal with the desired mutations in the *MYBPC3* gene were unsuccessful. The stillborn piglet apparently died due to heart failure and a connection to the introduced mutations is very likely, but further analysis to exclude other possible underlying mechanisms, such as large offspring syndrome, remain to be conducted. Nevertheless, reasons for the low efficiency of the SCNT remain unclear. One possible explanation was that compound heterozygous or homozygous mutations led to severe problems during delevopment. To avoid this problem, cells with a heterozygous genotype can be used. Nevertheless, piglets with a mutation in the *MYH7* gene died even in the heterozygous state (Montag et al. 2018) and it is possible that the pig is more prone to heart failure and genetically modified animals cannot be generated with the used methods. Therefore, other new approaches should be considered, e.g. a conditional strategy can be used to avoid possible problems during development caused by the knockout. One or several exons can be floxed and Cre recombinase can be conducted time-specific in the living animal. Another approach is the microinjection of the used gRNAs in oocytes, which have been fertilised *in vitro* beforehand, and transfer these in a surrogate. With this method complications occurring due to SCNT can be avoided.

6 Abbreviations

5`/3` UTR	five/three prime untranslated region
AAV	adeno-associated virus
ACTA1	sceletal muscle α-actin
BS	blasticidin S resistance gene
bp	base pair
cDNA	complementary DNA
cMyBP-C	cardiac myosin-binding protein C
Cs	Cockayne syndrome
CSA	Cockayne syndrome A ortholog or ERCC8
CSB	Cockayne syndrome B ortholog or ERCC6
CRISPR/Cas9	clustered regularly interspaced short palindromic repeats/ CRISPR associated protein 9
crRNA	CRISPR RNA
CVDs	Cardiovascular diseases
Da	dalton
DNA	Deoxyribonucleic acid
DSB	double-strand break
ECG	electrocardiography
ERCC1	excision repair cross-complementation group 1
ES cells	embryonic stem cells
f	female
g	acceleration of gravity
GAPDH	Glycerinaldehyd-3-phosphat-Dehydrogenase

Abbreviations

gRNA	guide RNA
HCM	Hypertrophic cardiomyopathy
HDR	homology-directed repair
HR	homologous recombination
iPSCs	induced pluripotent stem cells
kb	kilobase
KDF	kidney derived fibroblasts
KO	knockout
L1H	LINE1 element
LINE	long interspersed repetitive elements
Lmna	lamin A
LR	Landrace
m	male
MEF	mouse embryonic fibroblast
M motif	MyBP-C motif
mRNA	messenger RNA
MSC	mesenchymal stem cell
MYBPC3	cardiac myosin-binding protein C
MYH7	myosin heavy chain 7
neo	neomycin resistance gene
NER	nucleotide excixion repair
NMD	nonsense-mediated mRNA decay
NHEJ	Non-homologous end joining
No.	number
NPPA/B	natriuretic peptide A/B

Abbreviations

PAGE	polyacrylamide gelelectrophoresis
PAM	protospacer adjacent motive
PBS	Phosphate Buffered Saline
PCR	polymerase chain reaction
puro	puromycin resistance gene
Q-PCR	Quantitative real time PCR
R26/ROSA26	reverse oriented splice acceptor, clone 26
RAD23B	RAD 23 homolog B, nucleotide excision repair protein
RNA	Ribonucleic acid
RPA	replication protein A
RT	room temperature
SA	splice acceptor
SCNT	somatic cell nuclear transfer
SCR7	5,6-bis((E)-benzylideneamino)-2-mercaptopyrimidin-4-ol
SDS	sodiumdodecylsulfate
SINE	short interspersed repetitive elements
ssODN	single-stranded oligodeoxyribonucleotide
TALENS	transcription activator-like effector nucleases
TFIIH	transcription factor II Human
tracrRNA	trans-activating crRNA
TV	targeting vector
U	enzyme unit
UV	ultraviolet
v/v	volume percent
wt	wildtype

xp	xeroderma pigmentosum
Xpa	Xeroderma pigmentosum, complementation group A
XPB	Xeroderma pigmentosum, complementation group B
Xpc	Xeroderma pigmentosum, complementation group C
XPD	Xeroderma pigmentosum, complementation group D or ERCC2
XPF	excision repair cross-complementation group 4 or ERCC4
Xpg	Xeroderma pigmentosum, complementation group G or ERCC5
ZFN	zinc finger nuclease
Zmpste24	zinc metallopeptidase STE24

7 List of tables

8 List of figures

9 Bibliography

AHMAD A, ROBINSON AR, DUENSING A, VAN DRUNEN E, BEVERLOO HB, WEISBERG DB, HASTY P, HOEIJMAKERS JHJ AND NIEDERNHOFER LJ. 2008. ERCC1-XPF Endonuclease Facilitates DNA Double-Strand Break Repair. Molecular and cellular biology 28: 5082-5092.

AKAGI S, MATSUKAWA K AND TAKAHASHI S. 2014. Factors affecting the development of somatic cell nuclear transfer embryos in Cattle. The Journal of reproduction and development 60: 329-335.

AL-MINAWI AZ ET AL. 2009. The ERCC1/XPF endonuclease is required for completion of homologous recombination at DNA replication forks stalled by inter-strand cross-links. Nucleic Acids Res 37: 6400-6413.

ALDERS M ET AL. 2003. The 2373insG mutation in the MYBPC3 gene is a founder mutation, which accounts for nearly one-fourth of the HCM cases in the Netherlands. European heart journal 24: 1848-1853.

ARNOLD DR, BORDIGNON V, LEFEBVRE R, MURPHY BD AND SMITH LC. 2006. Somatic cell nuclear transfer alters peri-implantation trophoblast differentiation in bovine embryos. Reproduction (Cambridge, England) 132: 279-290.

ARORA S, KOTHANDAPANI A, TILLISON K, KALMAN-MALTESE V AND PATRICK SM. 2010. Downregulation of XPF-ERCC1 enhances cisplatin efficacy in cancer cells. DNA Repair (Amst) 9: 745-753.

BARNHOORN S ET AL. 2014. Cell-autonomous progeroid changes in conditional mouse models for repair endonuclease XPG deficiency. PLoS genetics 10: e1004686.

BARRANGOU R, FREMAUX C, DEVEAU H, RICHARDS M, BOYAVAL P, MOINEAU S, ROMERO DA AND HORVATH P. 2007. CRISPR provides acquired resistance against viruses in prokaryotes. Science 315: 1709-1712.

BAXTER GF. 2004. The natriuretic peptides. Basic research in cardiology 99: 71-75.

BENETOS A, WAEBER B, IZZO J, MITCHELL G, RESNICK L, ASMAR R AND SAFAR M. 2002. Influence of age, risk factors, and cardiovascular and renal disease on arterial stiffness: clinical applications. American journal of hypertension 15: 1101-1108.

BERGO MO ET AL. 2002. Zmpste24 deficiency in mice causes spontaneous bone fractures, muscle weakness, and a prelamin A processing defect. Proceedings of the National Academy of Sciences of the United States of America 99: 13049-13054.

BIBIKOVA M, BEUMER K, TRAUTMAN JK AND CARROLL D. 2003. Enhancing gene targeting with designed zinc finger nucleases. Science 300: 764.

BIBIKOVA M, CARROLL D, SEGAL DJ, TRAUTMAN JK, SMITH J, KIM YG AND CHANDRASEGARAN S. 2001. Stimulation of homologous recombination through targeted cleavage by chimeric nucleases. Molecular and cellular biology 21: 289-297.

BISHOP KA, HARRINGTON A, KOURANOVA E, WEINSTEIN EJ, ROSEN CJ, CUI X AND LIAW L. 2016. CRISPR/Cas9-Mediated Insertion of loxP Sites in the Mouse Dock7 Gene Provides an Effective Alternative to Use of Targeted Embryonic Stem Cells. G3 (Bethesda, Md) 6: 2051-2061.

BORGESIUS NZ, DE WAARD MC, VAN DER PLUIJM I, OMRANI A, ZONDAG GC, VAN DER HORST GT, MELTON DW, HOEIJMAKERS JH, JAARSMA D AND ELGERSMA Y. 2011. Accelerated age-related cognitive decline and neurodegeneration, caused by

deficient DNA repair. The Journal of neuroscience : the official journal of the Society for Neuroscience 31: 12543-12553.

BOROVIAK K, DOE B, BANERJEE R, YANG F AND BRADLEY A. 2016. Chromosome engineering in zygotes with CRISPR/Cas9. Genesis (New York, NY : 2000) 54: 78-85.

BOROVIAK K, FU B, YANG F, DOE B AND BRADLEY A. 2017. Revealing hidden complexities of genomic rearrangements generated with Cas9. Sci Rep 7: 12867.

BOSS GR AND SEEGMILLER JE. 1981. Age-related physiological changes and their clinical significance. The Western journal of medicine 135: 434-440.

BOUABE H AND OKKENHAUG K. 2013. Gene targeting in mice: a review. Methods in molecular biology (Clifton, NJ) 1064: 315-336.

BRACE LE, VOSE SC, VARGAS DF, ZHAO S, WANG XP AND MITCHELL JR. 2013. Lifespan extension by dietary intervention in a mouse model of Cockayne syndrome uncouples early postnatal development from segmental progeria. Aging cell 12: 1144-1147.

BRIOUDE F ET AL. 2018. Expert consensus document: Clinical and molecular diagnosis, screening and management of Beckwith-Wiedemann syndrome: an international consensus statement. Nature reviews Endocrinology 14: 229-249.

BURDON TG AND WALL RJ. 1992. Fate of microinjected genes in preimplantation mouse embryos. Molecular reproduction and development 33: 436-442.

CAMACHO P, FAN H, LIU Z AND HE JQ. 2016. Large Mammalian Animal Models of Heart Disease. Journal of cardiovascular development and disease 3.

CAMPBELL KH. 2002. A background to nuclear transfer and its applications in agriculture and human therapeutic medicine. Journal of anatomy 200: 267-275.

CARLSON DF, TAN W, LILLICO SG, STVERAKOVA D, PROUDFOOT C, CHRISTIAN M, VOYTAS DF, LONG CR, WHITELAW CB AND FAHRENKRUG SC. 2012. Efficient TALEN-mediated gene knockout in livestock. Proceedings of the National Academy of Sciences of the United States of America 109: 17382-17387.

CARRERO D, SORIA-VALLES C AND LOPEZ-OTIN C. 2016. Hallmarks of progeroid syndromes: lessons from mice and reprogrammed cells. Disease models & mechanisms 9: 719-735.

CARRIER L ET AL. 1997. Organization and sequence of human cardiac myosin binding protein C gene (MYBPC3) and identification of mutations predicted to produce truncated proteins in familial hypertrophic cardiomyopathy. Circulation research 80: 427-434.

CARRIER L ET AL. 2004. Asymmetric septal hypertrophy in heterozygous cMyBP-C null mice. Cardiovasc Res 63: 293-304.

CARRIER L, MEARINI G, STATHOPOULOU K AND CUELLO F. 2015. Cardiac myosin-binding protein C (MYBPC3) in cardiac pathophysiology. Gene 573: 188-197.

CARRIER L, SCHLOSSAREK S, WILLIS MS AND ESCHENHAGEN T. 2010. The ubiquitin-proteasome system and nonsense-mediated mRNA decay in hypertrophic cardiomyopathy. Cardiovasc Res 85: 330-338.

CHEN PP, PATEL JR, POWERS PA, FITZSIMONS DP AND MOSS RL. 2012. Dissociation of structural and functional phenotypes in cardiac myosin-binding protein C conditional knockout mice. Circulation 126: 1194-1205.

CHEN Z, ROBBINS KM, WELLS KD AND RIVERA RM. 2013. Large offspring syndrome: a bovine model for the human loss-of-imprinting overgrowth syndrome Beckwith-Wiedemann. Epigenetics 8: 591-601.

CHRISTIANSON WT. 1992. Stillbirths, mummies, abortions, and early embryonic death. The Veterinary clinics of North America Food animal practice 8: 623-639.

CHU VT, WEBER T, WEFERS B, WURST W, SANDER S, RAJEWSKY K AND KÜHN R. 2015. Increasing the efficiency of homology-directed repair for CRISPR-Cas9-induced precise gene editing in mammalian cells. Nature biotechnology 33: 543.

CONCORDET J-P AND HAEUSSLER M. 2018. CRISPOR: intuitive guide selection for CRISPR/Cas9 genome editing experiments and screens. Nucleic acids research.

CONG L ET AL. 2013. Multiplex genome engineering using CRISPR/Cas systems. Science 339: 819-823.

CRISTEA S, FREYVERT Y, SANTIAGO Y, HOLMES MC, URNOV FD, GREGORY PD AND COST GJ. 2013. In vivo cleavage of transgene donors promotes nuclease-mediated targeted integration. Biotechnology and bioengineering 110: 871-880.

CUI J, LI J, MATHISON M, TONDATO F, MULKEY SP, MICKO C, CHRONOS NA AND ROBINSON KA. 2005. A clinically relevant large-animal model for evaluation of tissue-engineered cardiac surgical patch materials. Cardiovascular revascularization medicine : including molecular interventions 6: 113-120.

DAVIS AJ AND CHEN DJ. 2013. DNA double strand break repair via non-homologous end-joining. Translational cancer research 2: 130-143.

DE BEAUFORT HWL, CODA M, CONTI M, VAN BAKEL TMJ, NAUTA FJH, LANZARONE E, MOLL FL, VAN HERWAARDEN JA, AURICCHIO F AND TRIMARCHI S. 2017. Changes in aortic pulse wave velocity of four thoracic aortic stent grafts in an ex vivo porcine model. PloS one 12: e0186080.

DE BOER J, DE WIT J, VAN STEEG H, BERG RJ, MORREAU H, VISSER P, LEHMANN AR, DURAN M, HOEIJMAKERS JH AND WEEDA G. 1998. A mouse model for the basal transcription/DNA repair syndrome trichothiodystrophy. Mol Cell 1: 981-990.

DE LAAT WL, SIJBERS AM, ODIJK H, JASPERS NG AND HOEIJMAKERS JH. 1998. Mapping of interaction domains between human repair proteins ERCC1 and XPF. Nucleic Acids Research 26: 4146-4152.

DE WAARD MC ET AL. 2010. Age-related motor neuron degeneration in DNA repair-deficient Ercc1 mice. Acta neuropathologica 120: 461-475.

DENG C AND CAPECCHI MR. 1992. Reexamination of gene targeting frequency as a function of the extent of homology between the targeting vector and the target locus. Molecular and cellular biology 12: 3365-3371.

DHATTERWAL P, MEHROTRA S AND MEHROTRA R. 2017. Optimization of PCR conditions for amplifying an AT-rich amino acid transporter promoter sequence with high number of tandem repeats from Arabidopsis thaliana. BMC research notes 10: 638.

DING Y, LI H, CHEN L-L AND XIE K. 2016. Recent Advances in Genome Editing Using CRISPR/Cas9. Frontiers in Plant Science 7: 703.

DOIG J, ANDERSON C, LAWRENCE NJ, SELFRIDGE J, BROWNSTEIN DG AND MELTON DW. 2006. Mice with skin-specific DNA repair gene (Ercc1) inactivation are hypersensitive to ultraviolet irradiation-induced skin cancer and show more rapid actinic progression. Oncogene 25: 6229-6238.

DOLLE ME ET AL. 2011. Broad segmental progeroid changes in short-lived Ercc1(-/Delta7) mice. Pathobiology of aging & age related diseases 1.

EDIFIZI D AND SCHUMACHER B. 2015. Genome Instability in Development and Aging: Insights from Nucleotide Excision Repair in Humans, Mice, and Worms. Biomolecules 5: 1855-1869.

EL-ARMOUCHE A, POHLMANN L, SCHLOSSAREK S, STARBATTY J, YEH YH, NATTEL S, DOBREV D, ESCHENHAGEN T AND CARRIER L. 2007. Decreased phosphorylation levels of

cardiac myosin-binding protein-C in human and experimental heart failure. Journal of molecular and cellular cardiology 43: 223-229.

ESTRADA J, SOMMER J, COLLINS B, MIR B, MARTIN A, YORK A, PETTERS RM AND PIEDRAHITA JA. 2007. Swine generated by somatic cell nuclear transfer have increased incidence of intrauterine growth restriction (IUGR). Cloning and stem cells 9: 229-236.

EVANS E, MOGGS JG, HWANG JR, EGLY JM AND WOOD RD. 1997. Mechanism of open complex and dual incision formation by human nucleotide excision repair factors. Embo j 16: 6559-6573.

FAGGIONI M AND KNOLLMANN BC. 2012. Calsequestrin 2 and arrhythmias. American journal of physiology Heart and circulatory physiology 302: H1250-1260.

FERRARI E, BERDAJS D, TOZZI P, SINISCALCHI G AND VON SEGESSER LK. 2015. Apical closure device for transapical valve procedures. Interactive cardiovascular and thoracic surgery 21: 561-564.

FERRARI E, DEMERTZIS S, ANGELELLA J, BERDAJS D, TOZZI P, MOCCETTI T, MAISANO F AND VON SEGESSER LK. 2017. Apical closure device for full-percutaneous transapical valve implantation: stress-test in an animal modeldagger. Interactive cardiovascular and thoracic surgery 24: 721-726.

FISCHER K ET AL. 2016. Efficient production of multi-modified pigs for xenotransplantation by 'combineering', gene stacking and gene editing. Scientific Reports 6: 29081.

FLISIKOWSKA T, KIND A AND SCHNIEKE A. 2013. The new pig on the block: modelling cancer in pigs. Transgenic research 22: 673-680.

FOUGEROUSSE F, DELEZOIDE AL, FISZMAN MY, SCHWARTZ K, BECKMANN JS AND CARRIER L. 1998. Cardiac myosin binding protein C gene is specifically expressed in heart during murine and human development. Circulation research 82: 130-133.

FREEMAN LM, RUSH JE, STERN JA, HUGGINS GS AND MARON MS. 2017. Feline Hypertrophic Cardiomyopathy: A Spontaneous Large Animal Model of Human HCM. Cardiology Research 8: 139-142.

FRIEDBERG EC. 2001. How nucleotide excision repair protects against cancer. Nature reviews Cancer 1: 22-33.

FRIEDEL RH ET AL. 2005. Gene targeting using a promoterless gene trap vector ("targeted trapping") is an efficient method to mutate a large fraction of genes. Proceedings of the National Academy of Sciences of the United States of America 102: 13188-13193.

FUJII W, ONUMA A, SUGIURA K AND NAITO K. 2014. Efficient generation of genome-modified mice via offset-nicking by CRISPR/Cas system. Biochemical and Biophysical Research Communications 445: 791-794.

GARSIDE EL AND MACMILLAN AM. 2014. Cas9 in close-up. Nature biotechnology 32: 338.

GAUTEL M AND DJINOVIC-CARUGO K. 2016. The sarcomeric cytoskeleton: from molecules to motion. The Journal of experimental biology 219: 135-145.

GEDICKE-HORNUNG C ET AL. 2013. Rescue of cardiomyopathy through U7snRNA-mediated exon skipping in Mybpc3-targeted knock-in mice. EMBO molecular medicine 5: 1128-1145.

GIROLAMI F, OLIVOTTO I, PASSERINI I, ZACHARA E, NISTRI S, RE F, FANTINI S, BALDINI K, TORRICELLI F AND CECCHI F. 2006. A molecular screening strategy based on beta-myosin heavy chain, cardiac myosin binding protein C and troponin T genes in Italian patients with hypertrophic cardiomyopathy. Journal of cardiovascular medicine (Hagerstown, Md) 7: 601-607.

GORDON JW, SCANGOS GA, PLOTKIN DJ, BARBOSA JA AND RUDDLE FH. 1980. Genetic transformation of mouse embryos by microinjection of purified DNA. Proceedings of the National Academy of Sciences of the United States of America 77: 7380-7384.

GOSSLER A, JOYNER AL, ROSSANT J AND SKARNES WC. 1989. Mouse embryonic stem cells and reporter constructs to detect developmentally regulated genes. Science 244: 463-465.

GREENWOOD RD, SOMER A, ROSENTHAL A, CRAENEN J AND NADAS AS. 1977. Cardiovascular abnormalities in the Beckwith-Wiedemann syndrome. American journal of diseases of children (1960) 131: 293-294.

GREGG SQ, ROBINSON AR AND NIEDERNHOFER LJ. 2011. Physiological consequences of defects in ERCC1-XPF DNA repair endonuclease. DNA repair 10: 781-791.

GRELON M. 2016. Meiotic recombination mechanisms. Comptes rendus biologies 339: 247-251.

GROENEN MA ET AL. 2012. Analyses of pig genomes provide insight into porcine demography and evolution. Nature 491: 393-398.

GUTSCHNER T, HAEMMERLE M, GENOVESE G, DRAETTA GF AND CHIN L. 2016. Post-translational Regulation of Cas9 during G1 Enhances Homology-Directed Repair. Cell reports 14: 1555-1566.

HALLIWELL B. 2003. Oxidative stress in cell culture: an under-appreciated problem? FEBS letters 540: 3-6.

HAMMER RE, PURSEL VG, REXROAD JR CE, WALL RJ, BOLT DJ, EBERT KM, PALMITER RD AND BRINSTER RL. 1985. Production of transgenic rabbits, sheep and pigs by microinjection. Nature 315: 680.

HANAWALT PC. 2002. Subpathways of nucleotide excision repair and their regulation. Oncogene 21: 8949-8956.

HARKEMA L, YOUSSEF SA AND DE BRUIN A. 2016. Pathology of Mouse Models of Accelerated Aging. Veterinary pathology 53: 366-389.

HARRIS SP, BARTLEY CR, HACKER TA, MCDONALD KS, DOUGLAS PS, GREASER ML, POWERS PA AND MOSS RL. 2002. Hypertrophic cardiomyopathy in cardiac myosin binding protein-C knockout mice. Circulation research 90: 594-601.

HASTY P, RIVERA-PEREZ J AND BRADLEY A. 1991. The length of homology required for gene targeting in embryonic stem cells. Molecular and cellular biology 11: 5586-5591.

HAWKINS S AND WISWELL R. 2003. Rate and mechanism of maximal oxygen consumption decline with aging: implications for exercise training. Sports medicine (Auckland, NZ) 33: 877-888.

HEES PS, FLEG JL, LAKATTA EG AND SHAPIRO EP. 2002. Left ventricular remodeling with age in normal men versus women: novel insights using three-dimensional magnetic resonance imaging. The American journal of cardiology 90: 1231-1236.

HENSLEY N, DIETRICH J, NYHAN D, MITTER N, YEE MS AND BRADY M. 2015. Hypertrophic cardiomyopathy: a review. Anesthesia and analgesia 120: 554-569.

HOMMELSHEIM CM, FRANTZESKAKIS L, HUANG M AND ÜLKER B. 2014. PCR amplification of repetitive DNA: a limitation to genome editing technologies and many other applications. Scientific Reports 4: 5052.

HOWARTH JW, RAMISETTI S, NOLAN K, SADAYAPPAN S AND ROSEVEAR PR. 2012. Structural insight into unique cardiac myosin-binding protein-C motif: a partially folded domain. J Biol Chem 287: 8254-8262.

HUANG L ET AL. 2017. CRISPR/Cas9-mediated ApoE-/- and LDLR-/- double gene knockout in pigs elevates serum LDL-C and TC levels. Oncotarget 8: 37751-37760.

IGOR RAFAEL S, RICARDO A, ERASMO SIMÃO DA S, SERGIO B, MARIA DE LOURDES H, VITOR CERVANTES G, PEDRO NOGUEIRA G, ANNA PAULA WEINHARDT B AND LUIZ FRANCISCO POLI DE F. 2011. Impact of Stent-Graft Oversizing on the Thoracic Aorta: Experimental Study in a Porcine Model. Journal of Endovascular Therapy 18: 576-584.

JAARSMA D ET AL. 2011. Age-related neuronal degeneration: complementary roles of nucleotide excision repair and transcription-coupled repair in preventing neuropathology. PLoS genetics 7: e1002405.

JAGANNATHAN L, CUDDAPAH S AND COSTA M. 2016. Oxidative stress under ambient and physiological oxygen tension in tissue culture. Current pharmacology reports 2: 64-72.

JASPERS NGJ ET AL. 2007. First Reported Patient with Human ERCC1 Deficiency Has Cerebro-Oculo-Facio-Skeletal Syndrome with a Mild Defect in Nucleotide Excision Repair and Severe Developmental Failure. American journal of human genetics 80: 457-466.

JO BS AND CHOI SS. 2015. Introns: The Functional Benefits of Introns in Genomes. Genomics & informatics 13: 112-118.

JOHANNES S, CLAUDIA H, FRIEDHELM B, MATTHIAS S, ROBERT MB, DITTMAR B, RANDALL BG AND MORITZ SB. 2012. Early Histological Changes in the Porcine Aortic Media After Thoracic Stent-Graft Implantation. Journal of Endovascular Therapy 19: 363-369.

KAJSTURA J, CHENG W, SARANGARAJAN R, LI P, LI B, NITAHARA JA, CHAPNICK S, REISS K, OLIVETTI G AND ANVERSA P. 1996. Necrotic and apoptotic myocyte cell death in the aging heart of Fischer 344 rats. The American journal of physiology 271: H1215-1228.

KARIKKINETH AC, SCHEIBYE-KNUDSEN M, FIVENSON E, CROTEAU DL AND BOHR VA. 2017. Cockayne syndrome: Clinical features, model systems and pathways. Ageing research reviews 33: 3-17.

KASHIYAMA K ET AL. 2013. Malfunction of nuclease ERCC1-XPF results in diverse clinical manifestations and causes Cockayne syndrome, xeroderma pigmentosum, and Fanconi anemia. American journal of human genetics 92: 807-819.

KASPAR BK ET AL. 2002. Adeno-associated virus effectively mediates conditional gene modification in the brain. Proceedings of the National Academy of Sciences of the United States of America 99: 2320-2325.

KEERAN KJ, JEFFRIES KR, ZETTS AD, TAYLOR J, KOZLOV S AND HUNT TJ. 2017. A Chronic Cardiac Ischemia Model in Swine Using an Ameroid Constrictor. e56190.

KIDANE D, CHAE WJ, CZOCHOR J, ECKERT KA, GLAZER PM, BOTHWELL AL AND SWEASY JB. 2014. Interplay between DNA repair and inflammation, and the link to cancer. Critical reviews in biochemistry and molecular biology 49: 116-139.

KITTLESON MD, MEURS KM AND HARRIS SP. 2015. The genetic basis of hypertrophic cardiomyopathy in cats and humans. Journal of veterinary cardiology : the official journal of the European Society of Veterinary Cardiology 17 Suppl 1: S53-73.

KLOCKE R, TIAN W, KUHLMANN MT AND NIKOL S. 2007. Surgical animal models of heart failure related to coronary heart disease. Cardiovascular Research 74: 29-38.

KOLBER-SIMONDS D ET AL. 2004. Production of alpha-1,3-galactosyltransferase null pigs by means of nuclear transfer with fibroblasts bearing loss of heterozygosity mutations. Proceedings of the National Academy of Sciences of the United States of America 101: 7335-7340.

KRAMER KM, BROCK JA, BLOOM K, MOORE JK AND HABER JE. 1994. Two different types of double-strand breaks in Saccharomyces cerevisiae are repaired by similar RAD52-independent, nonhomologous recombination events. Molecular and cellular biology 14: 1293-1301.

KUROME M ET AL. 2013. Factors influencing the efficiency of generating genetically engineered pigs by nuclear transfer: multi-factorial analysis of a large data set. BMC biotechnology 13: 43.

KUSTER DW ET AL. 2013. GSK3beta phosphorylates newly identified site in the proline-alanine-rich region of cardiac myosin-binding protein C and alters cross-bridge cycling kinetics in human: short communication. Circulation research 112: 633-639.

LAI L ET AL. 2002. Production of alpha-1,3-galactosyltransferase knockout pigs by nuclear transfer cloning. Science 295: 1089-1092.

LAKATTA EG. 2002. Age-associated cardiovascular changes in health: impact on cardiovascular disease in older persons. Heart failure reviews 7: 29-49.

LANDER ES ET AL. 2001. Initial sequencing and analysis of the human genome. Nature 409: 860-921.

LAPOSA RR, HUANG EJ AND CLEAVER JE. 2007. Increased apoptosis, p53 up-regulation, and cerebellar neuronal degeneration in repair-deficient Cockayne syndrome mice. Proceedings of the National Academy of Sciences of the United States of America 104: 1389-1394.

LEE J, CHUNG JH, KIM HM, KIM DW AND KIM H. 2016. Designed nucleases for targeted genome editing. Plant biotechnology journal 14: 448-462.

LEE SC AND CHAN JC. 2015. Evidence for DNA damage as a biological link between diabetes and cancer. Chinese medical journal 128: 1543-1548.

LEE SG ET AL. 2017. Age-associated molecular changes are deleterious and may modulate life span through diet. Science advances 3: e1601833.

LEKANNE DEPREZ RH, MUURLING-VLIETMAN JJ, HRUDA J, BAARS MJ, WIJNAENDTS LC, STOLTE-DIJKSTRA I, ALDERS M AND VAN HAGEN JM. 2006. Two cases of severe neonatal hypertrophic cardiomyopathy caused by compound heterozygous mutations in the MYBPC3 gene. Journal of medical genetics 43: 829-832.

LELOVAS PP, KOSTOMITSOPOULOS NG AND XANTHOS TT. 2014. A comparative anatomic and physiologic overview of the porcine heart. Journal of the American Association for Laboratory Animal Science : JAALAS 53: 432-438.

LI G, ZHANG X, ZHONG C, MO J, QUAN R, YANG J, LIU D, LI Z, YANG H AND WU Z. 2017. Small molecules enhance CRISPR/Cas9-mediated homology-directed genome editing in primary cells. Scientific Reports 7: 8943.

LI L, ELLEDGE SJ, PETERSON CA, BALES ES AND LEGERSKI RJ. 1994. Specific association between the human DNA repair proteins XPA and ERCC1. Proceedings of the National Academy of Sciences of the United States of America 91: 5012-5016.

LI S, FLISIKOWSKA T, KUROME M, ZAKHARTCHENKO V, KESSLER B, SAUR D, KIND A, WOLF E, FLISIKOWSKI K AND SCHNIEKE A. 2014a. Dual fluorescent reporter pig for Cre recombination: transgene placement at the ROSA26 locus. PloS one 9: e102455.

LI X AND HEYER WD. 2008. Homologous recombination in DNA repair and DNA damage tolerance. Cell research 18: 99-113.

LI X ET AL. 2014b. Rosa26-targeted swine models for stable gene over-expression and Cre-mediated lineage tracing. Cell research 24: 501-504.

LIU L, LEE J AND ZHOU P. 2010. Navigating the nucleotide excision repair threshold. Journal of cellular physiology 224: 585-589.

LU ZH, BOOKS JT, KAUFMAN RM AND LEY TJ. 2003. Long targeting arms do not increase the efficiency of homologous recombination in the beta-globin locus of murine embryonic stem cells. Blood 102: 1531-1533.

MA H ET AL. 2017. Correction of a pathogenic gene mutation in human embryos. Nature 548: 413-419.

MALI P, YANG L, ESVELT KM, AACH J, GUELL M, DICARLO JE, NORVILLE JE AND CHURCH GM. 2013. RNA-guided human genome engineering via Cas9. Science 339: 823-826.

MAN J, BARNETT P AND CHRISTOFFELS VM. 2018. Structure and function of the Nppa-Nppb cluster locus during heart development and disease. Cellular and molecular life sciences : CMLS 75: 1435-1444.

MANANDHAR M, BOULWARE KS AND WOOD RD. 2015. The ERCC1 and ERCC4 (XPF) genes and gene products. Gene 569: 153-161.

MANJI RA, LEE W AND COOPER DKC. 2015. Xenograft bioprosthetic heart valves: Past, present and future. International journal of surgery (London, England) 23: 280-284.

MARON BJ AND MARON MS. 2013. Hypertrophic cardiomyopathy. The Lancet 381: 242-255.

MARSTON S, COPELAND O, GEHMLICH K, SCHLOSSAREK S AND CARRIER L. 2012. How do MYBPC3 mutations cause hypertrophic cardiomyopathy? Journal of muscle research and cell motility 33: 75-80.

MARUYAMA T, DOUGAN SK, TRUTTMANN M, BILATE AM, INGRAM JR AND PLOEGH HL. 2015. Inhibition of non-homologous end joining increases the efficiency of CRISPR/Cas9-mediated precise [TM: inserted] genome editing. Nature biotechnology 33: 538-542.

MARZILIANO N, MERLINI PA, VIGNATI G, ORSINI F, MOTTA V, BANDIERA L, INTRIERI M AND VERONESE S. 2012. A case of compound mutations in the MYBPC3 gene associated with biventricular hypertrophy and neonatal death. Neonatology 102: 254-258.

MCCONNELL BK ET AL. 1999. Dilated cardiomyopathy in homozygous myosin-binding protein-C mutant mice. The Journal of clinical investigation 104: 1235-1244.

MCCREATH KJ, HOWCROFT J, CAMPBELL KH, COLMAN A, SCHNIEKE AE AND KIND AJ. 2000. Production of gene-targeted sheep by nuclear transfer from cultured somatic cells. Nature 405: 1066-1069.

MCLENACHAN S, SARSERO JP AND IOANNOU PA. 2007. Flow-cytometric analysis of mouse embryonic stem cell lipofection using small and large DNA constructs. Genomics 89: 708-720.

MCNEIL EM ET AL. 2015. Inhibition of the ERCC1-XPF structure-specific endonuclease to overcome cancer chemoresistance. DNA Repair (Amst) 31: 19-28.

MCWHIR J, SELFRIDGE J, HARRISON DJ, SQUIRES S AND MELTON DW. 1993. Mice with DNA repair gene (ERCC-1) deficiency have elevated levels of p53, liver nuclear abnormalities and die before weaning. Nat Genet 5: 217-224.

MEARINI G ET AL. 2014. Mybpc3 gene therapy for neonatal cardiomyopathy enables long-term disease prevention in mice. Nature communications 5: 5515.

MEARINI G ET AL. 2013. Repair of Mybpc3 mRNA by 5'-trans-splicing in a Mouse Model of Hypertrophic Cardiomyopathy. Molecular therapy Nucleic acids 2: e102.

MEIER ID, BERNREUTHER C, TILLING T, NEIDHARDT J, WONG YW, SCHULZE C, STREICHERT T AND SCHACHNER M. 2010. Short DNA sequences inserted for gene targeting can accidentally interfere with off-target gene expression. FASEB journal : official publication of the Federation of American Societies for Experimental Biology 24: 1714-1724.

MELIS JP ET AL. 2008. Mouse models for xeroderma pigmentosum group A and group C show divergent cancer phenotypes. Cancer Res 68: 1347-1353.

MIANNE J ET AL. 2016. Correction of the auditory phenotype in C57BL/6N mice via CRISPR/Cas9-mediated homology directed repair. Genome medicine 8: 16.

MILANI-NEJAD N AND JANSSEN PML. 2014. Small and large animal models in cardiac contraction research: advantages and disadvantages. Pharmacology & therapeutics 141: 235-249.

MILLER JC ET AL. 2011. A TALE nuclease architecture for efficient genome editing. Nature biotechnology 29: 143-148.

MOHAMED IA, KRISHNAMOORTHY NT, NASRALLAH GK AND DA'AS SI. 2017. The Role of Cardiac Myosin Binding Protein C3 in Hypertrophic Cardiomyopathy-Progress and Novel Therapeutic Opportunities. Journal of cellular physiology 232: 1650-1659.

MONTAG J, PETERSEN B, FLOGEL AK, BECKER E, LUCAS-HAHN A, COST GJ, MUHLFELD C, KRAFT T, NIEMANN H AND BRENNER B. 2018. Successful knock-in of Hypertrophic Cardiomyopathy-mutation R723G into the MYH7 gene mimics HCM pathology in pigs. Sci Rep 8: 4786.

MOOLMAN JA ET AL. 2000. A newly created splice donor site in exon 25 of the MyBP-C gene is responsible for inherited hypertrophic cardiomyopathy with incomplete disease penetrance. Circulation 101: 1396-1402.

MOORE JK AND HABER JE. 1996. Cell cycle and genetic requirements of two pathways of nonhomologous end-joining repair of double-strand breaks in Saccharomyces cerevisiae. Molecular and cellular biology 16: 2164-2173.

MULLINS LJ, WILMUT I AND MULLINS JJ. 2004. Nuclear transfer in rodents. The Journal of physiology 554: 4-12.

MUNOZ P, BLANCO R, FLORES JM AND BLASCO MA. 2005. XPF nuclease-dependent telomere loss and increased DNA damage in mice overexpressing TRF2 result in premature aging and cancer. Nat Genet 37: 1063-1071.

MYKEN PS AND BECH-HANSEN O. 2009. A 20-year experience of 1712 patients with the Biocor porcine bioprosthesis. The Journal of thoracic and cardiovascular surgery 137: 76-81.

NAKADE S ET AL. 2014. Microhomology-mediated end-joining-dependent integration of donor DNA in cells and animals using TALENs and CRISPR/Cas9. Nature communications 5: 5560.

NICCOLI T AND PARTRIDGE L. 2012. Ageing as a risk factor for disease. Current biology : CB 22: R741-752.

NIIMURA H ET AL. 1998. Mutations in the gene for cardiac myosin-binding protein C and late-onset familial hypertrophic cardiomyopathy. N Engl J Med 338: 1248-1257.

NOWAK-IMIALEK M AND NIEMANN H. 2012. Pluripotent cells in farm animals: state of the art and future perspectives. Reproduction, fertility, and development 25: 103-128.

NOWAK KJ, RAVENSCROFT G AND LAING NG. 2013. Skeletal muscle alpha-actin diseases (actinopathies): pathology and mechanisms. Acta neuropathologica 125: 19-32.

O'DONOVAN A, DAVIES AA, MOGGS JG, WEST SC AND WOOD RD. 1994. XPG endonuclease makes the 3' incision in human DNA nucleotide excision repair. Nature 371: 432-435.

OGITA M ET AL. 2016. Development of Accelerated Coronary Atherosclerosis Model Using Low Density Lipoprotein Receptor Knock-Out Swine with Balloon Injury. PloS one 11: e0163055.

OKADA N. 1991. SINEs. Current Opinion in Genetics & Development 1: 498-504.

OLIVETTI G, MELISSARI M, CAPASSO JM AND ANVERSA P. 1991. Cardiomyopathy of the aging human heart. Myocyte loss and reactive cellular hypertrophy. Circulation research 68: 1560-1568.

ORLANDO SJ ET AL. 2010. Zinc-finger nuclease-driven targeted integration into mammalian genomes using donors with limited chromosomal homology. Nucleic Acids Res 38: e152.

OSORIO FG ET AL. 2011. Splicing-directed therapy in a new mouse model of human accelerated aging. Science translational medicine 3: 106ra107.

PANDA SK, WEFERS B, ORTIZ O, FLOSS T, SCHMID B, HAASS C, WURST W AND KUHN R. 2013. Highly efficient targeted mutagenesis in mice using TALENs. Genetics 195: 703-713.

PENDAS AM ET AL. 2002. Defective prelamin A processing and muscular and adipocyte alterations in Zmpste24 metalloproteinase-deficient mice. Nat Genet 31: 94-99.

PIERCE AJ, HU P, HAN M, ELLIS N AND JASIN M. 2001. Ku DNA end-binding protein modulates homologous repair of double-strand breaks in mammalian cells. Genes Dev 15: 3237-3242.

POLEJAEVA IA AND CAMPBELL KH. 2000. New advances in somatic cell nuclear transfer: application in transgenesis. Theriogenology 53: 117-126.

POLLACK M AND LEEUWENBURGH C. 2001. Apoptosis and aging: role of the mitochondria. The journals of gerontology Series A, Biological sciences and medical sciences 56: B475-482.

PORTEUS M. 2007. Using homologous recombination to manipulate the genome of human somatic cells. Biotechnology & genetic engineering reviews 24: 195-212.

PURSEL VG, PINKERT CA, MILLER KF, BOLT DJ, CAMPBELL RG, PALMITER RD, BRINSTER RL AND HAMMER RE. 1989. Genetic engineering of livestock. Science 244: 1281-1288.

PUTINSKI C, ABDUL-GHANI M, STILES R, BRUNETTE S, DICK SA, FERNANDO P AND MEGENEY LA. 2013. Intrinsic-mediated caspase activation is essential for cardiomyocyte hypertrophy. Proceedings of the National Academy of Sciences of the United States of America 110: E4079-4087.

REEMTSMA K. 1995. Xenotransplantation: A Historical Perspective. ILAR journal 37: 9-12.

RICHARDSON CD, RAY GJ, DEWITT MA, CURIE GL AND CORN JE. 2016. Enhancing homology-directed genome editing by catalytically active and inactive CRISPR-Cas9 using asymmetric donor DNA. Nature biotechnology 34: 339-344.

RIET J, RAMOS LRV, LEWIS RV AND MARINS LF. 2017. Improving the PCR protocol to amplify a repetitive DNA sequence. Genetics and molecular research : GMR 16.

RUBIN JS, JOYNER AL, BERNSTEIN A AND WHITMORE GF. 1983. Molecular identification of a human DNA repair gene following DNA-mediated gene transfer. Nature 306: 206-208.

SABATER-MOLINA M, PEREZ-SANCHEZ I, HERNANDEZ DEL RINCON JP AND GIMENO JR. 2018. Genetics of hypertrophic cardiomyopathy: A review of current state. Clinical genetics 93: 3-14.

SADAYAPPAN S ET AL. 2011. A critical function for Ser-282 in cardiac Myosin binding protein-C phosphorylation and cardiac function. Circulation research 109: 141-150.

SAHDEV S, SAINI S, TIWARI P, SAXENA S AND SINGH SAINI K. 2007. Amplification of GC-rich genes by following a combination strategy of primer design, enhancers and modified PCR cycle conditions. Molecular and cellular probes 21: 303-307.

SAITO Y. 2010. Roles of atrial natriuretic peptide and its therapeutic use. Journal of Cardiology 56: 262-270.

SANDER JD AND JOUNG JK. 2014. CRISPR-Cas systems for editing, regulating and targeting genomes. Nature biotechnology 32: 347-355.

SAUER B AND HENDERSON N. 1988. Site-specific DNA recombination in mammalian cells by the Cre recombinase of bacteriophage P1. Proceedings of the National Academy of Sciences of the United States of America 85: 5166-5170.

SAUER B AND MCDERMOTT J. 2004. DNA recombination with a heterospecific Cre homolog identified from comparison of the pac-c1 regions of P1-related phages. Nucleic Acids Res 32: 6086-6095.

SCHARER OD. 2013. Nucleotide excision repair in eukaryotes. Cold Spring Harbor perspectives in biology 5: a012609.

SCHNIEKE AE, KIND AJ, RITCHIE WA, MYCOCK K, SCOTT AR, RITCHIE M, WILMUT I, COLMAN A AND CAMPBELL KH. 1997. Human factor IX transgenic sheep produced by transfer of nuclei from transfected fetal fibroblasts. Science 278: 2130-2133.

SELFRIDGE J, HSIA KT, REDHEAD NJ AND MELTON DW. 2001. Correction of liver dysfunction in DNA repair-deficient mice with an ERCC1 transgene. Nucleic Acids Res 29: 4541-4550.

SEPE S ET AL. 2016. Inefficient DNA Repair Is an Aging-Related Modifier of Parkinson's Disease. Cell reports 15: 1866-1875.

SIJBERS AM, VAN DER SPEK PJ, ODIJK H, VAN DEN BERG J, VAN DUIN M, WESTERVELD A, JASPERS NG, BOOTSMA D AND HOEIJMAKERS JH. 1996. Mutational analysis of the human nucleotide excision repair gene ERCC1. Nucleic Acids Research 24: 3370-3380.

SONG J, YANG D, XU J, ZHU T, CHEN YE AND ZHANG J. 2016. RS-1 enhances CRISPR/Cas9- and TALEN-mediated knock-in efficiency. Nature communications 7: 10548.

SOULIER J ET AL. 2005. Detection of somatic mosaicism and classification of Fanconi anemia patients by analysis of the FA/BRCA pathway. Blood 105: 1329-1336.

STRAIT JB AND LAKATTA EG. 2012. Aging-associated cardiovascular changes and their relationship to heart failure. Heart failure clinics 8: 143-164.

TAJSHARGHI H. 2008. Thick and thin filament gene mutations in striated muscle diseases. International journal of molecular sciences 9: 1259-1275.

TAYLOR EM, BROUGHTON BC, BOTTA E, STEFANINI M, SARASIN A, JASPERS NG, FAWCETT H, HARCOURT SA, ARLETT CF AND LEHMANN AR. 1997. Xeroderma pigmentosum and trichothiodystrophy are associated with different mutations in the XPD (ERCC2) repair/transcription gene. Proceedings of the National Academy of Sciences of the United States of America 94: 8658-8663.

THOMAS KR AND CAPECCHI MR. 1987. Site-directed mutagenesis by gene targeting in mouse embryo-derived stem cells. Cell 51: 503-512.

TRIPSIANES K, FOLKERS G, AB E, DAS D, ODIJK H, JASPERS NG, HOEIJMAKERS JH, KAPTEIN R AND BOELENS R. 2005. The structure of the human ERCC1/XPF interaction domains reveals a complementary role for the two proteins in nucleotide excision repair. Structure (London, England : 1993) 13: 1849-1858.

TYCKO J, MYER VE AND HSU PD. 2016. Methods for Optimizing CRISPR-Cas9 Genome Editing Specificity. Mol Cell 63: 355-370.

VAN DER HORST GT ET AL. 2002. UVB radiation-induced cancer predisposition in Cockayne syndrome group A (Csa) mutant mice. DNA Repair (Amst) 1: 143-157.

VAN DER HORST GT ET AL. 1997. Defective transcription-coupled repair in Cockayne syndrome B mice is associated with skin cancer predisposition. Cell 89: 425-435.

VAN DER PLUIJM I ET AL. 2007. Impaired genome maintenance suppresses the growth hormone--insulin-like growth factor 1 axis in mice with Cockayne syndrome. PLoS biology 5: e2.

VAN DUIN M, DE WIT J, ODIJK H, WESTERVELD A, YASUI A, KOKEN MHM, HOEIJMAKERS JHJ AND BOOTSMA D. 1986. Molecular characterization of the human excision repair gene ERCC-1: cDNA cloning and amino acid homology with the yeast DNA repair gene RAD10. Cell 44: 913-923.

VAN DUIN M, KOKEN MH, VAN DEN TOL J, TEN DIJKE P, ODIJK H, WESTERVELD A, BOOTSMA D AND HOEIJMAKERS JH. 1987. Genomic characterization of the human DNA excision repair gene ERCC-1. Nucleic Acids Research 15: 9195-9213.

VAN DUIN M, VAN DEN TOL J, WARMERDAM P, ODIJK H, MEIJER D, WESTERVELD A, BOOTSMA D AND HOEIJMAKERS JH. 1988. Evolution and mutagenesis of the mammalian excision repair gene ERCC-1. Nucleic Acids Research 16: 5305-5322.

VAN DUYNE GD. 2001. A structural view of cre-loxp site-specific recombination. Annual review of biophysics and biomolecular structure 30: 87-104.

VAN ROOIJ E, QUIAT D, JOHNSON BA, SUTHERLAND LB, QI X, RICHARDSON JA, KELM RJ, JR. AND OLSON EN. 2009. A family of microRNAs encoded by myosin genes governs myosin expression and muscle performance. Developmental cell 17: 662-673.

VERHAGEN-OLDENAMPSEN JH, HAANSTRA JR, VAN STRIEN PM, VALKHOF M, TOUW IP AND VON LINDERN M. 2012. Loss of ercc1 results in a time- and dose-dependent reduction of proliferating early hematopoietic progenitors. Anemia 2012: 783068.

VERMEIJ WP, HOEIJMAKERS JH AND POTHOF J. 2016. Genome Integrity in Aging: Human Syndromes, Mouse Models, and Therapeutic Options. Annual review of pharmacology and toxicology 56: 427-445.

VIGNIER N ET AL. 2009. Nonsense-mediated mRNA decay and ubiquitin-proteasome system regulate cardiac myosin-binding protein C mutant levels in cardiomyopathic mice. Circulation research 105: 239-248.

VOLKER M, MONE MJ, KARMAKAR P, VAN HOFFEN A, SCHUL W, VERMEULEN W, HOEIJMAKERS JH, VAN DRIEL R, VAN ZEELAND AA AND MULLENDERS LH. 2001. Sequential assembly of the nucleotide excision repair factors in vivo. Mol Cell 8: 213-224.

WANG W, BAGSHAW SM, NORRIS CM, ZIBDAWI R, ZIBDAWI M AND MACARTHUR R. 2014. Association between older age and outcome after cardiac surgery: a population-based cohort study. Journal of cardiothoracic surgery 9: 177.

WATANABE S AND NAGAI T. 2009. Death losses due to stillbirth, neonatal death and diseases in cloned cattle derived from somatic cell nuclear transfer and their progeny: a result of nationwide survey in Japan. Animal science journal = Nihon chikusan Gakkaiho 80: 233-238.

WEEDA G, DONKER I, DE WIT J, MORREAU H, JANSSENS R, VISSERS CJ, NIGG A, VAN STEEG H, BOOTSMA D AND HOEIJMAKERS JH. 1997. Disruption of mouse ERCC1 results in a novel repair syndrome with growth failure, nuclear abnormalities and senescence. Current biology : CB 7: 427-439.

WERFEL S ET AL. 2014. Rapid and highly efficient inducible cardiac gene knockout in adult mice using AAV-mediated expression of Cre recombinase. Cardiovasc Res 104: 15-23.

WESS G, SCHINNER C, WEBER K, KUCHENHOFF H AND HARTMANN K. 2010. Association of A31P and A74T polymorphisms in the myosin binding protein C3 gene and hypertrophic cardiomyopathy in Maine Coon and other breed cats. Journal of veterinary internal medicine 24: 527-532.

WESTERVELD A, HOEIJMAKERS JH, VAN DUIN M, DE WIT J, ODIJK H, PASTINK A, WOOD RD AND BOOTSMA D. 1984a. Molecular cloning of a human DNA repair gene. Nature 310: 425-429.

WESTERVELD A, HOEIJMAKERS JHJ, VAN DUIN M, DE WIT J, ODIJK H, PASTINK A, WOOD RD AND BOOTSMA D. 1984b. Molecular cloning of a human DNA repair gene. Nature 310: 425-429.

WITT CC, GERULL B, DAVIES MJ, CENTNER T, LINKE WA AND THIERFELDER L. 2001. Hypercontractile properties of cardiac muscle fibers in a knock-in mouse model of cardiac myosin-binding protein-C. J Biol Chem 276: 5353-5359.

WOOD RD. 2010. Mammalian nucleotide excision repair proteins and interstrand crosslink repair. Environmental and Molecular Mutagenesis 51: 520-526.

YANG D, SCAVUZZO MA, CHMIELOWIEC J, SHARP R, BAJIC A AND BOROWIAK M. 2016. Enrichment of G2/M cell cycle phase in human pluripotent stem cells enhances HDR-mediated gene repair with customizable endonucleases. Sci Rep 6: 21264.

YANG H, WANG H, SHIVALILA CS, CHENG AW, SHI L AND JAENISCH R. 2013. One-step generation of mice carrying reporter and conditional alleles by CRISPR/Cas-mediated genome engineering. Cell 154: 1370-1379.

YANG Q, SANBE A, OSINSKA H, HEWETT TE, KLEVITSKY R AND ROBBINS J. 1998. A mouse model of myosin binding protein C human familial hypertrophic cardiomyopathy. The Journal of clinical investigation 102: 1292-1300.

YANG Q, SANBE A, OSINSKA H, HEWETT TE, KLEVITSKY R AND ROBBINS J. 1999. In vivo modeling of myosin binding protein C familial hypertrophic cardiomyopathy. Circulation research 85: 841-847.

YOUNG LE, SINCLAIR KD AND WILMUT I. 1998. Large offspring syndrome in cattle and sheep. Reviews of reproduction 3: 155-163.

YU C ET AL. 2015. Small molecules enhance CRISPR genome editing in pluripotent stem cells. Cell stem cell 16: 142-147.

ZHANG JP ET AL. 2017. Efficient precise knockin with a double cut HDR donor after CRISPR/Cas9-mediated double-stranded DNA cleavage. Genome biology 18: 35.

ZHOU X ET AL. 2015. Generation of CRISPR/Cas9-mediated gene-targeted pigs via somatic cell nuclear transfer. Cellular and molecular life sciences : CMLS 72: 1175-1184.

10 Appendix

10.1 Sequences of DNA-fragments

Table 35: Sequences of DNA-fragments.
All fragments were purchased from Integrated DNA Technologies, Leuven, BEL.

DNA-fragments	Sequence (5`→ 3`)
ERCC1_Ex5_loxP	CTGTCCTCCTGAGCTCGCCAGGCCCTCTGCATTCCACTGAGCAGGACAAAGG GGTCTGGGGATGATAACTTCGTATAGCATACATTATACGAAGTTATACCGGG ACCTCCCAACCCCGCCGTCTCCCTGCCCGCAGCCTCCGCTACCACAACCTCCA TCCGGATTACATCCACCAGCGGCTGCAGAGTCTCGGCAAGAGCTTCGCACTC CGCGTCCTGCTCGTCCAGGTAGACGTGGTAAGCAGGGGTCACTCCATAACTT CGTATAGCATACATTATACGAAGTTATCCTGGCAGCCTCACTGTCCACATCTG TGAAATGGGGAGTGTTGGGCCTCAAGGTAGCCAGGTAGACTATTGACTCCC TTCCAATAAGAAATGCAAGTGGGAGCAGTTCCCGTTGTGGCTCAGAGGTAG TGAACCCAGCTAATATCCATAAGGACTCGGGTTCGATCCCTGGCCTCGCTCA ATGGGTTAAGGATCCAGCGTTGCTGTGAACTGTGGTGTAGGTCACAGACAC AGCTTGGATCTGGTATTGCTGTCATGTAGGTTGGGCAGCTGTAGCTCTGATT GGACCCCTAGCTTGGGAACCTCCATATGCCGTGGGTGCGGCCCTAAAATGAC CAAAAAAAAAAAAGAGAAAGAAAGAAACGCAAGTTGGAACCTTAGTGGGGA ATTTCTCACATCTGAGATGGACGCGTGTATTGCCCAGAAAATGGGAGGGTG AAATTACCCTTCCCCTCCTCCCCACA
ERCC1 minigene	GAATGCCGATCTCGTACTTGCTGCCGATGCTACGCCTTCATTTTCAGACCCCA GAAGGACCTTGCGATGGACGAAGAGGGAGGCCAGAAGCCGGCTGCCTCAC CCACAAGGAAGAAATTCGTCATACCACTGGACGAGGATGAAGTCCCTCCTCC TGGGGCCAAGCCCTTATTCAAATGCACACGGAGCCTGCCCACCGTGGAGACC CCACCCCAGCCGGCTCCACAAACCTATGCTGAGTACGCCATCTCAGGACCTCC AGGAGGGGCTGGAGCCACACACCCCACGGGGCCAGAACCCCTGGCAGGAG AGACCCCCAACCAGGCTCCCAAACCAGGAGCAAAATCCAACAGCATCATTGT GAGCCCCCGGCAGAGGGGCAACCCCGTGCTGAGGTTTGTGCGCAACGTGCC CTGGCAGTTTGGCGATGTGCTTCCCGACTACGTGCTGGGCCAGAGCACCTGT GCCCTCTTCCTCAGCCTCCGCTACCACAACCTCCATCCGGATTACATCCACCA GCGGCTGCAGAGCCTGGGGAAGAGCTTCGCCCTGCGGGTCCTGCTCGTCCA GGTAGACGTGAAAGATCCGCAGCAGGCCCTCAGGGACCTGGCTAAGATGTG CATCCTGGCCGACTGCACCCTCATTCTGGCATGGAGCCCCGAGGAGGCCGG GCGGTACCTGGAGACGTACAAGGCCTATGAGCAGAAGCCAGCAGATCTCCT GATGGAGAAGCTGGAGCAAGACTTCGTGTCCAGGGTAACTGAATGTCTGAC CACCGTGAAGTCAGTCAACAAAACCGACAGTCAGACCCTCCTGACTACTTTT GGGTCCTTGGAACAGCTCACAGCTGCATCGCGGGAAGATCTGGCCTTGTGCC CTGGCCTGGGGCCTCAGAAGGCCCGGAGACTCTTTGACGTCTTACATGAGCC CTTCTTGAAAGCGTCCCGATGAGCTTAGCTGCCCCCAGTGTGACATGCTAGC ATACCGGTATTCGCGAGG

10.2 Vectors containing gRNA sequences

Table 36: Vectors containing gRNA sequences

plasmid	source	No.
pX330-MCS-Cas9-gRNA-ERCC1-E10 2	generated during this work	25
pX459-Cas9-Puro-gRNA-ERCC1-E10 2	generated during this work	68
pBS-U6-chimaric-gRNA-ERCC1-E10 1	generated during this work	44
pBS-U6-chimaric-gRNA-ERCC1-E10 2	generated during this work	45
pX330-MCS-Cas9-gRNA-ERCC1-E5 1	generated during this work	40
pX330-MCS-Cas9-gRNA-ERCC1-I4 2	generated during this work	52
pX330-MCS-Cas9-gRNA-ERCC1-I5	generated during this work	53
pX459-Cas9-puro-gRNA-ERCC1-E5 1	generated during this work	63
pX459-Cas9-puro-gRNA-ERCC1-I4 2	generated during this work	64
pX459-Cas9-puro-gRNA-ERCC1-I5	generated during this work	65
pX330-Cas9-puro-gRNA-ERCC1-I3 2	generated during this work	60
pX330-Cas9-puro-gRNA-ERCC1-I4 1	generated during this work	61
pBS-U6-chimaric-gRNA-MYBPC3-E6 1	generated during this work	28
pBS-U6-chimaric-gRNA-MYBPC3-E6 2	generated during this work	29
pX330-Cas9-puro-gRNA-MYBPC3-E6 1	generated during this work	66
pX330-MCS-Cas9-gRNA-MYBPC3-E23 1	generated during this work	49
pX330-MCS-Cas9-gRNA-MYBPC3-E23 2	generated during this work	50
pX330-MCS-Cas9-gRNA-MYBPC3-E23 3	generated during this work	51
pX459-Cas9-Puro-gRNA-MYBPC3-E23 3	generated during this work	67
pX330-Cas9-puro-gRNA-ERCC1-E3 2	generated during this work	81
pX330-Cas9-puro-gRNA-ERCC1-E6 2	generated during this work	82

10.3 Materials for new strategy - *ERCC1* Minigene in *ROSA26* locus

10.3.1 Oligonucleotides

Table 37: Oligonucleotides

All Oligonucleotides were purchased from MWG Eurofins, Ebersberg, GER.

oligonucleotide	sequence (5`→ 3`)	No.
ERCC1_In1F4	ACAGCGTGATACTATCCTTTCAG	104
PGK-ERCC1-Ex06 R	CAGTTTGCTTTCAGTGCCCTGGTACCGTCGACTGCAGG	177
ERCC1-Ex10-pA R	CAGCAAGTACGAGATCGGCATTCGGTACCGTCGACTGCAGG	179
ERCC1-del7-pA R	GGCTTTACACTTTATGCTTCCG GTCGACCTATTATCA CTCATGTAAGACGTCAAAGAG	180
PGK-ERCC1-Ex06 F	CCTGCAGTCGACGGTACCAGGGCACTGAAAGCAAACTG	209
ERCC1-Ex10-pA F	TAGCTGCCCCCAGTGTGACCGGAAGCATAAAGTGTAAAGCC	211

ERCC1-del7-pA F	TGATAATAGGTCGACCGGAAGCATAAAGTGTAAAGCC	212
ERCC1-del7-pA F2	CGTCTTACATGAGTGATAATAGGTCGACCGGAAGCATAAAGTGTAAAGCC	213
SbfI-PGK F	CCTGCAGGCCAGTGCCAAGCTTAAGGTG	68g
NheI-PGK F	GCTAGCCCAGTGCCAAGCTTAAGGTG	69g
BGH-pA R	ACAACCGGTACCTCTAGAACT	70g
NheI-loxP F	GCTAGCATAACTTCGTATAGCATACATTATACGAAGTTATCCTGCAGGTAAGCCCCTAGGATAACTTCGTATAGCATACATTATACGAAGTTATGCTAGC	120b
NheI-loxP R	GCTAGCATAACTTCGTATAATGTATGCTATACGAAGTTATCCTAGGGGCTTACCTGCAGGATAACTTCGTATAATGTATGCTATACGAAGTTATGCTAGC	121b
gRNA target site oligonucleotides		
CRISP-ER_Ex3_F2 (rev)	CACC G GTACTCAGCATAGGTCTGCG	96b
CRISP-ER_Ex3_R2 (rev)	AAAC CGCAGACCTATGCTGAGTAC C	97b
CRISP-ER_Ex6_F2 (for)	CACC G ACTGCACCCTGATCCTCGCC	104b
CRISP-ER_Ex6_R2 (for)	AAAC GGCGAGGATCAGGGTGCAGT C	105b

10.3.2 Vectors

Table 38: Vectors

plasmid	source	No.
pSL1180-PGK-eGFP	Chair of Livestock Biotechnology, Prof. A Schnieke, Freising, GER	70
pGE-ROSA26-mTomato/mEGFP-loxP	Chair of Livestock Biotechnology, Prof. A Schnieke, Freising, GER	696

11 Acknowledgement

An dieser Stelle möchte ich mich recht herzlich bei allen bedanken, die mir meine Promotion ermöglichten:

Ich möchte Frau Prof. Angelika Schnieke recht herzlich dafür danken, dass sie es mir ermöglicht hat in Ihrem Lehrstuhl meine Promotion durchzuführen. Sie hatte immer ein offenes Ohr für mich und unterstützte mich dabei, meine Ideen einzubringen. Dabei konnten wir auch herzlich lachen. Vielen Dank für die Hilfestellungen, Ratschläge und das Aufzeigen meiner Möglichkeiten. Weiterhin möchte ich ihr für ihr aufgebrachtes Vertrauen mir und anderen gegenüber danken. Es ist keine Selbstverständlichkeit seinen Angestellten so viel Freiheiten zu ermöglichen und ich möchte ihr dafür einen riesen Dank aussprechen.

Weiterhin danke ich Dr. Alex Kind, der ebenfalls stets ein offenes Ohr für Probleme hatte und der mit Freuden seine Hilfe anbot. Vielen Dank für die vielen Stunden, die er in meine Arbeiten investiert hat. Auch danke ich ihm für die Geduld, die er bei Korrekturen aufbrachte, besonders bei der Kommasetzung. Many thanks, Alex!

Ich danke Dr. habil. Tatiana Flisikowska herzlich für ihre Betreuung. Sie hatte immer ein offenes Ohr für Probleme, hat mich bei all meinen Projekten bestmöglich unterstützt und hat es mir ermöglicht meine Projekte selbstständig zu planen und durchzuführen. Auch in den schwierigen Phasen gab sie mir aufmunternde Hilfestellungen und half mir nie aufzugeben. Vielen Dank!

Ich möchte Sulith Christan herzlich dafür danken, dass sie so ist, wie sie ist. Sie hat uns mit einer Engelsgeduld mit allen nötigen Materialien versorgt, war immer hilfsbereit zur Stelle, wenn es ein Problem gab und hat uns immer mit genügend Zucker und Optimismus versorgt. Vielen Dank Sulith!

Marlene Stumbaum möchte ich dafür danken, dass ich sie das ein oder andere Mal als Joker verwenden durfte. Waren die Klonierungen noch so schwierig, Marlene kam zur Rettung und war auch immer gerne hilfsbereit zur Stelle, wenn man Fragen zu Methoden hatte. Vielen Dank!

Ich möchte mich auch herzlich bei Peggy Müller-Fliedner bedanken. Gerade am Ende meiner Arbeit hat sie mir sehr geholfen und ich fand die Zusammenarbeit äußerst angenehm. Vielen Dank für deine zuverlässige und selbständige Arbeitsweise!

Kristina Mosandl möchte ich dafür danken, dass sie mir viel in der Zellkultur geholfen hat. Auch die Gespräche nebenher waren immer anregend. Vielen Dank für die angeneheme Zusammenarbeit.

Alexander Carrapeiro und Nina Simm möchte ich recht herzlich für ihre Hilfe danken. Wenn es euch möglich war, habt ihr mir Arbeit abgenommen und diese immer zuverlässig und ordentlich erledigt. Weiterhin möchte ich euch für die tolle Zeit bei den Mittagspausen danken. Mit euch kann man immer ratschen und lachen, vielen Dank!!!

Auch bei allen anderen TAs möchte ich mich bedanken. Vielen Dank an Kilian Skowranek, Toni Kuhnt, Robert Grötschel und Johanna Tebbing, für die angenehme Zusammenarbeit

Vielen herzlichen Dank an Barbara Bauer. Sie hat immer alles organisiert, ob Weihnachtsfeier oder Betriebsausflug, und hat dafür gesorgt, dass alles läuft. Auch wenn es mal knapp wurde, sie hat sich für uns durch den bürokratischen Dschungel gewühlt. Vielen Dank!

Steffen und Viola Löbnitz möchte ich für ihre gute Arbeit und ihren Einsatz danken. Vielen Dank für das Pflegen der Tiere und die Beschaffung von Probenmaterial.

Dr. habil. Krzysztof Flisikowski möchte ich dafür danken, dass er sich um die Organisation des Tierstalles kümmert und für Fragen immer ein offenes Ohr hatte. Vielen Dank für die Zusammenarbeit.

Dr. Konrad Fischer möchte ich für seine Hilfestellungen und sein offenes Ohr bei Problemen danken. Auch für die schönen Zeiten nach der Arbeit möchte ich mich bedanken. Weiterhin vielen Dank, dass du uns nie hast verhungern lassen, die Weihnachtsfeiern wären ohne dich nicht halb so lecker gewesen.

Ich möchte mich bei meiner Bachlorstudentin Anna Folz, und den Forschungspraktikanten Leonie Redlinger, Monika Frühschütz und Sandra Mellmann bedanken. Ihr habt dabei geholfen meine Projekte weiter voranzutreiben, Vielen Dank und ich wünsche ihnen alles Gute für ihre Zukunft!

Acknowledgement

Ganz besonders möchte ich mich bei meinem Masterstudenten Stefan Rambichler bedanken. Wir hatten sehr viel Spass und konnten viel Lachen. Vielen Dank für deine angenehme Art und die Leistung, die du gebracht hast!

Ein weiterer besonderer Dank gilt Melanie Manyet. Als Masterstudentin hat sie mit viel Fleiß und Engagement mein Projekt weitergebracht. Aber sie war nicht nur eine angenehme Studentin, sondern wurde auch zu einer neuen Kollegin und eine meiner engsten Freunde. Vielen Dank für deine seelische Unterstützung und die vielen schönen Stunden die wir gemeinsam verbracht haben. Ich wünsche ihr viel Glück bei ihrer Promotion.

Andrea Schäffler möchte ich vor allem für die unzähligen schönen Stunden in und außerhalb der Arbeit einen besonderen Dank aussprechen. Sie hatte immer ein offenes Ohr für meine Probleme und auch sie ist eine meiner engsten Freunde geworden. Vielen lieben Dank und ich wünsche ihr viel Glück bei ihrer Promotion.

Vielen Dank an Beate Rieblinger und Dr. Simone Kraner-Scheiber für die freundliche Aufnahme in ihr Büro. Sie waren die besten Büropartner, die man sich wünschen konnte. Ich danke euch beiden herzlich für das angenehme Arbeitsklima und die vielen freudigen Stunden. Besonders Beate Rieblinger möchte ich noch für weitere schöne Stunden nach der Arbeitszeit danken. Egal ob Shoppen oder Fast Food, oder einfach ratschen, es war immer eine Freude mit ihr. Vielen Dank.

Allen weiteren Promotionsstudenten besonders aber Rahul Dutta, Benedikt Baumer und Erica Schulze, möchte ich für die angenehmen Gespräche und die schönen Augenblicke am Lehrstuhl danken. Weiterhin gilt vor allem Carolin Perleberg ein besonderer Dank für die vielen schönen Stunden und die anregenden Gespräche. Sie war immer bedingungslos hilfsbereit und hatte auch für private Probleme ein Ohr. Vielen Dank! Außerdem möchte ich Bernhard Klinger, Romina Hellmich, Alessandro Grodziecki und Daniela Kalla danken. Ob in der Küche oder auch mal zufällig irgendwo im Labor oder Büro, mit euch konnte man immer schöne Gespräche führen und viel Lachen.

Ein riesiger Dank geht an meine Familie. Meine Eltern haben es mir ermöglicht diesen Weg zu gehen und haben mir seelische Unterstützung gegeben wann immer es nötig war. Vielen Dank, dass ihr mir immer den Rücken gestärkt habt und mir auch beigestanden habt, wenn es mal nicht so einfach war! Auch meinem Bruder möchte ich danken für die vielen Momente in denen er mir eine große Stütze war und mir in jeder schwierigen Situation

geholfen hat. Auf ihn konnte ich Tag und Nacht zählen, wenn ich wieder ein Problem zu lösen hatte. Vielen Dank Bruderherz!

Mein größter Dank gilt meinem wunderbaren Mann. Ich danke ihm für seine Geduld, Unterstützung, die aufbauenden Worte und die vielen glücklichen Stunden, die er mir geschenkt hat und die mich aus jeder schwierigen Situation gerettet haben. Ich kann froh sein, in ihm meinen Seelenverwandten gefunden zu haben, mit dem ich gemeinsam lachen, weinen, leben und jeden noch so schwierigen Lebensweg gehen kann. Mein Liebster, vielen Dank für alles, ich liebe dich!